

MOTOR PROTEIN-ENDOMEMBRANE-NUCLEAR DYNAMICS DURING
MAMMALIAN FERTILIZATION

by

Christopher J. Payne

A DISSERTATION

Presented to the Department of Cell and Developmental Biology

and the Oregon Health and Science University

School of Medicine

in partial fulfillment of

the requirements for the degree of

Doctor of Philosophy

September 2003

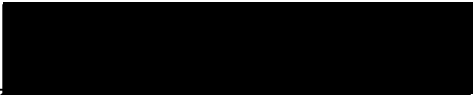
School of Medicine
Oregon Health Sciences University

CERTIFICATE OF APPROVAL

This is certify that the Ph.D. thesis of

Christopher J. Payne

has been approved



Professor in charge of thesis



Member



Member



Member

Member

TABLE OF CONTENTS

List of Figures and Tables.....	iv
List of Abbreviations.....	vii
Acknowledgments.....	ix
Abstract.....	xii
Chapter 1: Introduction.....	1
Localization of Motor Proteins and Endomembranes in Germ Cells.....	2
Role of the Centrosome During Fertilization.....	5
Use of Assisted Reproductive Technologies.....	8
Chapter 2: Materials and Methods.....	14
Chapter 3: Preferentially Localized Dynein and Perinuclear Dynactin Associate With Nuclear Pore Complex Proteins to Mediate Genomic Union During Mammalian Fertilization.....	31
Summary.....	32
Introduction.....	33
Results.....	34
Discussion.....	43
Chapter 4: LIS1 Association With Dynactin Is Required For Nuclear Motility and Genomic Union in the Fertilized Mammalian Oocyte.....	63

	Summary.....	64
	Introduction.....	65
	Results.....	66
	Discussion.....	70
Chapter 5:	Golgi Dynamics During Meiosis Are Distinct From Mitosis and Are Coupled to Endoplasmic Reticulum Dynamics Until Fertilization.....	77
	Summary.....	78
	Introduction.....	79
	Results.....	82
	Discussion.....	88
Chapter 6:	Summary and Conclusions.....	109
	Dynactin Association with Dynein, LIS1 and Nuclear Pore Complexes Mediates Female Pronuclear Migration.....	109
	Golgi Proteins Do Not Associate with Meiotic Spindle Poles, But Re-Distribute Around the Pronuclei During Fertilization.....	112
Appendix 1:	Biparental Inheritance of γ -Tubulin During Human Fertilization: Molecular Reconstitution of Functional Zygotic Centrosomes in Inseminated Human Oocytes and in Cell-Free Extracts Nucleated by Human Sperm.....	117
	Summary.....	118
	Introduction.....	119
	Results.....	121
	Discussion.....	127

Appendix 2: Non-Random Chromosome Positioning in Human Sperm and Sex Chromosome Anomalies Following Intracytoplasmic Sperm Injection.....	148
Appendix 3: Molecular Correlates of Primate Nuclear Transfer Failures.....	152
References.....	157

List of Figures and Tables

Chapter 1

Figure 1.1	Bull spermatozoa contain dynactin and nucleoporins but do not express either cytoplasmic dynein or Golgi proteins.....	11
Figure 1.2	Mature bovine oocytes contain dynactin, cytoplasmic dynein, and Golgi proteins but not organized nuclear pore complexes.....	12
Figure 1.3	Dynactin concentrates around the decondensing sperm- and oocyte-derived nuclei at 9 h post-insemination.....	13

Chapter 3

Figure 3.1	Sperm aster microtubules and dynein distribute to the female pronucleus.....	50
Figure 3.2	Dynactin subunits localize around both female and male pronuclei, while dynein distributes only to the female.....	51
Figure 3.3	Dynein and dynactin are required for pronuclear migration and apposition.....	52
Figure 3.4	Dynein does not localize to the female pronucleus in the absence of a sperm aster.....	54
Figure 3.5	Microtubules are required to retain dynein, but not dynactin, at pronuclear surfaces.....	55
Figure 3.6	Dynactin interacts with nucleoporins, vimentin and dynein during female pronuclear migration.....	57
Figure 3.7	Nucleoporins and vimentin are required for pronuclear migration and apposition.....	59
Figure 3.8	A model for pronuclear assembly, motility and union.....	61

Chapter 4

Table 1	Anti-LIS1 antibodies inhibit pronuclear union during fertilization.....	72
Figure 4.1	RT-PCR and cDNA sequence analysis of bovine and rhesus monkey Lis1.....	73
Figure 4.2	LIS1 RNA expression, protein expression and co-immunoprecipitation with dynactin.....	74
Figure 4.3	LIS1 and dynactin co-localize around the pronuclear surfaces in zygotes.....	75
Figure 4.4	LIS1 is required for pronuclear apposition.....	76

Chapter 5

Table 2	Distance between pronuclei in 1-cell zygotes.....	97
Table 3	Effect of brefeldin A (BFA) on bovine embryonic development in vitro.....	98
Figure 5.1	Golgi and ER dynamics during oocyte in vitro maturation, in vitro fertilization and early embryonic development.....	99
Figure 5.2	GM130 co-localizes with Sec23 at ER vesicle export sites but not with LCA at cortical granules.....	101
Figure 5.3	Phosphorylation cycle of GM130 during oocyte in vitro maturation, in vitro fertilization and early embryonic development.....	103
Figure 5.4	Brefeldin A (BFA) disrupts the Golgi apparatus but does not inhibit pronuclear apposition in zygotes.....	105
Figure 5.5	Effect of Brefeldin A (BFA) on development in early embryos.....	107

Chapter 6

Figure 6.1	A model for nuclear motility facilitated by a dynein-dynactin-LIS1 complex during fertilization.....	115
------------	--	-----

Appendix 1

Figure A1.1	γ -Tubulin in human and bovine sperm centrosomes.....	137
Figure A1.2	Centrin in human sperm centrosomes.....	139
Figure A1.3	Ultrastructural detection of centrin in the bovine mature sperm centrosome and its sensitivity to CSF-arrested cell-free extract.....	141
Figure A1.4	MPM-2 detection in human sperm and early bovine sperm penetration.....	143
Figure A1.5	Microtubule assembly in vitro nucleated by <i>X. laevis</i> , human and bovine sperm.....	145
Figure A1.6	γ -Tubulin, centrin, and MPM-2 detection in human and bovine zygotes.....	146

Appendix 2

Figure A2.1	Human sperm after in vitro decondensation and chromosome painting.....	151
-------------	--	-----

Appendix 3

Figure A3.1	Faulty mitotic spindles produce aneuploid embryos after primate nuclear transfer.....	156
-------------	---	-----

List of Abbreviations

ART	Assisted Reproductive Technologies
BFA	Brefeldin A
BSA	Bovine Serum Albumin
β -COP	β -Coatomer Protein
CSF	Cytostatic Factor
DTT	Dithiothreitol
ECNT	Embryonic Cell Nuclear Transfer
ER	Endoplasmic Reticulum
FITC	Fluorescein Isothiocyanate
GM130	Golgi Matrix protein of 130 kDa
GV	Germinal Vesicle
GVBD	Germinal Vesicle Breakdown
HPI	Hours Post-Insemination
HRP	Horseradish Peroxidase
ICC	Immunocytochemistry
ICSI	Intracytoplasmic Sperm Injection
IP	Immunoprecipitation; Immunoprecipitate
IVM	In Vitro Maturation
IVF	In Vitro Fertilization
KMT	KCl + MgCl ₂ + Tris-HCl buffer
LCA	<i>Lens culinaris</i> agglutinin
Met-2	Metaphase of second meiosis
MTs	Microtubules
NPC	Nuclear Pore Complex

Abbreviations (continued)

NT	Nuclear Transfer
NuMA	<u>N</u> uclear protein at interphase that associates with the poles of the <u>M</u> itotic <u>A</u> pparatus
PBS	Phosphate Buffered Saline
PN	Pronucleus
PVDF	Polyvinylidene Difluoride
RT-PCR	Reverse Transcription-Polymerase Chain Reaction
SCNT	Somatic Cell Nuclear Transfer
SDS-PAGE	SDS-Polyacrylamide Gel Electrophoresis
TALP	Tyrode's medium with Albumin, Lactate and Pyruvate
TL	Tyrode's medium with Lactate

Acknowledgments

My sincere gratitude - first and foremost – is for my advisor, Dr. Gerald Schatten, whose energy, passion and guidance have shaped me on many different levels, but whose support has been singular and steadfast. The work that comprises my Ph.D. thesis, which was performed entirely in his laboratory, is presented here as Chapters 3, 4, and 5. Additional work that relates to my thesis project, but which was performed in collaboration with others in the Schatten Lab, is presented here as Appendices 1, 2, and 3. I acknowledge that I am not the primary author on these appended chapters. It has been both a challenge and a reward conducting research in the laboratory during our move from Oregon to Pennsylvania, with experiences gained from such a transition being their own rewards. This would not have been achievable without the solid support of my Thesis Advisory and Examination Committees at OHSU: Drs. Jan Christian, Mike Danilchik, Gary Thomas, and David Battaglia. A very big thank you goes to Elaine Offield in the Department of Cell and Developmental Biology for helping me through the final process of completing my Ph.D. program from the other side of the country.

I would also like to extend my thanks to all of the wonderful individuals around the world with whom I have had the distinct pleasure of interacting during the past six years. Much of this interaction has occurred through my annual summer adventures in course coordination (“*Frontiers in Reproduction*”) at the Marine Biological Laboratory in Woods Hole, Massachusetts – a truly special place that now feels like a second home. Warm thanks to Dori-Chrysler Mebane, Martha Peterson, Herb Luther, Rudi Rottenfusser, Carol Hamel, Sandy Kaufmann, Dr. Louis Kerr, Dr. Lenny Dawidowicz

and everybody else on the MBL staff who welcomes me back each time. Recognition also goes to my fellow coordinators who helped keep me sane: Lisa de Speville, Sheila Roberts, and Drs. Michelle McMullen, Carrie Aldrich and Carrie Bivens.

Drs. Michael McClure, Martin Ionescu-Pioggia, Jerome Strauss, Charles Lockwood, Kelly Mayo, Joan Hunt, Asgi Fazleabas, Patricia Hunt, and Teresa Woodruff all deserve recognition for their unwavering support and trust in my scientific course coordinating skills, and for listening to what I had to say each year about the state of the reproductive biology course - even if it wasn't always good news at the time. Most importantly, I would like to thank all of the wonderful scientists I have met through the course, especially Drs. Dean Betts, Craig Hodges, Elizabeth McGee, Craig Richard, Nucharin Songsasen, and Joyce Tung.

I am grateful to Dr. Trina Schroer for the gift of anti-dynactin antibodies, and to Dr. Martin Lowe for the gift of anti-phospho-GM130 antibodies used during these studies. Betsy True and David McDougal provided the graphics that generated the model figures and schematic diagrams. Acknowledgments are also given to the National Institutes of the Health, especially the NICHD, NCRR and NIEHS, for their support through research grants awarded to Dr. Schatten. Thanks also to the Magee-Womens Health Foundation and Ms. Irma Goertzen.

Members of the Schatten Lab have all dispensed wisdom, both scientific and non-scientific in nature, and I wish to thank many for their contributions: Drs. Tanja Dominko, Laura Hewitson, Marc Luetjens, Ricardo Moreno, Chris Navara, Gabriel Sanchez-Partida, Cal Simerly, Peter Sutovsky, Anthony Chan, Kowit-Yu Chong, Kay Larkin, Paul Sammak, Yukihiro Terada, and Diana Takahashi, Crista Chace, Amanda

Dettmer, Heather Gray, and others for whom space limitations preclude acknowledgements. Special thanks to Drs. João Ramalho-Santos and Jus St. John for fruitful scientific collaborations, thoughtful discussions, and enduring friendships.

I would also like to acknowledge special friends and scientific colleagues from around the world: agradecimentos as minhas colegas Adriana Bos-Mikich, Denise Bongalhardo e Paula Navarro; un agradecimiento a Paula Cameo y sua Familia; un grand merci à Sylvie Fabre; un inmenso agradecimiento a Vanesa Rawe por su apoyo moral y conocimiento tecnico durante todo mi trabajo.

My thanks to classmates, peers and faculty members at OHSU: to Drs. Willy Lensch, Stephani Sutherland, and committee members for assistance with organizing and running the Student Research Forum all those years; to Anita Bechtholt for showing me the ‘time-saving’ shortcuts within Microsoft Word; to Drs. Bruce Magun and Richard Maurer for their support during my leave of absence; and to Drs. Gary Ciment and Phil Copenhaver for allowing me to teach first-year medical students the development of the urinary-genital system. Most importantly, I would like to thank Dr. Erin Jobst for always being there as a supportive friend and wonderful colleague during this long journey through graduate school.

Last, but not least, I would like to thank my parents, Dr. Jay Thomas and Janet Payne, my brother Michael, my grandparents Jesse and Jean LaDow, grandmother Mary Ruth Payne, and all of my relatives for their love, support and understanding of my goals and passions: Dr. Beth LaDow; Joshua, Kate and Samuel Alper; David, Margaret, Eva and Alice LaDow; Carolyn Payne; and Steven and Barbara Brown. I dedicate this dissertation to the memory of my grandfather, Jay Henry Payne.

Abstract

Mammalian fertilization dynamics unfold as a series of remarkable events, involving the active reorganization of the centrosome and cytoskeleton, the egg- and sperm-derived nuclei, and the endomembranes within the zygote. Despite the many advances in our knowledge of these events, the molecular mechanisms that regulate the cytoplasmic and nuclear dynamics of fertilization are still poorly understood. This work tests several hypotheses that involve the distribution and regulation of microtubule motor proteins, nuclear envelope proteins, and Golgi proteins within the cytoplasm, as well as nuclear dynamics during fertilization and assisted reproductive technologies (ART). In our first hypothesis, we propose a role for cytoplasmic dynein and dynactin in associating with pronuclear membranes to mediate genomic union. Our results show that dynactin associates with nuclear pore complex proteins, as well as the intermediate filament vimentin and dynein on the cytoplasmic surfaces of the pronuclei. Inhibition of the motor complex, as well as of nucleoporins and vimentin, blocks pronuclear apposition. Because it is known that the molecule LIS1 directly associates with dynein and dynactin to mediate neuronal migration, we also test whether LIS1 functions in the fertilized mammalian egg to facilitate genomic union. We find that LIS1 associates with dynactin on pronuclear surfaces, and that its inhibition blocks pronuclear apposition.

Cytoplasmic components that do not affect nuclear motility, in contrast, are Golgi proteins. During mitosis, the putative matrix protein GM130 is phosphorylated and relocalized to spindle poles, but when exposed to the drug brefeldin A the protein associates with vesicle export sites on the endoplasmic reticulum. Given that most

mammalian oocytes lack centrosomes at the meiotic spindle, we test the hypothesis that GM130 associates not with meiotic spindle poles, but with clusters of endoplasmic reticulum in the mature oocyte. Indeed, GM130 co-localizes with Sec23, a marker for ER vesicle export sites at Met-2 arrest, and does not distribute to the spindle region. We conclude that the absence of a maternal centrosome precludes Golgi association with the meiotic spindle, and show that when the sperm enters the egg, introducing the paternal centrosome, GM130 reorganizes around the pronuclei. The question of what, exactly, the sperm contributes to the zygotic centrosome is also addressed in the first of three appendices, detailing work that was performed as part of several collaborative projects. Cell-free *Xenopus* egg extracts and human sperm are used to characterize zygotic centrosome assembly. Our results support a model in which γ -tubulin, a major component of the centrosome, is biparentally inherited, and in which maternal components are attracted to a paternal template.

In many cases when human sperm cannot penetrate an oocyte by conventional means, successful fertilization can be achieved through direct microinjection of a single sperm into an oocyte – a technique known as ICSI (intracytoplasmic sperm injection). While it succeeds in introducing both the nuclear and centrosomal material into the egg, the technique has raised concerns with an increased report of sex chromosome anomalies in children conceived through its use. To investigate the relationship between sex chromosomes and ICSI, we identify a non-random localization of the X chromosome in the apical region of the sperm nucleus – a region that remains condensed for a longer period of time than the basal region – and describe the results in Appendix 2. Perhaps this finding may contribute to a greater general understanding of sperm nuclear remodeling

within an egg cytoplasm. What is perplexing, however, is why another form of ART used in animals – nuclear transfer -succeeds in some species but not in others. Specifically, we question why nuclear transfer has failed in non-human primates. Focusing on the role played by another set of motor proteins, Eg5, HSET and NuMA, to organize and maintain a bipolar meiotic spindle, we show in Appendix 3 that the conventional method of nuclear transfer removes these essential proteins from the primate egg cytoplasm and results in aberrant mitotic spindles.

With our increased understanding of the interactions among molecular motors, spindle microtubules, nuclear envelope components, Golgi proteins and vesicle export sites during fertilization, we are more fully defining the extensive cytoskeletal, membrane and nuclear dynamics in the fertilized mammalian egg. This should allow us to begin addressing the specific molecular mechanisms underlying this remarkable process.

Chapter 1

Introduction

It has been over one hundred years since the first micrographs of sea urchin fertilization were published by E.B. Wilson in *An Atlas of the Fertilization and Karyokinesis of the Ovum* (Wilson, 1895). In the intervening century, our understanding of the complex and remarkable dynamics occurring within the cytoplasm of the fertilized egg has been extended to fish, amphibians, birds and a variety of mammals (reviewed in Schatten, 1994). The process of fertilization unfolds in a series of events, involving the active reorganization of the centrosome and cytoskeleton, the egg- and sperm-derived nuclei, and the endomembranes within the zygote. Despite the many advances in our knowledge of these events, the molecular mechanisms that regulate the cytoplasmic and nuclear dynamics of fertilization are still poorly understood. This thesis investigates the regulation of dynamic events that occur during mammalian fertilization, examining the roles and interactions of molecular motors and microtubule-associated proteins on the migration of the egg-derived (female) pronucleus to the sperm-derived (male) pronucleus in zygotes, as well as the association between - and reorganization of - the Golgi apparatus and endoplasmic reticulum during meiotic maturation and fertilization in oocytes. The paternal and maternal contributions to zygotic centrosome assembly, the significance of chromosomal positioning in sperm nuclei, and the importance of mitotic spindle-associated molecular motors will also be described in the appendices that follow the main chapters.

Localization of Motor Proteins and Endomembranes in Germ Cells

Molecular motors function in nearly every cell to transport vesicles to their required location during interphase, and to build and maintain spindles to ensure proper chromosome separation during mitosis and meiosis. One specific microtubule motor is cytoplasmic dynein, which requires its cofactor dynactin to actively move cargo. The dynein-dynactin complex, in addition to its role in protein trafficking and spindle formation, also functions to localize the Golgi apparatus to the centrosome in the majority of cells. Often this location is juxtannuclear, in close proximity to nuclear membranes and the nucleoporins embedded within their envelopes. The roles of different cytoplasmic proteins will be examined in pronucleate-stage zygotes throughout this thesis, but first, the distribution of cytoplasmic dynein, dynactin, nucleoporins, and Golgi proteins will be presented in bull spermatozoa and bovine oocytes.

Mature bull sperm, at the time of insemination, contain a band of dynactin around the equatorial region of the sperm head, but lack cytoplasmic dynein (Figure 1.1A,B). This result is not surprising, given that the class of dynein found in sperm is axonemal, and not cytoplasmic (Gagnon, 1995). Axonemal dynein, which localizes to the tail and is required for its movement, is distinct from the cytoplasmic form of the molecule, sharing only 25% identity in the amino acid sequence (Gibbons, 1995). Cytoplasmic dynein contains two 532-kDa heavy chains, three 74-kDa intermediate chains, and four light chains of M_r 59, 57, 55, and 53 (Holzbaur et al., 1994). The 74-kDa intermediate chain of cytoplasmic dynein directly interacts with the p150^{Glued} subunit of dynactin (Karki and

Holzbaur, 1995; Vaughan and Vallee, 1995), itself a large complex that also contains: one p62 subunit (62 kDa), five p50 dynamin subunits (50 kDa), ten Arp-1/centractin subunits (45 kDa), and four additional subunits of M_r 37, 32, 27, and 22 (Holleran et al., 1998). Thus, during fertilization, sperm have the ability to contribute some dynactin but no cytoplasmic dynein.

Nuclear pore complex (NPC) proteins also localize to the equatorial region of the sperm head, as well as to the centrosome region of the midpiece in bull sperm (Figure 1.1C). NPC proteins comprise the complex that spans the nuclear pore, enabling transport of protein and RNA to and from the nucleus. Proteomic analysis of the mammalian NPC has identified 29 nucleoporins and 18 NPC-associated proteins (Cronshaw et al., 2002). The presence of some of these nucleoporins in mature bull sperm suggests that even in its remarkably compact form, communication between the highly condensed nucleus and the tiny volume of cytoplasm is retained. The similarity between dynactin and NPC distribution is also intriguing, given that dynactin localizes to the nuclear envelope in somatic cells entering prophase (Salina et al., 2002; Busson et al., 1998).

Bull spermatozoa do not contain a Golgi apparatus, however, as neither the putative matrix protein GM130 nor the ER-to-Golgi COPI vesicle coat protein β -coatamer (β -COP) are present (Figure 1.1D,E). This result agrees with recent data showing that other Golgi components, including Golgin-97 and Golgin-160, are lost during spermiogenesis, discarded in the cytoplasmic droplet that is cast off during the maturation process (Moreno et al., 2000). Mammalian sperm, therefore, no longer appear to retain the endomembranes necessary for protein secretion, and do not contribute Golgi proteins during fertilization.

Mature bovine oocytes, in contrast to spermatozoa, contain both dynein and cytoplasmic dynein that are enriched at the meiotic spindle (Figure 1.2A,B). This localization resembles the distribution of the dynein-dynactin complex in mitotic somatic cells, concentrated at the spindle to ensure proper assembly and maintenance of the microtubule array (Vaisberg et al., 1993). The process of meiotic maturation involves the expulsion of maternal DNA into two polar bodies by a mechanism that demands the accurate separation of chromosomes. Surprisingly, a high degree of meiotic errors can occur during oocyte maturation, resulting in aneuploidy that adversely affects subsequent embryo development (LeMaire-Adkins et al., 1997). Thus, the concentration of dynein and dynactin at the meiotic spindle suggests their importance in maintaining this structure with respect to normal development.

NPC proteins, however, are neither concentrated nor organized as a complex within the oocyte, but instead are distributed diffusely throughout the cytoplasm (Figure 1.2C). These observations confirm earlier findings that NPC staining is quite dim and unfocused in mature mammalian oocytes (Sutovsky et al., 1998). Given that NPCs assemble and insert into nuclear membranes at the onset of interphase, it is not surprising that the component proteins are not yet associated with each other at meiotic metaphase. Sutovsky et al. showed that NPCs concentrate around the decondensing sperm- and egg-derived pronuclei soon after insemination, and that their assembly is required for proper pronuclear formation. Fertilization, therefore, promotes the restoration of NPC protein associations with nuclear membranes.

The distribution of Golgi proteins in mature bovine oocytes, meanwhile, takes the form of punctate foci, broadly dispersed throughout the cytoplasm (Figure 1.2D,E). Both

GM130 and β -COP localize with this pattern, appearing as membrane vesicles. The highly fragmented appearance of the Golgi apparatus could explain the absence of a functional secretory pathway in the oocyte at this stage, as the fragmentation of the Golgi and the block in protein secretion coincide (Colman et al., 1985; Moreno et al., 2002). No preferential concentration of Golgi proteins is observed at the meiotic spindle in bovine oocytes, in contrast to mitotic somatic cells (Seemann et al., 2002).

Mature bull sperm, therefore, can conceivably contribute dynactin, nucleoporins and tubulin to the oocyte during fertilization, in addition to other cytoplasmic components like the centrosome and mitochondria (Sutovsky and Schatten, 2000). The overwhelming majority of proteins and endomembranes required for fertilization and early embryonic development, however, is provided by the oocyte and its large volume of cytoplasm. Sperm incorporation is accompanied by the expulsion of the second polar body, decondensation of the egg-derived and sperm-derived nuclei, and recruitment of maternal endomembranes around the two pronuclei. At 9 h post-insemination, for example, an accumulation of dynactin can be seen around the female pronucleus as well as near the surface of the newly forming male pronucleus (Figure 1.3). This distribution of dynactin resembles the localization of NPCs around the pronuclei at the time of their formation (Sutovsky et al., 1998), suggesting that perhaps there is an association between dynactin and NPCs. This interaction will be one of several that will be examined in this thesis.

Roles of the Centrosome During Fertilization

One of the important cytoplasmic structures that bull sperm contribute to the oocyte during fertilization is the centrosome. Still not completely understood at the structural and functional levels after more than one hundred years since its discovery, the centrosome serves as the dominant microtubule-organizing center in the majority of animal cells (Kellogg et al., 1994). Consisting of an orthogonal pair of centrioles, specialized organelles containing nine groups of triplet microtubules fashioned into cylinders, that are, in turn, surrounded by an amorphous cloud of pericentriolar material, the centrosome nucleates microtubules from a central structure known as the γ -tubulin ring complex (Zheng et al., 1995). In most mammalian species, including cow and monkey, the centrosome degenerates in the oocyte and is retained in the sperm during the maturation process (Schatten, 1994). Rodents, however, differ from this scenario and show maternal centrosomal inheritance and centrosome degeneration in the sperm (Schatten et al., 1986; Manandhar et al., 1999). Bovine and rhesus gametes, therefore, more closely resemble human oocytes and sperm, and will be used as model systems throughout this thesis.

Following the insemination of bovine or rhesus oocytes, the sperm centrosome, which lies attached to the sperm nucleus in the egg cytoplasm, nucleates microtubules to form a structure known as the sperm aster. Defined as a radial array of microtubules anchored at the centrosome, the sperm aster grows and expands to reach both the surface of the female pronucleus as well as the egg cortex (Schatten, 1994). Contact of the sperm aster with the cortex is thought to generate the force necessary to propel the male pronucleus to the center of the egg (Reinsch and Gönczy, 1998), and microtubule association with the surface of the female pronucleus is thought to facilitate the migration

of the female towards the male pronucleus that completes the fertilization process (Schatten, 1994). Thus, the paternally inherited centrosome plays an essential role in establishing and supporting the microtubule-based motility within the zygote.

Until recently, however, it has not been clear how the sperm centrosome becomes modified within the egg cytoplasm to become a fully functional microtubule-organizing complex. In *Xenopus*, for example, γ -tubulin is thought to be acquired solely from the maternal cytoplasm, with the assembly of γ -tubulin into the complex occurring only after sperm incorporation (Gard, 1994; Stearns and Kirschner, 1994). Centrin, a centrosome protein that is biparentally inherited, is a Ca^{2+} -sensitive molecule that is thought to sever axonemal microtubules from the sperm centrosome, and may be involved in centrosome duplication (Salisbury, 1995). Other components might also be biparentally inherited. Centrosome reconstitution during mammalian fertilization, therefore, requires further examination into which specific components are provided by the sperm and which are provided by the egg.

Pronuclear migration and apposition in the bovine zygote is followed by the breakdown of pronuclear envelopes, the formation of a mitotic spindle, and the first interactions between the maternal and paternal DNA. The role of the centrosome in anchoring a bipolar spindle is well known in somatic cells and cell-free extracts, and is slowly becoming better understood in mammalian zygotes (Doxsey, 2001). Molecular motors, interestingly, appear to serve even more important roles in spindle assembly and maintenance, with molecules such as HSET and NuMA crucial for preserving proper spindle structure and function (Mountain et al., 1999). When mammalian oocytes are parthenogenetically activated, development to the blastocyst stage in the absence of a

paternal centrosome ensues – raising two possibilities of how mitotic spindles might be formed in these cells: either that molecular motors exclusively assemble the spindles in the absence of a centrosome, or that a centrosome forms *de novo* to organize the microtubules (Kuntziger and Bornens, 2000). Further analysis will be needed to clarify this developmental phenomenon.

Use of Assisted Reproductive Technologies

The use of in vitro fertilization (IVF) as an alternative method for human reproduction has proven to be an unparalleled success since its introduction in 1978 (Thornton, 2000). Modifications and refinements to the technique, which created other assisted-fertilization methods such as partial zona dissection (PZD) and subzonal insemination (SUZI), inadvertently led to the successful microinjection of a single spermatozoon directly into an oocyte to achieve pregnancies and normal, healthy live births – a technique known as intracytoplasmic sperm injection (ICSI; Palermo et al., 1992; Van Steirteghem et al., 1993). ICSI is now used in human IVF clinics to overcome various types of male factor infertility, and the procedure bypasses many of the normal steps that unfold during insemination, such as the sperm acrosome reaction, sperm-zona binding and penetration, and sperm-oolemma binding and fusion (Ramalho-Santos et al., 2000; Hewitson et al., 2000a; Sutovsky and Schatten, 2000). Although ICSI appears to be a relatively safe and effective method to treat many cases of male factor infertility and to produce healthy babies (Van Steirteghem et al., 2002), questions have been raised

regarding the safety and long-term consequences of the technique (In't Veld et al., 1995; Bowen et al., 1998; Lamb, 1999; Nudell and Lipshultz, 2001).

Recent evidence has shown that sperm DNA decondensation occurs asynchronously following ICSI, with the apical region of the sperm head remaining highly condensed for a longer period of time than the basal region (Ramalho-Santos et al., 2000). The apical region contains the acrosome and perinuclear theca, structures normally lost during IVF, and these components are still retained on the male pronucleus even after pronuclear apposition – over 12 h after ICSI. Furthermore, paternal DNA synthesis, as evaluated by BrdU incorporation into the male pronucleus, occurs only once the spermatozoon completely decondenses, and thus is delayed when compared to IVF (Ramalho-Santos et al., 2000). These observations raise many questions concerning the alteration of normal cell biological events that occur during fertilization, especially in light of the reported higher incidence of sex chromosome anomalies in embryos and fetuses produced by ICSI (In't Veld et al., 1995; Bonduelle et al., 1998). These concerns warrant additional investigation and experimental analysis using animal models to shed light on the underlying mechanisms involved in this process.

Another method that falls within the category of assisted reproductive technologies in animals, and especially in domestic livestock, is nuclear transfer (NT). This technique involves the transfer of a nucleus – either with the entire cell via electrofusion or with cell remnants via microinjection – from a donor embryonic or adult somatic cell into an enucleated oocyte (Wolf, et al. 1999). First demonstrated in amphibians, NT using embryonic donor nuclei has successfully produced live offspring in mice, rabbits, pigs, sheep, goats, cows and other mammalian species in the past decade

(Sun and Moor, 1995). In 1997, the first live mammalian birth using an adult donor nucleus resulted in a lamb named Dolly (Wilmut et al., 1997), and in the intervening years live offspring using adult somatic cell NT have been generated in cows, goats, pigs, mice, rabbits, and one cat (Kato et al., 1998; Baguisi et al., 1999; Polejaeva et al., 2000; Wakayama et al., 1998; Chesne et al., 2002; Shin et al., 2002). One report of successful NT in rhesus monkeys using embryonic donor nuclei has been published (Meng et al., 1997), but thus far no live monkey births using adult somatic cells have been achieved.

The majority of mammals produced by somatic cell NT, unfortunately, die *in utero* and display abnormalities related to large offspring syndrome, with metabolic and respiratory disorders and enlarged, dysfunctional placentas (Young et al., 1998; Rideout et al., 2001; Jaenisch et al., 2002). The challenges of reprogramming the donor nucleus, combined with the hurdles presented in the host cytoplasm, are thought to be the chief obstacles that decrease the efficiency of this technique and increase the developmental abnormalities observed in embryos. Optimization strategies, therefore, need to be pursued with respect to nuclear reprogramming and the donor-host cytoplasmic environment. For example, it is possible that vital components within the cytoplasm of the oocyte are lost during enucleation and are not replenished during NT, reducing the likelihood of embryonic survival. These components might consist of molecular motors, endomembranes, or other molecules that associate with the nuclear apparatus in the mature oocyte, and that could be discarded during the enucleation process. The exploration of this possibility would shed light on the dynamics of motors, membranes, and nuclear material during fertilization, and would have implications on the success of assisted reproductive technologies like ICSI and NT.

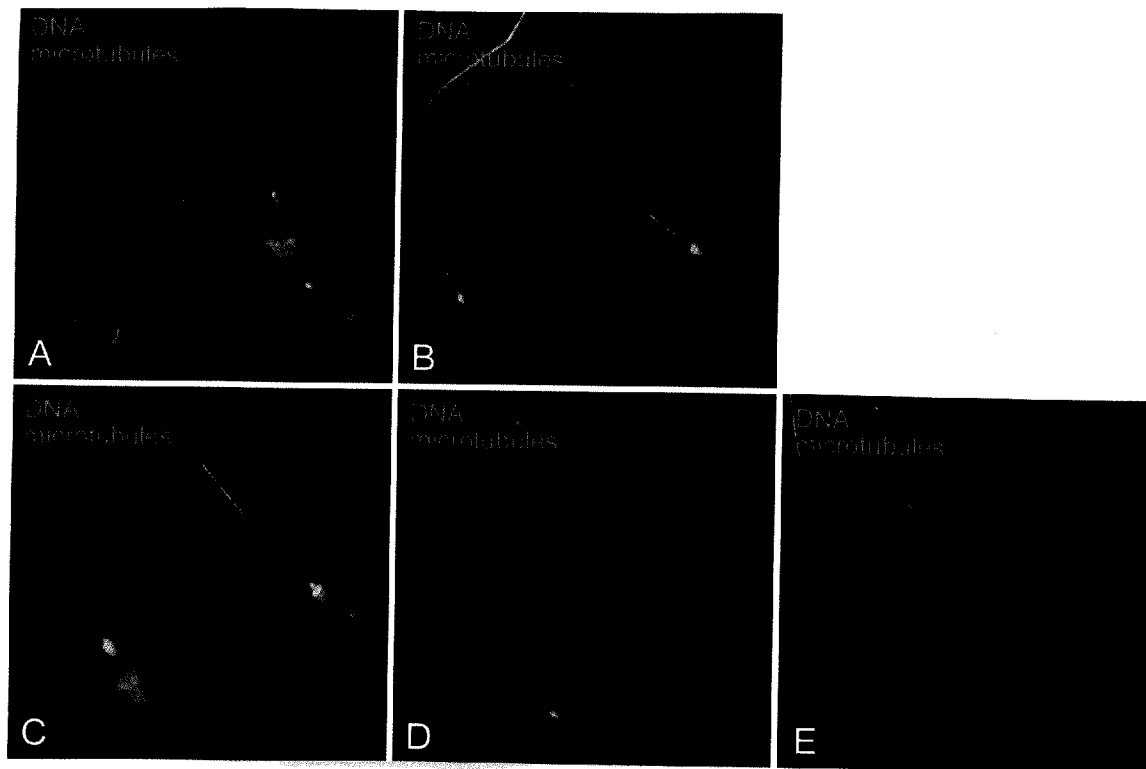


Figure 1.1. Bull spermatozoa contain dynactin and nucleoporins but do not express either cytoplasmic dynein or Golgi proteins. (A) Dynactin subunit p150^{Glued} (red) localizes to the equatorial region of the mature sperm head; DNA (blue) and microtubules (green) are also shown for A-E. In contrast, the intermediate chain of cytoplasmic dynein (B) is not detected in either the heads or the tails. (C) Nucleoporins, which comprise the nuclear pore complex (red), distribute to both the centrosomal region where the head connects the tail, as well as the equatorial region of the head. Neither Golgi matrix protein GM130 (D) nor vesicle trafficking β -coatamer protein (β -COP; E) are detected.

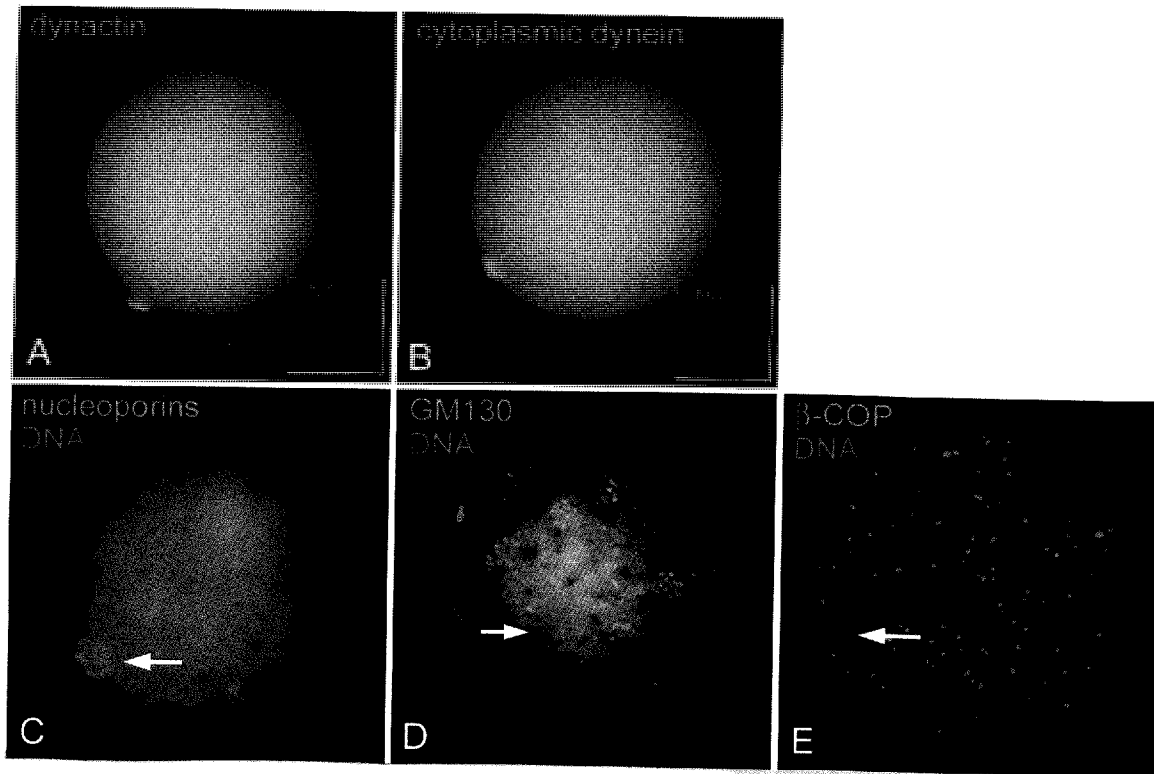


Figure 1.2. Mature bovine oocytes contain dynactin, cytoplasmic dynein, and Golgi proteins but not organized nuclear pore complexes. (A) Dynactin subunit p150^{Glued} (green) concentrates at the site where the maternal DNA is aligned on the metaphase plate (inset: DNA, blue). (B) Cytoplasmic dynein intermediate chain (green) also localizes to the region of the meiotic spindle (inset: DNA, blue), showing a slightly broader distribution than dynactin. (C) Nucleoporins show weak, diffuse staining, with no identifiable nuclear pore complexes evident; arrow denotes DNA (blue). Both Golgi matrix protein GM130 (D; green) and vesicle trafficking protein β -COP (E; green) distribute throughout the ooplasm as punctate foci; arrows denote DNA (blue).

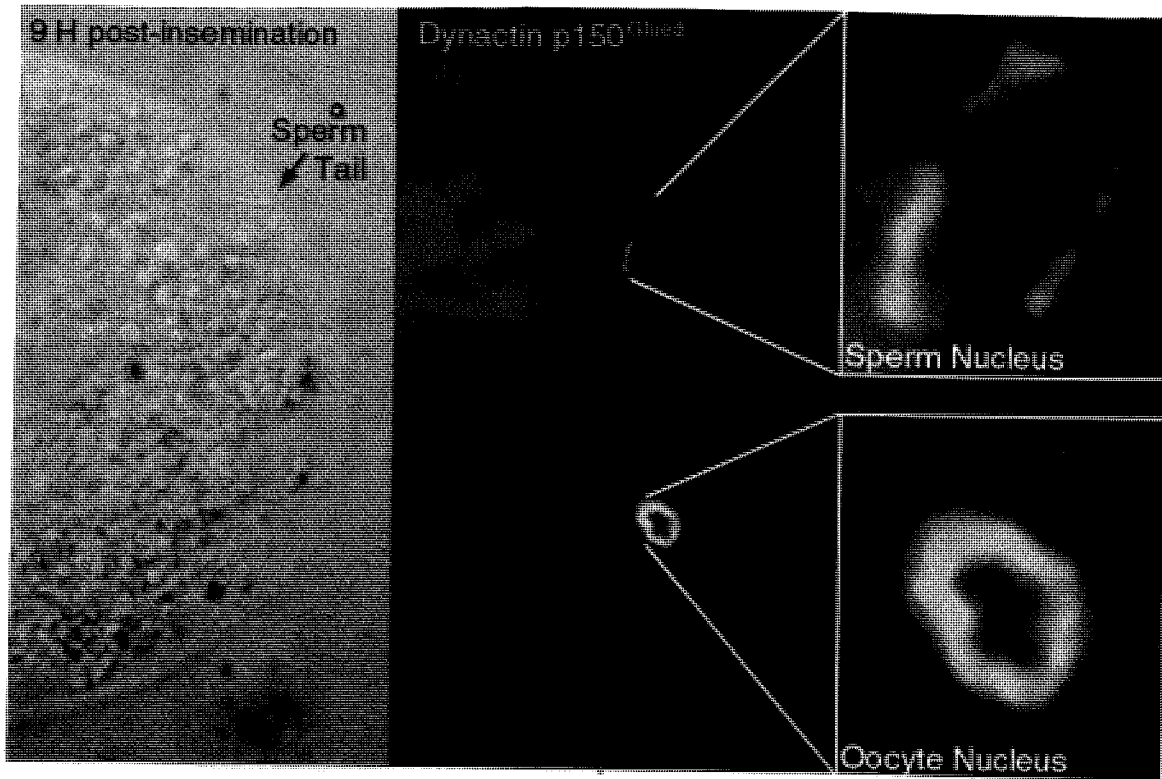


Figure 1.3. Dynactin concentrates around the decondensing sperm- and oocyte-derived nuclei at 9 h post-insemination. The p150^{Glued} subunit (green) localizes at the surfaces of both nuclei (blue), with the oocyte nucleus showing a greater accumulation of dynactin than the sperm nucleus at this time point (top and bottom inset). Differential interference contrast optics allow for the identification of the sperm tail (arrow; left panel).

Chapter 2

Materials and Methods

Bovine and Rhesus Monkey Oocyte In Vitro Maturation and In Vitro Fertilization

In vitro maturation (IVM) and in vitro fertilization (IVF) are carried out according to standard protocols (Sirard et al., 1988; Wolf et al., 1989; Navara et al., 1994; Hewitson et al., 1998), with bovine oocytes obtained either from a local abattoir or from BOMED, Inc. (Madison, WI), and rhesus oocytes obtained from the Assisted Reproductive Technology Cores at the Oregon National Primate Research Center (Beaverton, OR) and the Pittsburgh Development Center (Pittsburgh, PA).

Bovine ovaries obtained after slaughter are transported in thermoses containing normal saline at 39°C. Immature oocytes are then recovered by aspiration of 3- to 5-mm large ovarian follicles using an 18-gauge needle; only those oocytes having an homogenous cytoplasm and surrounded by at least three layers of cumulus cells are selected. These oocytes are then washed through three rinses in Tyrode's medium (114 mM NaCl, 3.2 mM KCl, 2 mM CaCl₂·2H₂O, 5 mM MgCl₂·6H₂O, 25 mM NaHCO₃, 0.4 mM NaH₂PO₄, 10 mM Na lactate, 100 IU/ml penicillin; TL stock), modified with 10 mM Hepes, 1 mg/ml BSA, 2 mM pyruvate, and 25 µg/ml gentamycin (TALP-Hepes; Bavister et al., 1983). Oocytes are matured for 24 h in 50-µl drops of TC199 medium modified with 10% fetal calf serum, 5 µg/ml follicle stimulating hormone (FSH), 1 µg/ml estrogen, and 25 µg/ml gentamycin at 39°C in 5% CO₂ under mineral oil.

Rhesus oocytes are recovered by laparoscopy from gonadotropin-stimulated female rhesus monkeys (Zelinski-Wooten et al., 1995; Hewitson et al., 1996; Meng et al., 1997). Beginning at menses, females are down-regulated with the gonadotropin-releasing hormone (GnRH) antagonist Antide (Serono), administered sub-cutaneously at 0.5 mg/kg body weight, for six days during which recombinant human FSH is administered twice daily, followed by 1, 2 or 3 days of rhFSH + recombinant human luteinizing hormone (rhLH; Serono), administered intra-muscularly at 30 IU each, twice daily. Ultrasonography is performed on day 7 to assess the follicular response, and recombinant human chorionic gonadotropin (rHCG; Serono) is administered at 1000 IU when follicles are 3-4 mm in diameter. Follicular aspiration is then performed 27 h after HCG administration. Oocytes are aspirated from the follicles using a needle suction device at ~40-60 mm Hg pressure into heparinized blood collection tubes, which are transported to the laboratory for oocyte recovery and evaluation.

Mature bovine and rhesus oocytes, arrested in metaphase of second meiosis (Met-2), are then placed into 50- μ l drops of TALP medium (Bavister et al., 1983). Frozen bull semen (American Breeders Service) is thawed to room temperature, layered over a 2-part 45%, 90% percoll gradient and centrifuged at 700 g for 15 min to isolate live sperm. Rhesus semen is collected by penile electro-ejaculation (Bavister et al., 1983; Boatman and Bavister, 1984). Following liquefaction at 37°C for 30 min, the sample is washed twice in 10 ml TALP-Hepes by centrifugation at 400 g for 5 min, and the live sperm are incubated for 4 h at 37°C in 5% CO₂ before the addition of 1 mM caffeine and 1 mM dibutyryl cyclic AMP (Bavister et al., 1983). Sperm are then added to the drops of culture medium containing the oocytes to give a final concentration of 1×10^6 sperm/ml. Bovine

oocytes and sperm are incubated at 39°C under 5% CO₂, and rhesus gametes at 37°C under 5% CO₂, until the desired stages in development (Long et al., 1993; Laurinčík et al., 1998).

To examine the effects of microtubule depolymerization on the localization of dynein and dynactin in pronucleate-stage zygotes, some oocytes and sperm are incubated until 14 h post-insemination, at which time the zygotes are transferred into drops of culture medium containing 20 μ M nocodazole (Sigma-Aldrich) and cultured in the presence of the drug for 1 h. To examine the role of the sperm aster on the distribution of dynein and dynactin to the female pronucleus, some oocytes are parthenogenetically activated with two 5-min incubations in 5 μ M ionomycin, given 4 h apart (Navara et al., 1994). These activated oocytes extrude a second polar body, form a female pronucleus in the absence of a sperm aster, and are cultured for 16 h.

To examine the effects of Golgi apparatus disruption on the migration and apposition of the female and male pronuclei, some zygotes and embryos are cultured in the presence of the fungal metabolite brefeldin A (BFA; Sigma-Aldrich). BFA concentration in the medium ranges from 1 μ g/ml to 20 μ g/ml. Zygotes incubated with BFA are either fixed 18-20 h post-insemination, or cultured with BFA for an additional 70 h. At 36 h post-insemination, embryos are transferred into BFA-containing CR1 medium: 115 mM NaCl, 3 mM KCl, 26 mM NaHCO₃, 0.4 mM pyruvate, 1 mM L-glutamine, 5 mM L (+) hemi-Ca²⁺ lactate, 0.3% BSA, 1X BME and MEM amino acids. Embryos are then transferred into fresh drops of BFA-CR1 medium every 12 h, and allowed to develop until 90 h post-insemination. BODIPY FL conjugate of BFA

(Molecular Probes) is used to verify that the BFA enters the zygotes and embryos in culture.

Nuclear Transfer and Embryo Transfer

Oocyte enucleation is accomplished using a 30- μ m inner diameter pipette (Humagen) to aspirate the first polar body and underlying cytoplasm, including the second meiotic spindle (Dominko et al., 1999). This is performed after a brief incubation in TALP-Hepes containing 7.5 μ g/ml cytochalasin D and 1 μ g/ml Hoechst 33342 (Sigma-Aldrich). Maternal chromosome removal is confirmed by DNA epifluorescence imaging. For nuclear transfer, one of two methods is used: a) the single donor cell is microinjected directly into the enucleated oocyte, or b) the donor cell is fused into the enucleated oocyte by electric current. For the second method, the single cell is micropipetted into the perivitelline space of the enucleated oocyte. After a recovery of 30-60 min, they are fused with two DC pulses (1.2 kV/cm, 30 μ sec) using a BTX Cell Manipulator 2001 (Genentronics, Inc.) in 0.3 M sorbitol, 0.1 mM Ca^{2+} -acetate, 0.1 mM Mg^{2+} -acetate and 0.5 mg/ml BSA (Sigma-Aldrich).

Rhesus cumulus, granulosa, umbilical endothelial, cultured inner cell mass cells, fibroblasts, and dissociated blastomeres from 4- to 32-cell embryos are used for nuclear transfer. Activation of the fused single cell-oocyte is induced 1-4 h after fusion by microinjection of 120-240 pg/ml rhesus sperm extract prepared in 120 mM KCl, 20 mM HEPES, 100 μ M EGTA, 10 mM sodium glycerolphosphate (Swann, 1990), or by 5 μ M ionomycin (5 min) and 1.9 mM DMAP for 4 h (Susko-Parrish et al., 1994) Nuclear transfer into concomitantly fertilized oocytes is accomplished by performing nuclear

transfer first, then performing IVF or intracytoplasmic sperm injection (ICSI). Fertilization of reconstituted oocytes is performed by fusing the enucleated oocyte with the cytoplasmic fragment removed during the enucleation process, followed by IVF or ICSI 2-3 h later. Surrogate female rhesus monkeys are selected on the basis of serum estradiol and progesterone levels, and following embryo transfer, pregnancies are ascertained by endocrine profiles and fetal ultrasound performed 24-30 d later.

Preparation of Human, Bovine, and *Xenopus* Sperm For Use in Cell-Free Extracts

Human sperm are obtained from fertile donors at in vitro fertilization clinics (University of Wisconsin-Madison or Rush Medical Center, Chicago, IL) or from a sperm bank (Follas Labs, West Lafayette, IN, or Cryobiology, Columbus, OH). Bovine sperm are obtained from American Breeders Service (DeForest, WI). Frozen sperm specimens are thawed and selected for viable sperm by centrifugation through a 2-part 45%, 90% percoll gradient, adjusted to a concentration of 1×10^7 sperm/ml, and sedimented onto coverslips. The sperm are treated with 0.05% lysophosphatidylcholine (lysolecithin; Sigma) in KMT buffer (100 mM KCl, 2 mM $MgCl_2$, 10 mM Tris-HCl, pH 7.0, and 5 mM EGTA), followed by 3% BSA in KMT. For male pronuclear decondensation in vitro (also referred to as “priming”), the methods of Ohsumi et al. (1986) are followed. Sperm are incubated in 5 mM DTT (pH 8.2) followed by 1 mM *N*-ethylmaleimide (pH 8.2) to irreversibly block thiol groups by alkylation. *Xenopus* sperm are prepared according to the methods of Félix et al. (1994).

Preparation of Cell-Free *Xenopus* Egg Extracts

Concentrated CSF-arrested *Xenopus* egg extracts are prepared according to the methods of Stearns and Kirschner (1994). Before experimental use, the extract is fortified with an “energy mix” containing 150 mM creatine phosphate, 20 mM ATP, pH 7.4, 2 mM EGTA, pH 7.7, and 20 mM MgCl₂ (5 μ l/100 μ l extract), plus the addition of 10 μ g/ml each of cytochalasin B and a protease inhibitor cocktail (leupeptin, chymostatin, and pepstatin A; completed extract). In addition, 2 μ g/ml nocodazole (Sigma) is added to the thawed extract before incubation with sperm in all cases except those in which in vitro microtubule aster growth is desired. Immunodepletion of γ -tubulin from CSF-arrested extracts is performed as reported previously by Stearns and Kirschner (1994).

Incubation of Sperm in Egg Extracts

For immunocytochemical experiments, ~1000 sperm/ μ l are added to 10 μ l of complete extract and incubated at 37°C for 40 min. After extensive washing in KMT buffer, sperm are affixed to clean 12-mm-round coverslips, fixed, and then processed for immunocytochemistry. For aster formation in vitro, sperm are treated with 1 μ M ionomycin for 5 min and then washed in KMT buffer. Sperm are permeabilized in 0.05% lysolecithin in KMT buffer for 10 min at ambient temperature before subsequent exposure to 5 mM DTT in KMT buffer (pH 8.2) for 1 h at 37°C. After several washes in KMT buffer, 1 μ l of the treated sperm is added to 8 μ l of completed extract containing 0.08 mg/ml rhodamine-labeled tubulin prepared from bovine brain (a gift from G. Borisy, University of Wisconsin, Madison, or purchased from Cytoskeleton, Inc.). The mixture is

incubated for 60–90 min at 29°C. Nucleation and growth of the sperm asters are analyzed according to the methods of Stearns and Kirschner (1994).

Isolation of Total RNA and Reverse Transcribed (RT)-PCR

Total RNA from rhesus and bovine oocytes, as well as from bovine zygotes, is isolated and prepared using the StrataPrep[®] Total RNA Microprep Kit following the manufacturer's protocol (Stratagene). Reverse transcription and amplification of cDNA are performed on the PTC-200 DNA Engine Cycler from MJ Research, using the ProSTAR[™] HF Single-Tube RT-PCR System (High Fidelity) from Stratagene. Oligonucleotide primers designed for Lis1 RT-PCR yield a 329 bp product: 5'-GTCGTAGCAACAAAGGAATGC-3' and 5'-CGCTTGTTCTTGTAATCCCATAC-3' (primers LIS1(71)1001F and LIS1(71)1329R, respectively; Lo Nigro et al. 1997). For β -actin RT-PCR, primers yield a 225 bp product: 5'-CTGGCATTGTCATGGACTCT-3' and 5'-TCGAAGTCTAGGGCGACATA-3'. Control primers provided by the ProSTAR[™] system are used to amplify control products with a size of 500 bp. This control amplification is recommended by the manufacturer to ensure that the kit reagents are working properly.

The reverse transcription (RT) and PCR steps occur consecutively in the same tube: reverse transcription is performed at 42°C for 15 min and PCR amplification is carried out with an initial denaturation at 95°C for 1 min, followed by 40 cycles of denaturation at 95°C for 30 s, annealing at 55°C for 30 s, and extension at 68°C for 1 min. A final extension of the PCR products occurs at 68°C for 10 min. A negative control reaction is carried out excluding the reverse transcriptase from the reaction mixture. RT-

PCR fragments are electrophoresed on 2.5% (w/v) agarose gels and referenced with the 100 bp ladder by Life Technologies. Visualization and analysis of RT-PCR products are achieved using the Gel Doc 2000™ system from Bio-Rad. Quantitation of RT-PCR is performed using the software included with the Gel Doc Imaging system, comparing levels of the *Lis1* products with the normalized standards of the β -actin products.

DNA Sequencing and Sequence Alignment

PCR products were end-sequenced using the *Lis1* oligonucleotide primers with dye terminators (373 DNA ABI Sequencer; Perkin-Elmer Biosystems). The cDNA sequences for the rhesus and two bovine *Lis1* fragments were submitted to GenBank and given the accession numbers AY260741, AY260742 and AY260743, respectively. Sequence alignments are performed using ClustalW Multiple Sequence Alignment computer program, comparing the bovine and rhesus cDNA sequences to human *LIS1* exons 8, 9 and 10 (GenBank accession numbers U72339, U72340 and U72341, respectively; Lo Nigro et al. 1997). Human *LIS1* coding sequence used in the alignment encompasses bases 534-650 from U72339, bases 295-396 from U72340, and bases 404-513 from U72341. Deduced protein sequence is generated from the bovine and rhesus nucleotide sequences.

SDS-PAGE and Western Blotting

Sperm, oocyte and zygote proteins are separated on 4%-20% linear gradient Tris-HCl polyacrylamide gels (Bio-Rad) for 16 h at 20 V. Equal amounts of protein are loaded into each lane, determined using the Bradford assay. Following electrophoresis, the gels

are soaked in Towbin's transfer buffer (25 mM Tris, 192 mM glycine, 0.037% SDS, 20% methanol) and the proteins are transferred onto polyvinylidene difluoride (PVDF) membranes using a SemiPhor semi-dry blotting apparatus (Hoefer Scientific Instruments) at a current of 0.8 A/cm² for 2 h. The membranes are then blocked with Tris-buffered saline + Tween (25 mM Tris, 137 mM NaCl, 2.7 mM KCl, and 0.2% Tween) supplemented with 3% IgG-free BSA and 5% fetal calf serum (complete blocking solution) for 1 h on a rotating platform. After blocking, the membranes are washed with Tris-buffered saline and incubated for 16 h at 4 C with primary antibodies diluted in complete blocking solution.

Gels are also silver-stained using the Silver Stain Plus system (Bio-Rad) to verify the presence and relative amounts of protein. LIS1 is identified on the Western blots using goat and rabbit polyclonal anti-LIS1 antibodies (Santa Cruz Biotechnology) at a concentration of 1.25 µg/ml. Mouse monoclonal anti-dynactin p150^{Glued} antibody (BD Biosciences) is also used at 1.25 µg/ml.

Following incubation with primary antibodies, the membranes are washed four times (15 min each) with Tris-buffered saline and then incubated for 1 h with 1:5000 dilutions of horseradish peroxidase (HRP)-conjugated secondary antibodies, diluted in complete blocking solution. HRP-conjugated secondary antibodies are obtained from Molecular Probes and Jackson ImmunoResearch.

Membranes are washed again as described above. To induce enzymatic reactions, the membranes are incubated with chemiluminescence reagents (ECL Plus, AP Biotech) for 1 min, covered in plastic wrap, and immediately exposed to autoradiographic HyperFilm (AP Biotech). Protein bands are referenced to Kaleidoscope pre-stained

standards (Bio-Rad), and analyzed by a densitometer. Preimmune serum is used in place of primary antibodies for negative control reactions.

In some cases, Western blots are reprobed with different primary antibodies. Membranes are first stripped of primary and secondary antibodies by incubation in 0.1 M glycine (pH 2.7) for 30 min at room temperature. To ensure that primary antibodies are completely removed, the stripped membranes are incubated with secondary antibodies (as described above) and exposed to chemiluminescence reagents. Films obtained after this control procedure show a complete absence of immunostaining. These membranes are then immunostained with different primary antibodies.

Immunoprecipitation of Proteins

Immunoprecipitation of dynactin subunit p150^{Glued}, with the accompanying co-immunoprecipitation of associated proteins, is performed using Protein A Sepharose 4 Fast Flow medium (AP Biotech). Mature bovine oocytes are either lysed immediately or fertilized in vitro and cultured until 14 h post-insemination, at which time they are lysed and prepared for antibody incubations. The lysis buffer consists of 50 mM Triethanolamine (TEA), 500 mM NaCl, 0.5% Triton X-100, 1 mM DTT, 1 mM PMSF and 1:1,000 dilution of CLAP protease inhibitors (10 mg/ml each of chymostatin, leupeptin, antipain and pepstatin A). Lysates are cleared by centrifugation at 10,000 g for 10 min at 4°C, and protein concentrations are determined using the Bradford assay. Equal amounts of protein from each sample are used for immunoprecipitation.

Lysates are incubated with ~3 µg of either anti-p150^{Glued} dynactin antibody or, as a negative control, pre-immune mouse IgG antibody for 1 h at 4°C. Protein A Sepharose

4 Fast Flow medium is then added to the samples for a 16 h incubation at 4°C. Samples are centrifuged at 10,000 g for 2 min to isolate supernatants from the Protein A Sepharose pellets. Supernatants are concentrated to a volume of 15 μ l by centrifugation at 5000 g for 6 h at 4°C through Centricon spin column filters, which allows the entire sample of proteins that do not immunoprecipitate with p150^{Glued} dynactin (or control IgG) to be loaded into one lane of a polyacrylamide gel as a control for SDS-PAGE. Pellets, which contain the Protein A Sepharose beads bound with the anti-p150^{Glued} antibody, dynactin protein and associated proteins that co-immunoprecipitate, are washed, resuspended in Laemmli buffer, and denatured at 100°C for 3 min. Concentrated supernatants (non-immunoprecipitated), proteins denatured from the Protein A Sepharose beads (immunoprecipitated), the beads alone, and whole egg lysates are carefully loaded onto 4%-20% linear gradient Tris-HCl polyacrylamide gels and processed by SDS-PAGE and Western blotting as described above. The Silver Stain Plus system from Bio-Rad is used to verify the presence of proteins on the gels.

Antibodies For Immunodetection, Microinjection and Transfection

Three monoclonal antibodies raised against dynein intermediate chain are used for immunocytochemistry (ICC), Western blotting and transfection/protein inhibition studies: MAb1618 (1:50 for ICC, 1:500 for Westerns; Chemicon), clone 74.1 (1:200 for ICC; Covance/Babco) and clone 70.1 (1:150 for transfections; Sigma-Aldrich). Anti-dynein heavy chain antibody clone 440.4 (Sigma-Aldrich) is also used for both transfection and immunocytochemistry, at 1:20 dilution. Three monoclonal and two polyclonal antibodies raised against p150^{Glued} dynactin are utilized: MAb150.1 and MAb150B (1:20 each for

ICC and transfections; kind gifts from Trina Schroer), MAb clone 1 (1:20 for ICC, 1:250 for Westerns; BD Biosciences), and polyclonal N-19 and G-18 (1:50, for ICC; Santa Cruz Biotechnology). The p62 subunit of dynactin is labeled with polyclonal antibody N-17 (1:50 for ICC and transfections; Santa Cruz Biotechnology), and the p50 subunit is labeled with MAb clone 25 (1:20 for ICC and transfections; BD Biosciences).

To identify the nuclear pore complex, MAb414 (1:250; Covance/Babco) and anti-nucleoporin p62 antibodies clone RL31 (1:50 for ICC, 1:500 for Westerns; Affinity BioReagents) and polyclonal N-19 (1:50 for ICC and transfections; Santa Cruz Biotechnology) are used for immunocytochemistry, Western blotting and transfection/protein inhibition studies. Anti-vimentin polyclonal antibodies H-84 and C-20 (1:50 each; Santa Cruz Biotechnology) and anti- β -tubulin antibodies clone E7 (1:5 for ICC; Developmental Studies Hybridoma Bank) and polyclonal ATN02 (1:200; Cytoskeleton, Inc.) are also used. LIS1 is identified using both goat and rabbit anti-LIS1 polyclonal antibodies (1:50 for ICC and transfections, 1:500 for Westerns; Santa Cruz Biotechnology).

Golgi protein GM130 is identified using mouse monoclonal antibody clone 35 (1:20 for ICC, 1:250 for Westerns; BD Biosciences). Rabbit polyclonal antibody PS25 (kind gift from Martin Lowe) is an antibody that specifically recognizes GM130 when it is phosphorylated on serine residue 25, and it is used at 1:50 for ICC, 1:500 for Westerns. Anti- β -COP rabbit polyclonal antibody (1:400; Affinity BioReagents) and anti-giantin mouse monoclonal antibody (1:50 for ICC; Calbiochem) are used to identify Golgi components on COP I vesicles. Anti-mannosidase II mouse clone 53FC3 (1:1600; Covance/Babco) is used to recognize the Golgi enzyme found within the *cis*/medial Golgi

apparatus. Calreticulin, a Ca^{2+} -binding resident protein of the endoplasmic reticulum, is identified using a rabbit polyclonal antibody (1:1600; Affinity BioReagents). Sec23, a component of the COP II vesicle coat that is a marker for export sites on the endoplasmic reticulum, is identified using a goat polyclonal antibody (1:50 for ICC; Santa Cruz Biotechnology). NuMA, HSET and Eg5 are detected as described in Mountain et al. (1999).

Microtubules and sperm tails are labeled with monoclonal antibodies raised against acetylated α -tubulin 6-11B-1 (Sigma-Aldrich) and glutamate α -tubulin (a gift of C. Bulinsky, Columbia University, New York, NY), respectively. γ -Tubulin is detected with an affinity-purified rabbit polyclonal antibody raised against the entire sequence of *Xenopus* γ -tubulin (XG-1-4; Stearns et al., 1991; Stearns and Kirschner, 1994). Anti-centrin antibody 20H5, a mouse monoclonal antibody raised against bacterially derived *Chlamydomonas reinhardtii* centrin (Errabolu et al., 1994; Salisbury, 1995), is used to detect the centrosome. Two other anti-centrosomal antibodies are used in these studies: MPM-2, a mouse monoclonal antibody raised against mitotic HeLa cell extracts that detects phosphorylated epitopes, and anti- γ -tubulin antibody XG-1-4.

Control experiments are performed using pre-immune mouse IgG antibodies (Chemicon). Pre-incubation of antibodies for 1 h with either their corresponding antigens or human endothelial cell (HEC) lysates is performed as an additional control for both immunocytochemistry and antibody transfection. HEC lysates are provided by the cell culture core facilities at the ONPRC and PDC. AlexaFluor 488- and 568- conjugated secondary antibodies are obtained from Molecular Probes and used at 1:200 dilutions. Secondary antibodies are also obtained from Jackson ImmunoResearch. To label cortical

granules in some experiments, FITC-conjugated *Lens culinaris* agglutinin (FITC-LCA; Sigma-Aldrich) is added to 10 mM PBS + 0.3% BSA to prepare a 10 μ g/ml solution. Mature, zona pellucida-free oocytes are incubated in the FITC-LCA solution for 30 min, then washed three times in 10 mM PBS + 0.3% BSA and attached to coverslips for fixation and immunocytochemistry (ICC).

For the microinjection and transfection experiments, antibodies are dialyzed overnight using Slide-A-Lyzer cassettes (Pierce) in multiple changes of 10 mM PBS to remove sodium azide from the storage buffer. Microinjection of rhesus oocytes is performed using front-loaded 9- μ m inner diameter micropipettes (Humagen). Approximately 5% of the oocyte volume (~700 pl) is microinjected with antibodies at 2-10 mg/ml. Final antibody concentrations are between 70-350 pg total Ig protein per oocyte.

Transfection of bovine zygotes at 12 h post-insemination is achieved using the Chariot™ reagent following the manufacturer's protocol (Active Motif). Briefly, for each antibody transfection into 20 zygotes, we prepare a 20- μ l volume mix containing a 1:10 dilution of Chariot™ reagent and one of the following concentrated dilutions of antibodies: 1:2 of anti-dynactin (MAb150.1), 1:5 of anti-dynactin p62 (N-17), 1:15 of anti-dynein (clone 70.1), 1:2 of anti-dynein (clone 440.4), 1:25 of MAb414, 1:5 of anti-nucleoporin p62 (N-19), 1:5 of anti-vimentin (H-84), 1:150 of anti-calreticulin (PA3-900), 1:2 of anti-GM130 (clone 35), 1:5 of anti-LIS1 antibodies, and 1:20 of pre-immune IgG. These dilutions are determined empirically by performing antibody titrations on oocytes and zygotes and assessing staining specificity and function-blocking ability. The concentrated mixtures of Chariot™ reagent and antibodies are made in serum-free TALP

medium and incubate at room temperature for 30 min. Following this Chariot™ reagent-antibody binding step, each 20 μ l volume is added to one well of a 96-well plate that contains 20 cumulus cell-free, zona pellucida-free zygotes in 80 μ l of serum-free TALP medium. The samples are incubated at 39°C for 1 h, after which an additional 100 μ l of serum-containing TALP medium is added to each well; samples are cultured for an additional 7-11 h, and then fixed for immunocytochemistry at 20-24 h post-insemination.

Immunocytochemistry, Conventional Microscopy and Confocal Microscopy

For immunocytochemistry (ICC), the methods used here are described in Navara et al. (1994) and Payne and Schatten (2003). The attached cumulus cells and zona pellucidae of oocytes, zygotes and embryos are removed with short incubations in TALP-Hepes medium containing 1 mg/ml hyaluronidase and 2 mg/ml pronase, respectively. Gametes and embryos are then gently attached to poly-L-lysine coated coverslips (2 mg/ml solution for coating) in Ca^{2+} -free, BSA-free culture medium, fixed for 40 min in 2% formaldehyde, and permeabilized in 10 mM PBS + 0.1% Triton X-100 for an additional 40 min. Alternatively, samples are fixed in absolute methanol using the methods of Simerly and Schatten (1993). After fixation and permeabilization/protein extraction, the samples are blocked for 1 h in 10 mM PBS + 0.3% BSA + 1% fetal calf serum (ICC blocking solution) prior to incubation with primary and secondary antibodies.

The primary antibody is applied for up to 16 h in a humidified chamber at room temperature, and the samples are then rinsed with four changes of 10 mM PBS at 10 min for each wash. To detect the primary antibodies, fluorochrome-conjugated secondary antibodies are applied for 1 h in a humidified chamber at room temperature in the dark.

Following incubation with secondary antibodies, samples are once again rinsed 4 x 10 min with 10 mM PBS. DNA is labeled using one of three dyes: DAPI (Vector Laboratories) at 1 $\mu\text{g/ml}$, Hoechst 33342 (Sigma-Aldrich) at 5 $\mu\text{g/ml}$ or TOTO-3 (Molecular Probes) at 10 $\mu\text{g/ml}$. If TOTO-3 is used to detect DNA, then 200 $\mu\text{g/ml}$ RNase is added to the secondary antibody incubation to reduce the background labeling of RNA. Coverslips are mounted in an anti-fade medium (Vectashield H-1000, Vector Laboratories) to retard photobleaching.

Fixed oocytes, zygotes and embryos are imaged with a Leica TCS SP2 spectral confocal microscope, using laser lines at 488 nm, 568 nm and 633 nm wavelengths. Differential Interference Contrast optics are also used for imaging on both the Leica confocal, as well as on a Nikon E1000 epifluorescence microscope equipped with CCD camera (Hamamatsu) and controlled by MetaMorph software (Universal Imaging). Live oocytes, zygotes and embryos are visualized in 50 μl drops of TALP-Hepes under mineral oil in 35-mm or 60-mm diameter plastic petri dishes using a Nikon TE300 inverted microscope equipped with Hoffman Modulation Contrast optics. Live sperm and extract-treated sperm are imaged between coverglass and microslides, and are analyzed on the Nikon E1000. For the extract-treated sperm experiments, counts of at least three microscopic fields with a minimum number of 100 spermatozoa are recorded.

Immunogold Electron Microscopy

Immunogold electron microscopy is performed using a modification of the method described previously by Sutovsky et al. (1993). Briefly, sperm are pelleted by centrifugation at 700 g and fixed for 2 h at 4°C in 3% glutaraldehyde in 0.05 M

piperazine-*N,N* 9-bis[2-ethanesulfonic acid] buffer (pH 7.3) containing 2 mM CaCl₂ and 0.5 mM MgCl₂. After washing in piperazine-*N,N* 9-bis[2-ethanesulfonic acid] buffer, the sperm pellet is embedded in hot 1% agar and the fixed sperm are dehydrated in an ice-cold graded ethanol series up to 90%, then embedded in LR White resin (Electron Microscopy Sciences) at 220°C. Polymerization is performed by the addition of 1 ml/ml LR White accelerator (Electron Microscopy Sciences). Ultra-thin sections are cut using a Sorvall MT2B ultramicrotome and collected on formvarcoated 100-mesh nickel grids.

Colloidal gold labeling is performed by sequential incubation in 5% normal goat serum (Sigma) in PBS with: 0.1% BSA (Sigma) for 1 h, 20H5 anti-centrin (1:50) in PBS with 0.1% BSA and 1% normal goat serum for 90 min, and 5-nm colloidal gold-conjugated anti-mouse immunoglobulin G plus immunoglobulin M for 1 h (British BioCell International, Cardiff, UK; purchased from Ted Pella, Redding, CA). Grids are stained with uranyl acetate for 10 min and examined with a Phillips CM 120 transmission electron microscope (Phillips, Eindhoven, Netherlands). Negatives are scanned with an Eastman Kodak image scanner, recorded onto computer disk, and processed using Adobe Photoshop software. Negative controls are performed by the omission of 20H5 from the labeling protocol.

Chapter 3

Preferentially Localized Dynein and Perinuclear Dynactin Associate With Nuclear Pore Complex Proteins to Mediate Genomic Union During Mammalian Fertilization

Christopher Payne^{1,2}, Vanesa Rawe², João Ramalho-Santos^{2,3}, Calvin Simerly² and Gerald Schatten²

¹ Program in Molecular and Cellular Biosciences, Department of Cell and Developmental Biology, Oregon Health and Science University, Portland, Oregon 97201

² Pittsburgh Development Center, Magee-Womens Research Institute, Departments of Obstetrics, Gynecology and Reproductive Sciences, and Cell Biology and Physiology, University of Pittsburgh School of Medicine, Pittsburgh, Pennsylvania 15213

³ Center for Neuroscience and Cell Biology, Department of Zoology, University of Coimbra, 3004-517 Coimbra, Portugal

Accepted for publication in the *Journal of Cell Science* (2003). In press.

Summary

Fertilization, complete once the parental genomes unite, requires the migration of the egg nucleus to the sperm nucleus (female and male pronuclei, respectively) on microtubules within the inseminated egg. Neither the molecular mechanism of pronuclei binding to microtubules nor the role of motor proteins in regulating pronuclear motility have been fully characterized, and the failure of zygotic development in some patients suggests their contribution to human infertility. Based on the minus-end direction of female pronuclear migration, we propose a role for cytoplasmic dynein and dynactin in associating with the pronuclear envelope and mediating genomic union. Our results show that dynein intermediate and heavy chains preferentially concentrate around the female pronucleus, while dynactin subunits p150^{Glued}, p50 and p62 localize to the surfaces of both pronuclei. Transfection of antibodies against dynein and dynactin block female pronuclear migration in zygotes. Both parthenogenetic activation in oocytes and microtubule depolymerization in zygotes significantly reduce the localization of dynein to the female pronucleus, but do not inhibit the pronuclear association of dynactin. When immunoprecipitated from zygotes, p150^{Glued} associates with nuclear pore complex proteins, as well as the intermediate filament vimentin and dynein. Antibodies against nucleoporins and vimentin inhibit pronuclear apposition when transfected into zygotes. We conclude that preferentially localized dynein and perinuclear dynactin associate with the nuclear pore complex and vimentin and are required to mediate genomic union. These data suggest a model in which dynein accumulates and binds to the female pronucleus on sperm aster microtubules, where it interacts with dynactin, nucleoporins and vimentin.

Introduction

The molecular motor cytoplasmic dynein, together with its cofactor dynactin, transports cargo organelles towards the minus ends of microtubules (Karki and Holzbaur, 1999). Both are large multi-subunit complexes that coordinate many events throughout the cell cycle, including interphase trafficking of vesicles from the endoplasmic reticulum (ER) to the Golgi (Presley et al., 1997), mitotic spindle assembly (Vaisberg et al., 1993), and prophase nuclear envelope breakdown (Salina et al., 2002; Beaudouin et al., 2002). Association of dynein and dynactin with the nuclear envelope has been observed in somatic cells (Salina et al., 2002; Busson et al., 1998) and localization of dynein heavy chain to pronuclei has been detected in *C. elegans* zygotes (Gönczy et al., 1999), but specific nuclear envelope binding partners have not yet been identified.

Pronuclear migration and apposition, the events concluding the fertilization process, are hypothesized to involve dynein and dynactin based upon the directionality of female pronuclear movement and the dynamics of its motion along sperm aster microtubules (Schatten, 1994; Rouvière et al., 1994; Reinsch and Karsenti, 1997; Reinsch and Gönczy, 1998). The sperm aster, a radial array of microtubules nucleated by the sperm centrosome, is essential to unite the female with the male pronucleus in most mammalian zygotes (Navara et al., 1994). Interestingly, rodents do not utilize a sperm aster during fertilization, precluding their use for investigating sperm aster-mediated motility in mammals (Schatten, 1994). Bovine and non-human primate zygotes, on the contrary, both rely upon sperm asters to mediate genomic union and serve as ideal models for studying the dynamics of human fertilization (Navara et al., 1994; Hewitson

et al., 2000b). Synthetic nuclei assembled in *Xenopus* egg extracts have been shown to require dynein to move along centrosome-anchored microtubules towards their minus ends in vitro (Reinsch and Karsenti, 1997), but a role for dynein and dynactin in mediating pronuclear movement has not yet been demonstrated in vivo.

Embedded within the envelopes of somatic nuclei and zygotic pronuclei, nuclear pore complexes (NPCs) are macromolecular assemblies involved in nucleocytoplasmic transport, cell cycle progression and gene expression (Allen et al., 2000; Takizawa and Morgan, 2000; Cronshaw et al., 2002). Recent characterization of mammalian NPCs using mass spectrometry identifies approximately 30 core nucleoporins and additional NPC-associated proteins (Cronshaw et al., 2002). One of these NPC-associated proteins, vimentin, not only corresponds with the 10 nm filaments attached to the ring structure at the nuclear pore cytoplasmic face (Fujitani et al., 1989), but also associates with microtubules, dynein and dynactin (Helfand et al., 2002). Given this evidence of interaction among microtubules, motor proteins, intermediate filaments and NPCs, we questioned whether dynein and dynactin associate with pronuclear NPCs and vimentin during mammalian fertilization. Our results identify a novel physical interaction between motor proteins and NPCs, and suggest that dynein and dynactin bind to nucleoporins and vimentin at the cytoplasmic surface of the female pronuclear envelope to mediate pronuclear migration along sperm aster microtubules.

Results

Dynein concentrates exclusively around the migrating female pronucleus

Following insemination in bovine and rhesus oocytes, the distinct sperm and egg genomic material becomes enclosed within separate pronuclear envelopes. The sperm-derived male pronucleus and egg-derived female pronucleus occupy predominantly central and cortical locations, respectively, within the majority of zygotes examined (91%; 2486/2724). Male pronuclei can be discerned by identifying attached sperm tails (data not shown). The female then migrates through the egg cytoplasm to join the male pronucleus in the center. During female pronuclear migration, microtubules extend from a region adjacent to the male pronucleus and contact the surface of the female pronucleus (Figure 3.1A, left panel). Subsequent movement of the female to the male pronucleus results in pronuclear apposition (Figure 3.1A, right panel). Previous studies have shown that when microtubules are either depolymerized with nocodazole or stabilized with taxol, female pronuclear migration to the male is inhibited (Schatten, 1982).

The organization of microtubules and orientation of female pronuclear motility suggest that the minus-end directed motor cytoplasmic dynein might facilitate this pronuclear migration. We therefore first examined where dynein localizes in the zygote, and whether it might be able to transport the female towards the male pronucleus. During both pronuclear migration and apposition, dynein intermediate chain concentrates exclusively around the female pronucleus (Figure 3.1B, left and middle panels). Weak, diffuse staining is also detected throughout the cytoplasm. When pre-absorbed with its antigen, the anti-dynein antibody no longer shows staining within the zygotes (Figure 3.1B, right panel). Dynein heavy chain shows a similar distribution as the intermediate chain, localized around the female but not the male pronucleus (data not shown). The

presence of dynein at the surface of the female pronucleus, and absence from the male, suggests that it may have a specific temporal and spatial function to mediate female pronuclear migration.

Dynactin concentrates around both female and male pronuclei

In order for dynein to transport cargo on microtubules, the cofactor dynactin is required. Consisting of at least eight distinct subunits, the dynactin complex contains domains that bind directly to dynein, microtubules, and cargo proteins (Schafer et al., 1994; Waterman-Storer et al., 1995; Vaughan and Vallee, 1995; Karki and Holzbaur, 1995; Echeverri et al., 1996; Burkhardt et al., 1997). We therefore examined the distribution of three different dynactin subunits in bovine zygotes to determine whether they also concentrate around the female pronucleus. The p150^{Glued} subunit, which binds to dynein intermediate chain, concentrates around not only the female pronucleus but also the male pronucleus (Figure 3.2A, far left panel). Dynactin subunit p50, which maintains the structure of the complex with respect to microtubule organization, also concentrates around both pronuclei during migration and apposition (Figure 3.2A, center left panel). The p62 subunit, which resides in the domain that binds to cargo, localizes around the pronuclei in a pattern similar to the other two subunits (Figure 3.2A, center right panel). When pre-incubated with human endothelial cell lysates, the primary antibodies against all three dynactin subunits are no longer detected by secondary antibodies in the zygotes; anti-p150^{Glued} is shown as an example (Figure 3.2A, far right panel). This association of dynactin around both female and male pronuclei is distinct from that of dynein, examined further by double-labeling zygotes with both anti-dynein and anti-dynactin antibodies

(Figure 3.2B, top panel). Zygotes stained with antibodies against calreticulin, which distributes throughout the cytoplasm, reveal that not all proteins concentrate around the pronuclei during their migration (Figure 3.2B, bottom panel). The enriched distribution and differential staining of dynein and dynactin at pronuclear surfaces may indicate specific functions performed during fertilization.

Dynein and dynactin are required for female pronuclear migration

To determine whether dynein and dynactin are necessary for pronuclear migration and apposition, we transfected antibodies against dynein intermediate and heavy chains, as well as dynactin subunits p150^{Glued} and p62, into pronucleate-stage bovine zygotes using ChariotTM reagent (Morris et al., 2001). Transfection of antibodies occurred after pronuclear formation but before pronuclear apposition, optimizing the temporal and spatial effects of the antibodies. Zygotes were allowed to develop until just prior to mitosis, when they were fixed and the distances between the male and female pronuclei scored for inhibition of pronuclear union. Measured from edge-to-edge, inter-pronuclear distances $\geq 10 \mu\text{m}$, the average diameter of a pronucleus, indicate disrupted pronuclear migration.

The majority of zygotes transfected with antibodies against dynein intermediate and heavy chains show pronuclei $\geq 10 \mu\text{m}$ apart (94% and 93% respectively), while all zygotes transfected with pre-immune mouse IgG antibodies and ChariotTM reagent alone have inter-pronuclear distances $< 10 \mu\text{m}$ (Figure 3.3A,B). Antibodies against dynactin subunits p150^{Glued} and p62 also block pronuclear union, with the majority of pronuclei at distances $\geq 10 \mu\text{m}$ from one another (98% and 74% respectively). Pre-absorption of anti-

dynein and anti-dynactin antibodies with either their corresponding antigens or human endothelial cell lysates prior to transfection results in all pronuclei to be $< 10 \mu\text{m}$ apart (Figure 3.3B).

Zygotes transfected with antibodies against dynein and dynactin display a modest alteration in staining when compared to control zygotes examined at earlier stages: dynein 70.1 is enriched at the surface of the female pronucleus proximal, but not distal, to the sperm aster, and dynactin p150^{Glued} distribution around both pronuclear surfaces, as well as along microtubules, exhibits decreased concentration (Figure 3.3A). These alterations can be attributed to the effects of the different antibodies on the ability of dynein and dynactin to bind to membranes and microtubules. Despite the failure of pronuclear apposition in the zygotes transfected with anti-dynein and anti-dynactin antibodies, the sperm aster microtubules appear unperturbed between the male and female pronuclei (Figure 3.3A). Thus, while both dynein and dynactin are required for female pronuclear motility, disruption of these proteins with antibodies does not reorganize the sperm aster. The stabilizing presence of the centrosome likely precludes such alteration.

The sperm aster is necessary for dynein localization to the female pronucleus

We next examined the role of the sperm aster in distributing dynein and dynactin to the female pronuclear surface by parthenogenetically activating oocytes. Parthenogenesis generates polymerized microtubules throughout the ooplasm, but the absence of a sperm centrosome prevents aster formation. In all of the parthenogenotes observed (131 total; $n=3$), dynactin concentrates around the female pronucleus while

dynein redistributes towards the cortex, strikingly absent from the female pronuclear surface (Figure 3.4). Microtubules are also enriched at the cortex, unfocused in their orientation. These results suggest that dynein association with the female pronucleus requires a sperm aster, and that polymerized microtubules alone are not sufficient.

Microtubules are necessary for dynein retention at the female pronucleus but are not required for dynactin concentration around both pronuclei

Because the localization of dynein, but not dynactin, to the female pronucleus depends upon the formation of a sperm aster, we then questioned whether microtubules are necessary to retain dynein and dynactin at the female pronuclear surface once they are there. Nocodazole was administered to pronucleate-stage zygotes to depolymerize microtubules; exposure occurred after the female pronucleus is contacted by the sperm aster but before its apposition with the male pronucleus. In nocodazole-treated zygotes, the association of dynein with the female pronucleus is only $7\% \pm 2.7\%$, compared to $82\% \pm 5.6\%$ in controls ($p < 0.001$; $n=4$; Figure 3.5A,B). In contrast, nocodazole does not cause significant redistribution of dynactin from male and female pronuclear surfaces (i.e. $80\% \pm 4.3\%$ in controls vs. $62\% \pm 8.3\%$ in nocodazole-treated zygotes; Figure 3.5A,B), even though the microtubules are clearly disassembled.

Microtubules distribute near the surface of the male pronucleus in controls in the absence of dynein, suggesting that microtubule localization to male pronuclear surfaces is dynein-independent. The loss of dynein from the female pronuclear surface after nocodazole supports the hypothesis of a microtubule-dependent distribution of dynein to the female pronucleus. The retention of dynactin at the surfaces of both pronuclei in the

absence of microtubules raises the possibility that dynactin associates with structural components found near, at or within pronuclear membranes.

Nuclear pore complex proteins associate with dynactin and dynein and are required for pronuclear apposition

Because dynactin concentration around both pronuclei is retained after microtubules are depolymerized, we examined whether a physical interaction exists between dynactin and pronuclear envelope proteins. Embedded within the pronuclear envelope, nuclear pore complexes (NPCs) discriminate pronuclear membranes from ER and Golgi membranes and are attractive candidates for an association with dynein, dynactin and microtubules (Salina et al., 2002; Lénárt and Ellenberg, 2003). The p150^{Glued} subunit of dynactin was immunoprecipitated from pronucleate-stage zygotes and unfertilized oocytes, and an antibody with wide specificity against nucleoporins was used to probe the dynactin immunoprecipitate (IP). We chose the pan-nucleoporin antibody MAb414 to detect the NPCs, since it has been shown to recognize nucleoporins with molecular mass 270 kDa, 175 kDa and 62 kDa (Davis and Blobel, 1987), and depending on the cell type being used for SDS-PAGE and Western blotting, can detect up to an additional 3-4 nucleoporins of varying molecular mass (Aris and Blobel, 1989; Cronshaw et al., 2002).

Comparing the pellets and supernatants of the dynactin IP, along with protein A Sepharose beads alone and whole cell lysates from both zygotes and unfertilized oocytes, we detect five bands corresponding to nucleoporins with molecular mass 270 kDa, 175 kDa, 62 kDa, 35 kDa and 18 kDa in the IP pellets isolated from zygotes (Figure 3.6A).

These nucleoporins are also detected in the whole zygote lysates, but not in the IP supernatants or beads alone. This observation contrasts with the samples isolated from oocytes, in which the nucleoporins are identified in the IP supernatants as well as the whole oocyte lysates, but not in the IP pellets or beads alone (Figure 3.6A). Thus, nucleoporins co-immunoprecipitate with dynactin in pronucleate-stage zygotes, but not in unfertilized oocytes.

Vimentin is also detected in the IP pellets isolated from zygotes, and is identified with molecular mass 58 kDa (Figure 3.6B). Found at low abundance in the IP supernatants, vimentin is absent from the beads-alone samples. In the oocyte-derived samples, vimentin is detected in the IP supernatants and the whole cell lysates, but not in the IP pellets or beads alone (Figure 3.6B). The low level of vimentin detected in the zygote IP supernatants suggests that not all of the vimentin protein associates with dynactin during pronuclear migration. We conclude that like nucleoporins, however, vimentin co-immunoprecipitates with dynactin specifically under zygotic conditions. When the Western blots are then probed for dynein intermediate chain and dynactin p150^{Glued}, both proteins are detected in the IP pellets and whole cell lysates of both zygotes and oocytes, and are identified with molecular mass 74 kDa and 150 kDa, respectively (Figure 3.6C).

The distribution of nucleoporins and vimentin during pronuclear migration and apposition was then characterized by confocal microscopy. Nucleoporin p62, recognized in the dynactin immunoprecipitate by MAb414, localizes predominantly to the surfaces of the male and female pronuclei, with additional punctate cytoplasmic foci (Figure 3.6D). Co-distribution of this NPC protein with dynactin p150^{Glued} is observed when the

images are merged. Vimentin, meanwhile, displays a branched staining pattern between the two pronuclei, concentrating around their surfaces and extending throughout the cytoplasm (Figure 3.6E). Co-localization of vimentin and dynactin p150^{Glued} at pronuclear surfaces is detected when the images are merged, with additional distinct patterns of vimentin observed between pronuclei.

The association of nucleoporins and vimentin with both dynactin and dynein suggests that they might also be required for female pronuclear migration. To determine whether nucleoporins and vimentin are necessary for pronuclear apposition, we transfected antibodies against them into pronucleate-stage zygotes once again using the ChariotTM reagent. Inter-pronuclear distances were scored as before to determine the level of inhibition of pronuclear union. When transfected with MAb414 and anti-nucleoporin p62 antibodies, the majority of zygotes show pronuclei $\geq 10 \mu\text{m}$ apart (83% and 91% respectively), while all zygotes transfected with pre-immune mouse IgG antibodies have inter-pronuclear distances $< 10 \mu\text{m}$ (Figure 3.7A,B). Antibodies against vimentin also block pronuclear union, with the majority of pronuclei at distances $\geq 10 \mu\text{m}$ from one another (98%; Figure 3.7A,B). Pre-absorption of anti-nucleoporin and anti-vimentin antibodies with their corresponding antigens prior to transfection results in all pronuclei to be $< 10 \mu\text{m}$ apart (Figure 3.7B).

Nucleoporins show normal distribution around pronuclei in both control IgG-transfected and anti-nucleoporin-transfected zygotes, despite the arrest in female pronuclear migration seen in the latter group (Figure 3.7A). Vimentin, meanwhile, branches around and between the two pronuclei in zygotes transfected with anti-vimentin antibodies. Dynactin p150^{Glued} shows normal localization to pronuclei in control IgG-

transfected and anti-nucleoporin-transfected zygotes, while its distribution around pronuclear surfaces appears reduced following transfection with anti-vimentin antibodies (Figure 3.7A). This reduction could be due to an alteration in binding between vimentin and dynactin in the presence of the antibodies, or a masking effect revealed during the immunocytochemistry. Dynein distributes around female pronuclei in transfected zygotes, with decreased concentration at pronuclear surfaces following transfection with anti-vimentin antibodies (data not shown). Antibodies against the ER resident protein calreticulin and the Golgi apparatus protein GM130 do not inhibit pronuclear union, as all zygotes transfected with these antibodies have inter-pronuclear distances $< 10 \mu\text{m}$ (Figure 3.7B). Thus, specifically, nuclear pore complex proteins and vimentin appear to be necessary for pronuclear migration and apposition.

Discussion

We have shown that mammalian fertilization requires both dynein and dynactin to mediate genomic union, and that dynein concentrates exclusively around the female pronucleus. Dynactin, in contrast, localizes around both pronuclei and associates with nucleoporins and vimentin, in addition to dynein. The finding that a sperm aster is required for dynein to localize at the female pronucleus, and that microtubules are necessary to retain dynein, but not dynactin, at its surface, suggests that nucleoporins, vimentin and dynactin may associate upon pronuclear formation, and that subsequent

sperm aster contact with the female pronuclear surface allows dynein to interact with these proteins.

Dynein and dynactin exhibit distinct spatial and temporal pronuclear associations during fertilization

The dependence of dynein on the sperm aster to localize at the female pronuclear surface is consistent with earlier observations that female pronuclear movement does not begin until sperm aster contact has been established (Schatten, 1982; Navara et al., 1994). We conclude from the parthenogenetic activation experiments that the preferential distribution of dynein around the female pronucleus is due to sperm aster-mediated delivery of dynein to the female pronuclear surface on the plus ends of microtubules. Recent studies in budding yeast provide evidence in support of this mechanism for dynein transport to its target membrane, showing that dynein is delivered to the cell cortex on the plus ends of polymerizing astral microtubules (Sheeman et al., 2003). Such accumulation of dynein at microtubule plus ends would be expected to occur in the absence of dynactin, and indeed, Sheeman and colleagues saw this when they examined dynactin mutants. Given the differential distribution of dynein and dynactin observed during mammalian fertilization and parthenogenesis, and the necessity of a sperm aster for proper dynein concentration, this mechanism could explain how dynein localizes to the female pronuclear surface independent of dynactin.

The preferential localization of dynein likely depends upon the spatiotemporal control of the cell cycle. Fertilized eggs enter S-phase after the formation of the sperm aster and during the migration of the pronuclei, as detected with 5-bromo-2'-

deoxyuridine-5'-monophosphate (BrdU) (Nomura et al., 1991; Eid et al., 1994). Recent evidence has shown that centrosome-anchored microtubule arrays in fibroblasts do not accumulate dynein at their minus ends until after entering S-phase (Quintyne and Schroer, 2002). Because maintenance of the sperm aster is also likely to be dynein-independent until after S-phase entry, proximity of the centrosome to the male pronucleus might preclude dynein from both associating with the male pronuclear surface and accumulating at the centrosome until after pronuclear migration commences.

Dynactin concentration around zygotic pronuclei, meanwhile, resembles its localization to prophase nuclear envelopes in somatic cells, where it is thought to facilitate nuclear envelope breakdown (Salina et al., 2002; Beaudouin et al., 2002). Neither dynein nor dynactin, to our knowledge, has previously been reported to associate with interphase nuclear envelopes. Because migrating pronuclei are in S-phase, dynactin concentration around pronuclear envelopes is likely to persist throughout zygotic interphase, revealing a unique functional association during fertilization.

Dynactin interacts with pronuclear envelopes independent of the sperm aster

Retention of dynactin around both pronuclei in the presence of nocodazole demonstrates a microtubule-independent, dynein-independent association of dynactin with pronuclear membranes. While not required to retain dynactin at pronuclei once they have formed, microtubules are necessary for recruiting membrane material around paternal and maternal chromatin, bringing nuclear pore complexes to these membranes for insertion, and allowing pronuclei to form properly as shown through the use of *Xenopus* egg extracts (Sutovsky et al., 1998; Ewald et al., 2001). Microtubules involved

in these roles do not require the formation of a sperm aster, however, as female pronuclear membranes complete their formation around the maternal chromatin in parthenogenetically-activated oocytes, as well as in zygotes prior to contact by the sperm aster (C. Payne, unpublished observations). In phyla where oocytes complete meiosis prior to fertilization, as in many echinoderms, a female pronucleus is fully formed before sperm entry, demonstrating its independence from the sperm aster (Gilbert, 1997).

Nuclear pore complexes and vimentin act with dynein and dynactin to mediate pronuclear apposition

Immunoprecipitation of dynactin p150^{Glued} from pronucleate-stage zygotes identifies a physical interaction between dynactin and nucleoporins of molecular mass 270 kDa, 175 kDa, 62 kDa, 35 kDa and 18 kDa, as well as vimentin and dynein. The nucleoporins appear enriched in the zygote immunoprecipitate when compared to whole zygote lysates, showing a slight increase in intensity as analyzed by Western blotting. Similar enrichment may also be seen for vimentin, dynein and dynactin. Localization of the different immunoprecipitate components to pronuclear surfaces, including the co-distribution of dynactin with nucleoporin p62 and vimentin, reinforces the association of dynactin with nuclear pore complexes and intermediate filaments. Given that nucleoporin p62 resides within the center of the nuclear pore, which has an estimated maximum channel diameter of 40 nm (Ryan and Wentz, 2000; Panté and Kann, 2002), the interaction between nucleoporins and dynactin is most likely indirect. Recent evidence of a direct interaction between the dynein-dynactin complex and vimentin at the ultrastructural level (Helfand et al., 2002), combined with observations demonstrating an

association between intermediate filaments and nuclear pores (Jones et al., 1982; Fujitani et al., 1989), supports the hypothesis that dynactin may interact with nucleoporins through vimentin.

Transfection of antibodies into pronucleate-stage zygotes has allowed us to determine that dynein, dynactin, nucleoporins and vimentin are specifically required during pronuclear migration and apposition. Inhibition of both the intermediate and heavy chains of dynein, as well as the p150^{Glued} and p62 subunits of dynactin dramatically blocks genomic union. Perturbation of the motor complex, however, does not significantly alter the microtubule network between the pronuclei. Blocking nucleoporins and vimentin also inhibits pronuclear apposition, with a slight decrease in dynein and dynactin concentration at pronuclear surfaces. Mammalian fertilization could thus provide distinct roles for dynein and dynactin in the zygote: dynein, together with dynactin, trafficking the female pronucleus towards the centrosome attached to the male pronucleus, and dynactin, together with vimentin, associating with nuclear pore complex proteins to provide attachment sites for dynein and sperm aster microtubules at the female pronucleus.

Model for pronuclear assembly, motility and union

We propose a model for pronuclear formation, migration and apposition in which dynactin, nucleoporins and vimentin interact together with microtubules and dynein to mediate genomic union (Figure 3.8). Nuclear pore complex assembly and insertion into the envelopes of newly forming pronuclei bring dynactin and vimentin filaments to the cytoplasmic face of nuclear pores, where they interact as a macromolecular complex.

This formation likely depends upon sperm aster-independent microtubules, appearing within the ooplasm after egg activation and contacting the surfaces of the pronuclei during their assembly. The sperm aster, meanwhile, concomitantly develops as a focused set of microtubules radiating out from the centrosome, now serving as the dominant microtubule-organizing center in the zygote. Enlargement of the sperm aster extends the microtubule plus ends away from the male pronucleus, some of which then reach the female pronuclear envelope. Growth of the sperm aster towards the cortex could deliver dynein to the surface of the female pronucleus on these microtubule plus ends, allowing it to bind to dynactin and vimentin at nuclear pores and activate its motor activity. The dynein-dynactin complex would then be able to transport the female pronucleus to the sperm aster minus ends, culminating in pronuclear apposition.

Understanding these protein interactions may shed light on certain cases of clinical idiopathic infertility in which inseminated eggs arrest in development after the pronuclei fail to unite (Simerly et al., 1995). It has been observed that in approximately 6% of human fertilization failures, characterized in embryos discarded from infertility clinics, the sperm aster shows abnormal morphology within the zygote (Asch et al., 1995). Both incomplete assembly and disarrayed organization of sperm aster microtubules would compromise the association of dynein with the female pronucleus. Should microtubules fail to bind to the female pronucleus, preventing dynein from localizing to its surface, genomic union would be unsuccessful.

From these studies, we conclude that dynactin associates with nucleoporins and vimentin at the surfaces of both pronuclei upon their formation and throughout the fertilization cell cycle. Dynein, in contrast, depends upon sperm aster microtubules to

associate with dynactin, nucleoporins and vimentin exclusively at the female pronucleus to facilitate motility. The interaction between dynactin and nuclear envelope proteins common to both pronuclei, together with the spatial distribution of dynein to these proteins at the female pronucleus, may ensure successful genomic union that completes mammalian fertilization.

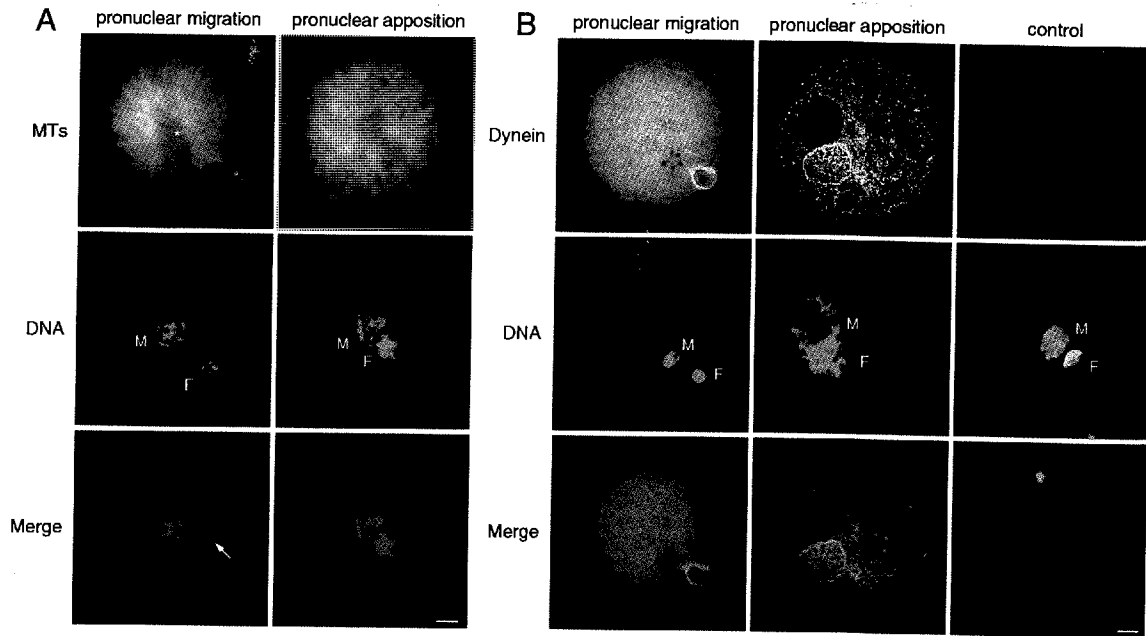


Figure 3.1. Sperm aster microtubules and dynein distribute to the female pronucleus. (A) Fluorescent micrographs of microtubules (MTs) and DNA in bovine zygotes during pronuclear migration and apposition. The male pronucleus (M) occupies a central position throughout these processes, while the female pronucleus (F) initially occupies a cortical position (left panel) and then migrates to the center to meet the male pronucleus (right panel). During pronuclear migration, sperm aster microtubules radiate out from a region next to the male pronucleus (asterisk) and extend to the surface of the female pronucleus. The arrow indicates the direction of female pronuclear movement. (B) During pronuclear migration and apposition, dynein intermediate chain concentrates around the female pronucleus (left and center panels). Dynein also distributes as dim cytoplasmic foci, but is absent from the surface of the male pronucleus. Pre-absorption of anti-dynein antibodies with their antigens results in a loss of detection in zygotes (right panel). Dynein localization is observed in both rhesus monkey zygotes (left panel) and bovine zygotes (center panel). Bars, 10 μ m.

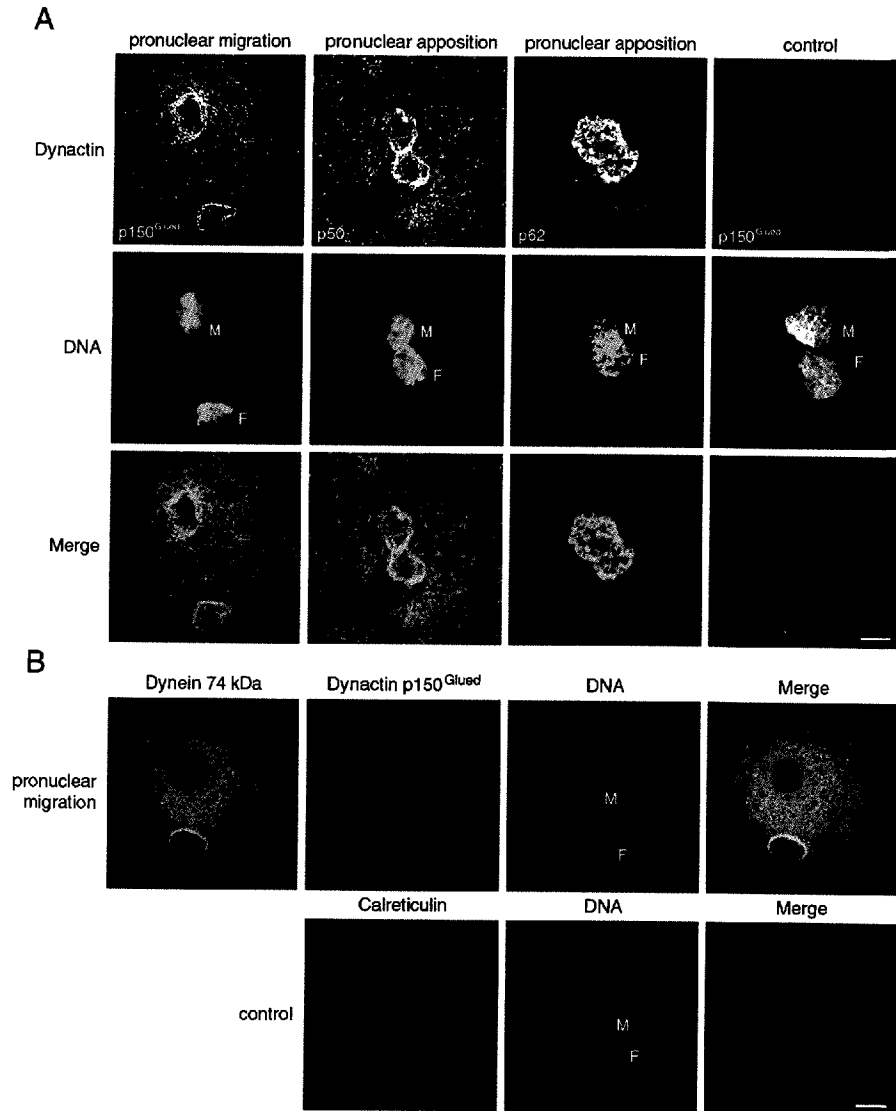
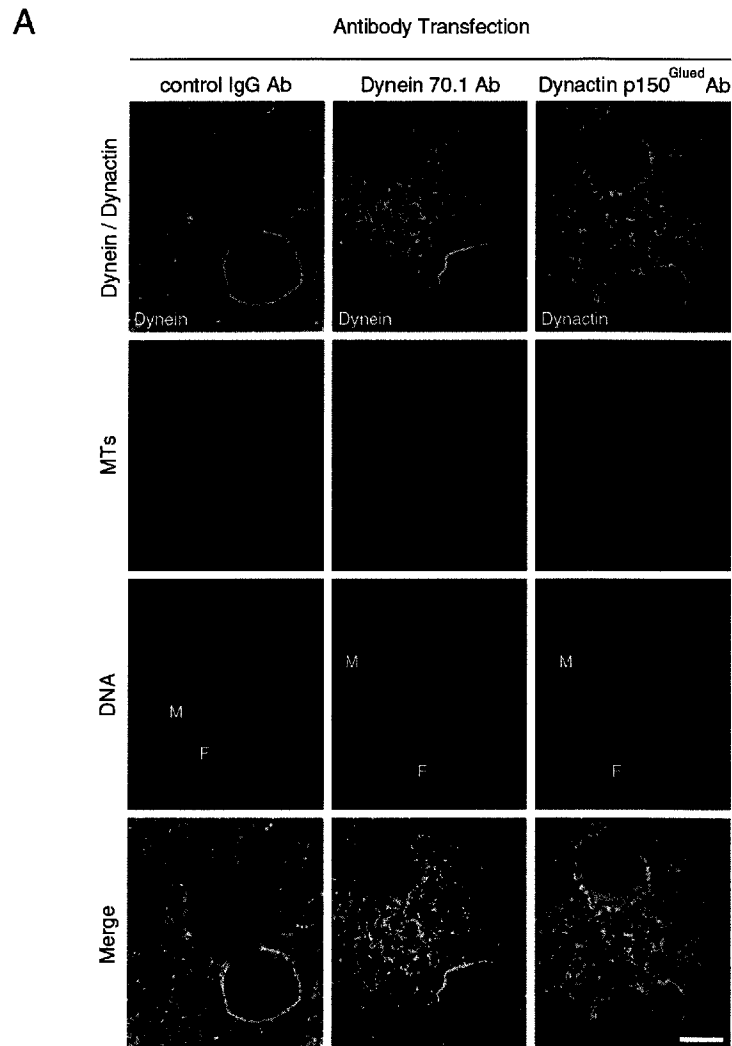


Figure 3.2. Dynactin subunits localize around both female and male pronuclei, while dynein distributes only to the female. (A) Dynactin subunits p150^{Glued}, p50 and p62 distribute around both female (F) and male (M) pronuclei during pronuclear migration and apposition in bovine zygotes. Additional diffuse staining is detected in the cytoplasm for both p150^{Glued} (far left panel) and p50 (center left panel). Pre-incubation of anti-dynactin p150^{Glued} antibodies with human endothelial cell lysates results in a loss of detection in zygotes (far right panel). (B) Double-staining of dynein 74 kDa (green) and dynactin p150^{Glued} (red) shows co-localization around the female, but not the male, pronucleus (Merge; top panel). Staining of calreticulin (red) shows distribution throughout the cytoplasm, but no localization to pronuclear surfaces (Merge; bottom panel). Bars, 10 μ m



B

Transfection of zygotes 12 HPI: Chariot™ reagent + 1° Ab	Fixation of zygotes 24 HPI: Distance between pronuclei	
1° Ab	≥ 10 μm apart	< 10 μm apart
Chariot™ reagent alone	0% (0/129)	100% (129/129)
pre-immune mouse IgG	0% (0/108)	100% (108/108)
Dynein Intermediate Chain (70.1)	94% (112/119)	6% (7/119)
Dynein Heavy Chain (440.4)	93% (99/107)	7% (8/107)
Dynactin p150 ^{Glued}	98% (124/127)	2% (3/127)
Dynactin p62	74% (75/101)	26% (26/101)
pre-absorbed antibodies	0% (0/92)	100% (92/92)

Figure 3.3. Dynein and dynactin are required for pronuclear migration and apposition. (A) Pronuclear apposition is normal when control IgG antibodies are transfected into bovine zygotes, but female pronuclear migration is inhibited following transfection of antibodies against either dynein intermediate chain (70.1) or dynactin p150^{Glued}. Dynein shows normal distribution around the female (F),

but not the male (M) pronucleus in controls (left panel), and localizes to the female pronuclear surface proximal to the sperm aster after anti-dynein antibody transfection (center panel). Dynactin concentration around both pronuclei appears less intense following anti-dynactin antibody transfection (right panel). Microtubule (MTs) organization is unperturbed in zygotes transfected with anti-dynein and anti-dynactin antibodies, with sperm asters clearly visible. Bar, 10 μm . (B) Quantification of the effects of antibody transfection on pronuclear apposition. Zygotes were transfected 12 h post-insemination (HPI) and developed until 24 HPI, when they were then fixed and analyzed by immunocytochemistry. Pronuclear apposition was scored by measuring the distance between pronuclei, with 10 μm representing the average diameter of a pronucleus. Pre-absorbed antibodies refer to anti-dynein and anti-dynactin antibodies incubated with their antigens or cell lysates prior to transfection.

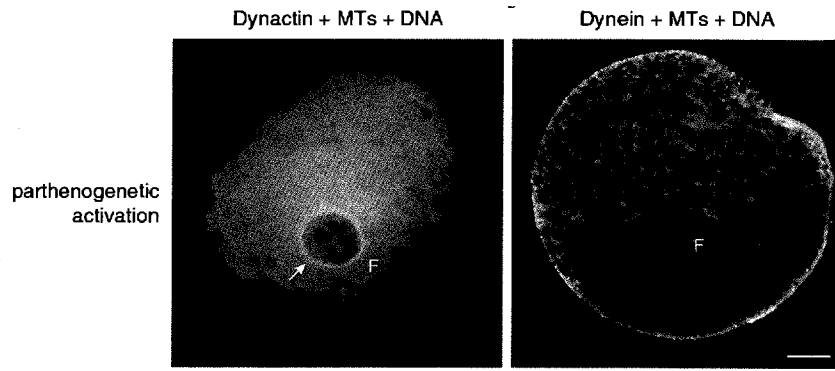
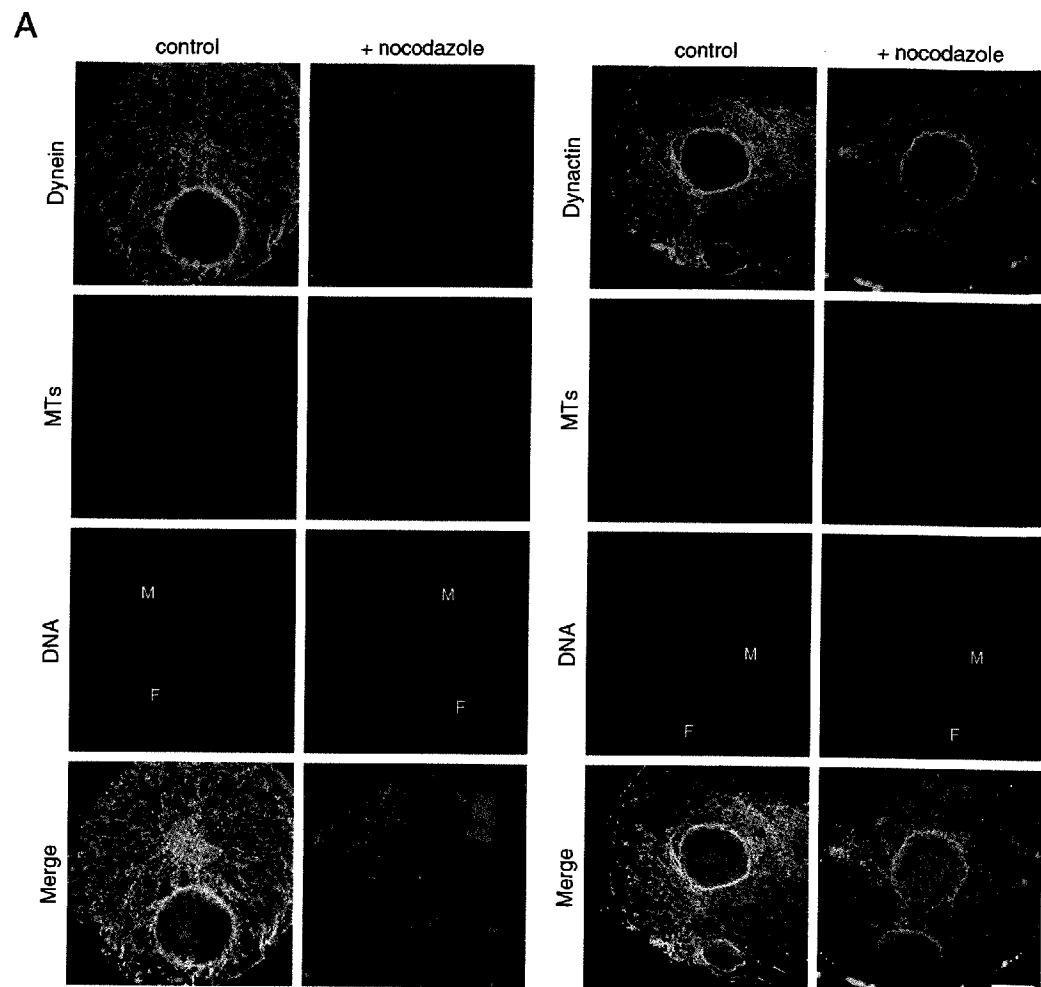


Figure 3.4. Dynein does not localize to the female pronucleus in the absence of a sperm aster. Parthenogenetic activation of bovine oocytes induces female (F) pronuclear formation and microtubule polymerization without aster formation. Dynactin p150^{Glued} (green; left) concentrates around the female pronucleus (blue), while dynein intermediate chain (green; right) distributes near the cortex, enriched with unfocused microtubules (red). Dynein is not detected at the female pronuclear surface. The arrow shows dynactin surrounding the female pronucleus. Bar, 10 μ m.



B

Staining Pattern Around Pronuclei	% Fertilized Eggs	
	control	+ nocodazole
Dynein Intermediate Chain		
Both Male and Female	0	0
Female only	82 \pm 5.6	7 \pm 2.7
Male only	0	0
Neither Male nor Female	18 \pm 5.6	93 \pm 2.7
Dynactin p150 ^{Glued}		
Both Male and Female	60 \pm 4.3	62 \pm 8.3
Female only	5 \pm 3.4	19 \pm 7.1
Male only	3 \pm 1.4	10 \pm 4.4
Neither Male nor Female	12 \pm 4.3	9 \pm 3.4

Figure 3.5. Microtubules are required to retain dynein, but not dynactin, at pronuclear surfaces. (A) Dynein intermediate chain localization to the female pronucleus is no longer detected in bovine zygotes following nocodazole treatment (left panels). Microtubules (MTs), observed around both female (F) and male (M) pronuclei in controls, are not seen in nocodazole-treated zygotes. Dynactin p150^{Glued}, however,

localizes to both pronuclei in nocodazole-treated bovine zygotes, even when microtubules (MTs) are no longer detected (right panels). Bars, 10 μ m. (B) Quantification of the effects of nocodazole treatment on dynein and dynactin association with pronuclei. Results represent the average \pm s.d. of 4 sets of experiments, with a total of 512 zygotes examined for dynein staining; $p < 0.001$ compared to controls (Student's t test). A total of 504 zygotes were examined for dynactin staining, with the differences not statistically significant compared to controls (Student's t test).

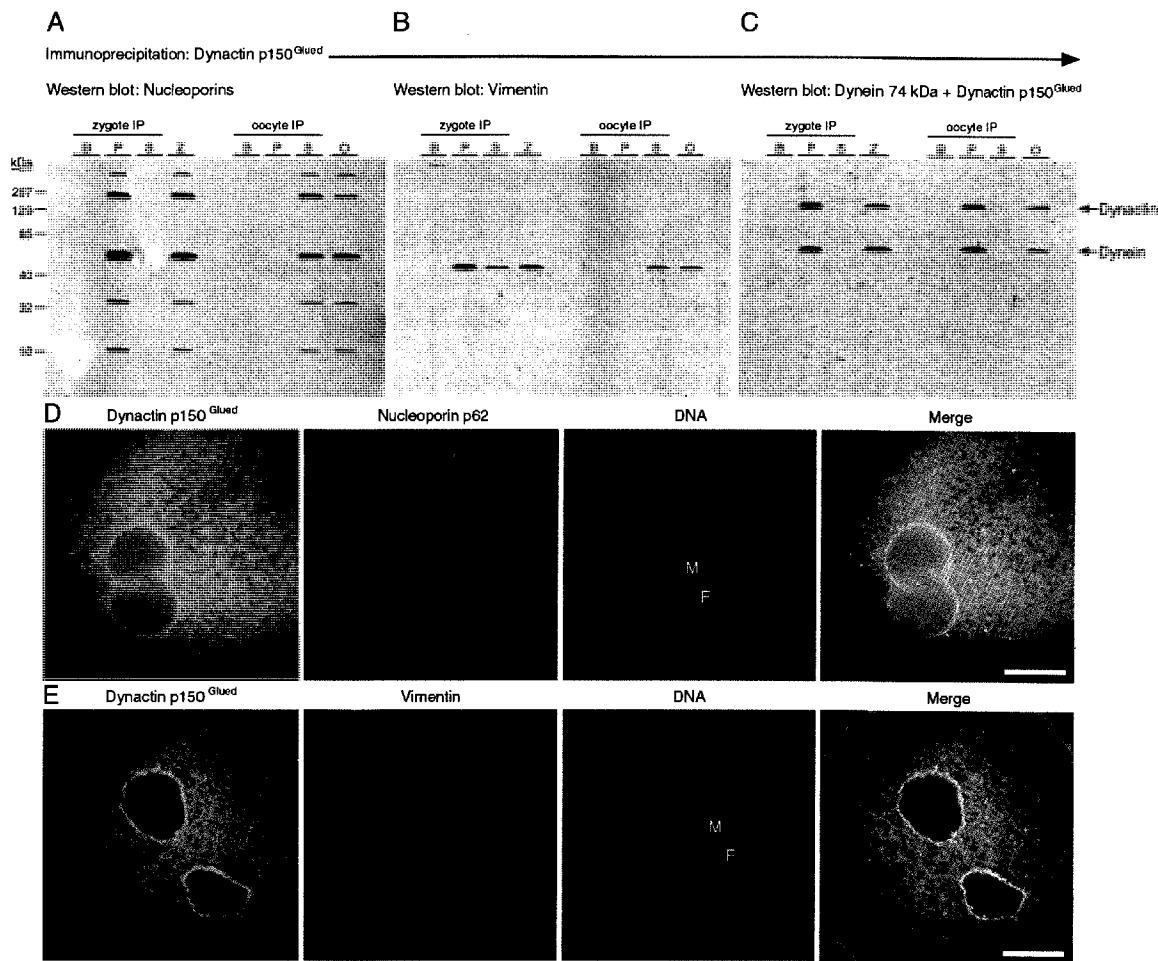


Figure 3.6. Dynactin interacts with nucleoporins, vimentin and dynein during female pronuclear migration. (A-C) Western blots following immunoprecipitation (IP) of dynactin p150^{Glued} from either pronucleate-stage zygotes or unfertilized oocytes. Lanes on the blots are beads-only (B), IP pellets (P), IP supernatants (S), and whole cell lysates from either zygotes (Z) or oocytes (O). (A) Five nucleoporins of molecular mass 270 kDa, 175 kDa, 62 kDa, 35 kDa and 18 kDa are detected in the zygote IP pellet and whole zygote lysate, as well as in the oocyte IP supernatant and whole oocyte lysate. Nucleoporins in the IP pellet show modest enrichment. (B) Vimentin, identified at 58 kDa, is enriched in the zygote IP pellet and detected in both zygote and oocyte IP supernatants, as well as in whole zygote and oocyte lysates. (C) Dynein, 74 kDa, and dynactin, 150 kDa, are enriched in zygote and oocyte IP pellets and detected in whole zygote and oocyte lysates. (D) Dynactin p150^{Glued} (green) and nucleoporin p62 (red) co-localize around the female (F) and male (M) pronuclei and at cytoplasmic foci when the channels are merged (yellow). (E)

Dynactin p150^{Glued} (green) and vimentin (red) co-localize around the pronuclei when the channels are merged (yellow), with vimentin showing additional branching in the region between and surrounding the pronuclei. Bar, 10 μ m.

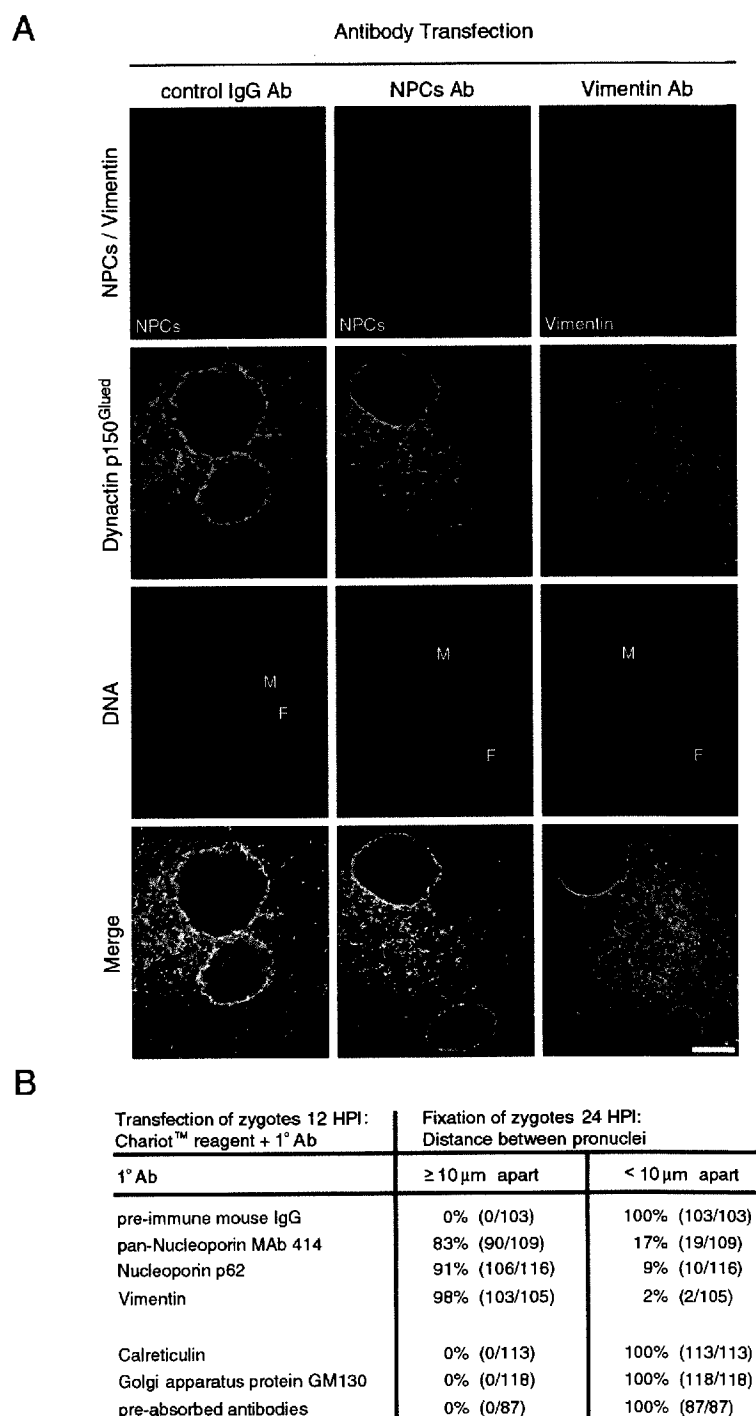


Figure 3.7. Nucleoporins and vimentin are required for pronuclear migration and apposition. (A) Pronuclear apposition is normal when control IgG antibodies are transfected into bovine zygotes, but female pronuclear migration is inhibited following transfection of antibodies against either nuclear pore complex proteins (NPCs) or vimentin. NPCs show normal distribution around the female (F) and the male

(M) pronucleus in controls (left panel), and similar localization is seen following anti-nucleoporin antibody transfection (center panel). Vimentin branching around and between the distant pronuclei is detected after anti-vimentin antibody transfection (right panel). Dynactin p150^{Glued} shows normal localization to pronuclei in control IgG-transfected and anti-nucleoporin-transfected zygotes, while its distribution around pronuclear surfaces appears reduced following transfection with anti-vimentin antibodies. Bar, 10 μ m. (B) Quantification of the effects of antibody transfection on pronuclear apposition. Zygotes were transfected 12 h post-insemination (HPI) and developed until 24 HPI, when they were then fixed and analyzed by immunocytochemistry. Pronuclear apposition was scored by measuring the distance between pronuclei, with 10 μ m representing the average diameter of a pronucleus. Pre-absorbed antibodies refer to anti-nucleoporin and anti-vimentin antibodies incubated with their antigens prior to transfection.

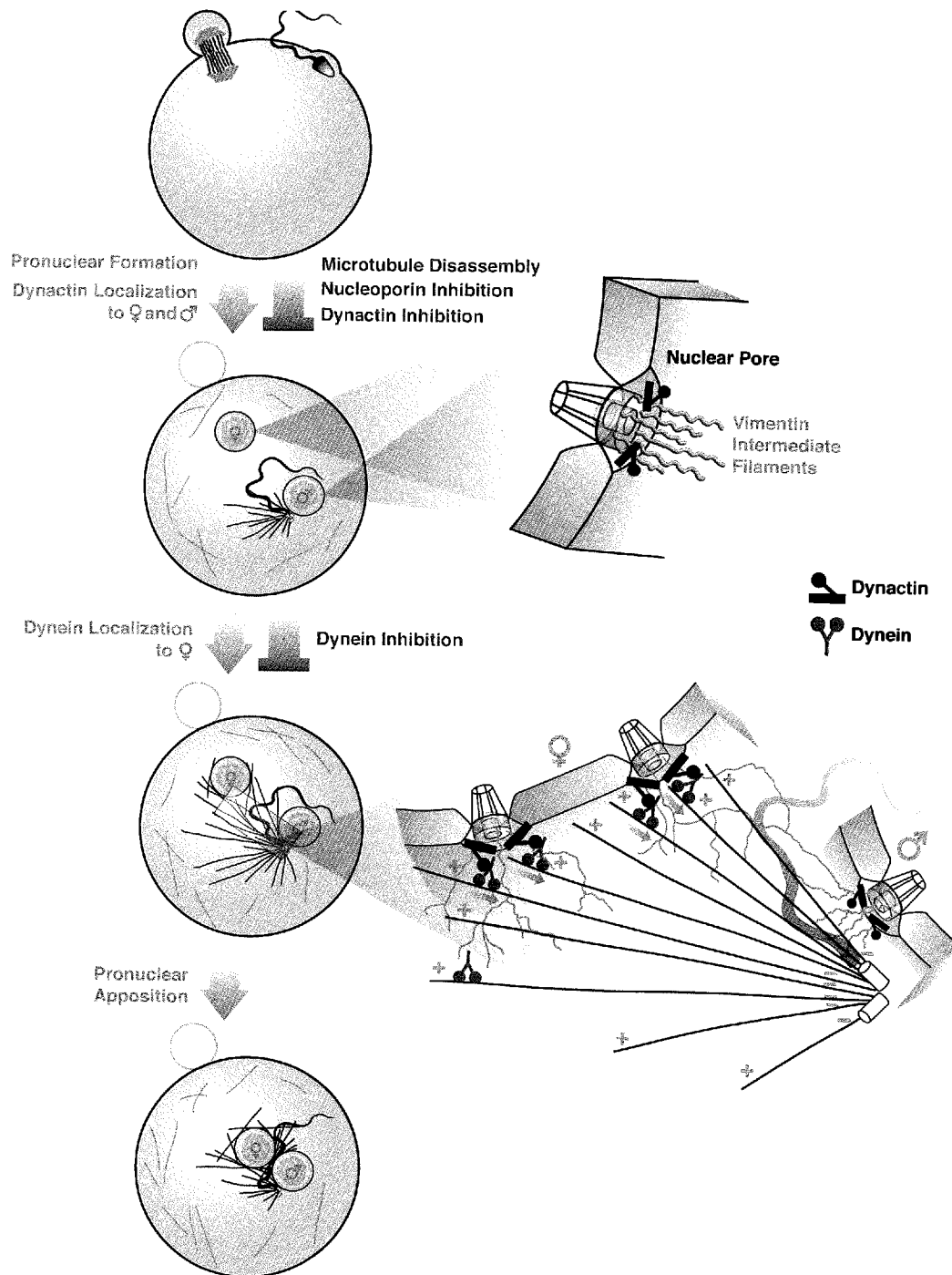


Figure 3.8. A model for pronuclear assembly, motility and union. Sperm entry activates the mature oocyte, leading to second polar body extrusion (top; first polar body not shown). Formation of pronuclei is accompanied by sperm aster-independent microtubules (second from top, left), which bring dynein (black

rectangle with side arm) and vimentin filaments (squiggly green lines) to the cytoplasmic face of the nuclear pore complex (basket structure) (enlargement, upper right). Disassembly of microtubules and inhibition of nucleoporins and dynactin block proper complex formation at the outer surfaces of both pronuclei. Growth of sperm aster microtubules, nucleated by the centrosome attached to the male pronucleus, extends microtubule plus ends away from the male pronucleus, some of which then reach the female pronuclear surface (second from bottom, left). These microtubule plus ends could deliver dynein (red wishbone) preferentially to the surface of the female pronucleus, allowing dynein to bind to dynactin and vimentin at nuclear pores, and enabling the dynein-dynactin complex to transport the female pronucleus to the minus ends along the sperm aster (enlargement, lower right). The inhibition of either dynactin or dynein blocks migration and prevents apposition (bottom).

Chapter 4

LIS1 Association With Dynactin Is Required For Nuclear Motility and Genomic Union in the Fertilized Mammalian Oocyte

Christopher Payne^{1,2}, Justin C. St. John³, João Ramalho-Santos^{2,4} and Gerald Schatten²

¹ Program in Molecular and Cellular Biosciences, Department of Cell and Developmental Biology, Oregon Health and Science University, Portland, Oregon 97201

² Pittsburgh Development Center, Magee-Womens Research Institute, Departments of Obstetrics, Gynecology and Reproductive Sciences, and Cell Biology and Physiology, University of Pittsburgh School of Medicine, Pittsburgh, Pennsylvania 15213

³ Reproductive Biology and Genetics Group, Department of Medicine, University of Birmingham, Birmingham, B15 2TH, UK

⁴ Center for Neuroscience and Cell Biology, Department of Zoology, University of Coimbra, 3004-517 Coimbra, Portugal

Accepted for publication in *Cell Motility and the Cytoskeleton* (2003). In press.

Summary

Mutations in the human *LIS1* gene cause the devastating brain disorder lissencephaly. LIS1 also regulates microtubule dynamics; it interacts with the molecular motor cytoplasmic dynein and its cofactor dynactin, and is necessary for neuronal migration. Recently, LIS1 has been suggested to mediate pronuclear migration during fertilization. Here we use rhesus monkey and bovine oocytes, as well as pronucleate-stage bovine zygotes, to determine: Lis1 RNA expression using reverse transcription-polymerase chain reaction; LIS1 protein association with dynactin using immunoprecipitation, Western blot analysis, and immunocytochemistry; and LIS1 function in mediating genomic union using antibody transfection. We find that Lis1 RNA expression increases during fertilization, that LIS1 and dynactin subunit p150^{Glued} co-immunoprecipitate and co-localize to pronuclear surfaces, and that anti-LIS1 antibodies transfected into zygotes dramatically inhibit pronuclear migration and apposition. LIS1 is therefore essential to mediate genomic union in a process that involves the dynein-dynactin complex. These results shed light on an additional role for LIS1 and raise implications for human reproduction.

Introduction

Human type I lissencephaly is a severe brain disorder caused by the failure of neurons to migrate from the paraventricular zone to the cerebral cortex during development (Dobyns et al., 1993). This results in disorganized cortical layers and reduced gyri, inducing epilepsy and severe mental retardation with death at an early age. Haplo-insufficiency of the *Lis1* gene product leads to both isolated lissencephaly sequence (ILS) and Miller-Dieker Syndrome (MDS), which together comprise a majority of cases seen in the clinic (Lo Nigro et al., 1997). Whereas total loss of *Lis1* is embryonic lethal, heterozygous mutations generated in mice result in neuronal migration defects (Hirotsume et al., 1998). The LIS1 protein, also a subunit of platelet-activating factor acetylhydrolase (PAFAH), has been shown to modulate microtubule dynamics in vitro (Sapir et al., 1997).

LIS1 shares 42% identity with NUDF, one of many nuclear distribution (NUD) proteins in the filamentous fungus *Aspergillus nidulans* (Xiang et al., 1995). During development in *A. nidulans*, nuclei migrate into the germtube and distribute within the cell, and many of the genes that regulate this process share striking homology to members of the cytoplasmic dynein-dynactin motor complex, including *NUDM*, a homologue of dynactin subunit *p150^{Glued}* (Xiang and Morris, 1999). Mutations in *Drosophila LIS1*, *C. elegans LIS1*, and the yeast homologue, *PAC1*, generate dynein-related defects in nuclear migration, nuclear orientation, and oogenesis (Swan et al., 1999; Dawe et al., 2001; Geiser et al., 1997).

Fertilization in most mammals requires a sperm aster, a radial array of microtubules nucleated by the sperm centrosome, upon which the egg-derived female pronucleus migrates to the sperm-derived male pronucleus in a process mediated by the dynein-dynactin motor complex (Payne et al., 2003; Reinsch and Karsenti, 1997; Schatten, 1994). Surprisingly, rodents do not utilize a sperm aster during fertilization, precluding their use for investigating sperm aster-mediated motility in mammals (Schatten, 1994), though *Lis1* expression was recently identified in mouse oocytes and zygotes (Cahana and Reiner, 1999). Because of the relationship that exists among LIS1, dynein, dynactin, and nuclear migration in non-mammalian species, we questioned whether *Lis1* is expressed in rhesus monkey and bovine oocytes, and whether LIS1 is required for pronuclear motility and union in bovine zygotes.

Results

Cloning and Expression of *Lis1* in Rhesus Monkey and Bovine Oocytes and Zygotes

To characterize the expression of *Lis1* in mammalian oocytes that utilize a sperm aster during fertilization, we isolated total RNA from rhesus monkey and bovine oocytes and performed RT-PCR. Amplification of cDNA was performed using oligonucleotide primers that recognize a coding region within the human *LIS1* gene and which were previously used to predict outcome associated with ILS and MDS (Lo Nigro et al., 1997). This portion of the gene is relevant to the current study, as it is a region that might show genetic variability across species. RT-PCR using these primers yielded 329 bp products

(Figure 4.1A). Two bovine Lis1 products (1031A and 1031B) and one rhesus Lis1 product (Rh6) were then sequenced and compared to the human *LIS1* coding sequence of that region (Figure 4.1B). Human Lis1 is 95% identical to rhesus Lis1 and 91% identical to bovine Lis1 over the length of the isolated cDNA. This high degree of homology is not entirely surprising, since the recent comparison between human and rhesus UDP-glucuronosyl-transferase also revealed 95% identity, reflecting the extensive conservation of sequence among primates (Dean et al., 2002). The deduced protein sequence is shown in Figure 4.1C.

Mammalian Lis1 expression at fertilization was examined further by performing RT-PCR and comparing the levels of Lis1 products isolated from unfertilized bovine oocytes and zygotes against the levels of β -actin products (Figure 4.2A). Semi-quantitation of the Lis1 products indicates that levels in the zygotes are nearly double those in the oocytes (~190%). These results suggest that Lis1 mRNA might be transcribed in the fertilized zygote. Recent evidence has shown that 1-cell bovine embryos are indeed transcriptionally and translationally active for genes important for embryonic development (Memili and First, 1999). Lis1 transcription has also been reported to occur in mouse zygotes, indicating the importance of this gene's expression in the early mammalian embryo (Cahana and Reiner, 1999).

LIS1 Associates with Dynactin in Pronucleate-Stage Bovine Zygotes

Western blot analysis was performed to determine whether LIS1 translation occurs during fertilization. LIS1 protein is detected here as a single 45-kD band in unfertilized bovine oocytes and zygotes (Figure 4.2B), with densitometry analysis

showing levels approximately one-third (~30%) higher in zygotes than in oocytes. This putative increase in mRNA and protein expression in the zygote suggests a potential function for LIS1 during fertilization and early embryogenesis.

LIS1 interacts with the p150^{Glued} subunit of dynactin in embryonic, neonatal and adult mammalian neurons, and its association with dynactin is particularly enriched at the cortical plate and marginal zone of the embryonic brain, sites of neuronal migration (Smith et al., 2000). We therefore questioned whether LIS1 associates with dynactin in bovine zygotes during pronuclear migration. Co-immunoprecipitation experiments show that the anti-dynactin p150^{Glued} antibody pulls down LIS1 from pronucleate-stage zygotes, but not from unfertilized oocytes (Figure 4.2C). The p150^{Glued} subunit is enriched in both samples. This result indicates that LIS1 interacts with dynactin at fertilization, perhaps to mediate pronuclear motility.

Co-distribution of LIS1 and Dynactin to Pronuclear Surfaces

The distribution of LIS1 and dynactin p150^{Glued} during pronuclear migration and apposition was then characterized by confocal microscopy. Both proteins localize at the surfaces of the two pronuclei (Figure 4.3A). While some dim cytoplasmic foci can be seen for LIS1 and dynactin, both proteins concentrate along the pronuclear rims. Pre-absorption of anti-LIS1 antibodies with their antigens and pre-incubation of anti-p150^{Glued} antibodies with human endothelial cell lysates result in no LIS1 or dynactin staining within the zygotes (Figure 4.3B). LIS1 has recently been identified to localize at nuclear envelopes in prophase somatic cells (Coquelle et al., 2002), and dynactin has been proposed to interact with cytoplasmic dynein to facilitate nuclear envelope

breakdown (Salina et al., 2002). Another possible function of LIS1 and the dynein-dynactin complex might be to facilitate pronuclear migration.

Requirement of LIS1 for Genomic Union

Co-localization of LIS1 and dynactin to pronuclear surfaces suggests their importance in mediating genomic union. To determine whether LIS1 is required for pronuclear migration and apposition, we transfected antibodies against LIS1 into pronucleate-stage bovine zygotes using Chariot[™] reagent (Morris et al., 2001). Antibody transfection occurred after the formation but before the union of the pronuclei, specifically targeting pronuclear motility. Development of the transfected zygotes was allowed until just prior to mitosis, whereupon distances between the two pronuclei were measured to score the inhibition of genomic union. Measured from surface-to-surface, inter-pronuclear distances $\geq 10 \mu\text{m}$ reflect inhibition, with $10 \mu\text{m}$ representing the average pronuclear diameter.

The majority of zygotes transfected with anti-LIS1 antibodies show pronuclei $\geq 10 \mu\text{m}$ apart (81%; Table 1). LIS1 concentrates around both pronuclei and distributes throughout the cytoplasm as punctate foci (Figure 4.4). All of the zygotes transfected with pre-immune mouse IgG antibodies display inter-pronuclear distances $< 10 \mu\text{m}$ and normal LIS1 distribution (Table 1, Figure 4.4). We conclude from these data that LIS1 is essential for pronuclear migration and genomic union. Recent observations of *C. elegans* zygotes noted that pronuclear apposition does not occur when the animals are subjected to Lis1 RNAi (Dawe et al., 2001). Our results here demonstrate a role for LIS1 on nuclear motility during mammalian fertilization, with implications for human infertility.

Discussion

LIS1 is required for early mouse embryogenesis, with homozygous null mutants exhibiting post-implantation lethality (Hirotsune et al., 1998). Morphological analysis of homozygous null blastocysts revealed defects in inner cell mass growth and development, resulting in embryonic death prior to neuronal differentiation or migration. While the precise cause of such defects has not yet been identified, the ability of these embryos to develop until implantation suggests that maternally-inherited *Lis1* transcripts and protein levels are sufficient in the zygote to permit development in the absence of gene expression. This current study shows that when LIS1 protein is inhibited by antibody transfection into the zygote, specific defects in genomic union are observed.

Co-immunoprecipitation and co-localization of LIS1 with dynactin in the zygote identify a possible role for LIS1 in modulating the dynein-dynactin complex. Recent studies report that LIS1, dynein, and dynactin localize to mitotic kinetochores and microtubule 'plus' ends in somatic cells (Faulkner et al., 2000; Coquelle et al., 2002), and that LIS1 interacts with specific regions in the dynein and dynactin molecules (Tai et al., 2002). Indeed, in unfertilized oocytes LIS1 localizes to regions along the meiotic spindle that are enriched with dynein and dynactin (C. Payne, unpublished observations). Given the proposed role of dynein and dynactin in mediating pronuclear migration and apposition during fertilization (Payne et al., 2003; Reinsch and Karsenti, 1997; Schatten, 1994), LIS1 likely regulates the motor complex at the surfaces of the pronuclei to

facilitate nuclear motility and union. Recent evidence shows that when anti-dynein and anti-dynactin antibodies are transfected into pronucleate-stage zygotes, the migration of the female pronucleus is dramatically inhibited (Payne et al., 2003). Thus, the similarity in outcome of blocking dynein, dynactin, and LIS1 during fertilization suggests their involvement in an interactive complex that mediates pronuclear movement.

It is remarkable that a gene highly expressed in neurons and critical for neuronal migration should also be expressed and functionally important at fertilization. Recent studies illustrate, however, that neurons and gametes share more commonalities than were once appreciated. The RNA binding protein CPEB (cytoplasmic polyadenylation element binding protein), for example, regulates key functions in both cell types (Richter, 2001), and SPNR (spermatid perinuclear RNA-binding protein) shows abundant expression in brain, ovary and testis (Pires-daSilva et al., 2001). Thus, proteins essential for proper development of the nervous system might also, if defective, contribute to infertility. With a role identified for LIS1 in mediating pronuclear migration and genomic union, we might now add fertilization defects together with lissencephaly as devastating consequences induced, respectively, by faulty LIS1 protein and gene expression.

Table 1

Anti-LIS1 antibodies inhibit pronuclear union during fertilization

Transfection of zygotes at 12 h with Chariot™ reagent + antibodies:	Distance between pronuclei at 20 h:	
	≥ 10 μm apart	< 10 μm apart
pre-immune mouse IgG	0% (0/92)	100% (92/92)
anti-LIS1	81% (69/85)	19% (16/85)

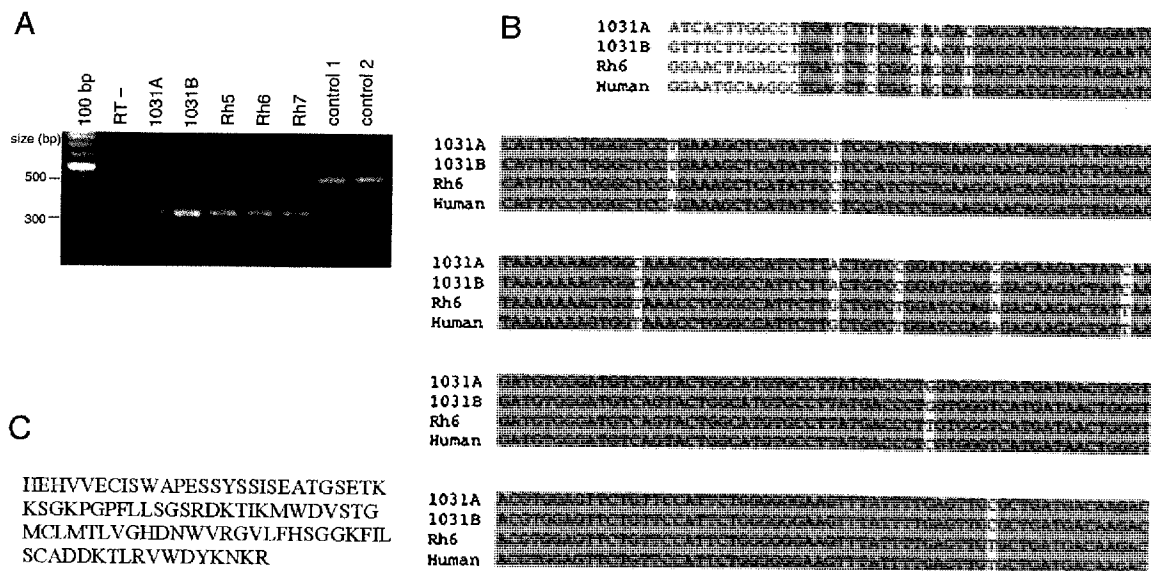


Figure 4.1. RT-PCR and cDNA sequence analysis of bovine and rhesus monkey Lis1. (A) Detection of the 329 bp Lis1 product, reverse transcribed and amplified from total RNA, isolated from bovine (1031A, 1031B) and rhesus (Rh5, Rh6, and Rh7) oocytes. Positive controls 1 and 2 yield a 500 bp product, and negative control (RT-) shows no product. (B) Sequence comparison among bovine (1031A, 1031B), rhesus (Rh6) and human Lis1 cDNA. Data are taken from GenBank as listed in Materials and Methods, and sequence analysis was performed with the Multiple Sequence Alignment computer program using the ClustalW algorithm. Conserved residues are highlighted with gray boxes. (C) The deduced protein sequence of this portion of the Lis1 gene, generated from the bovine and rhesus nucleotide sequences.

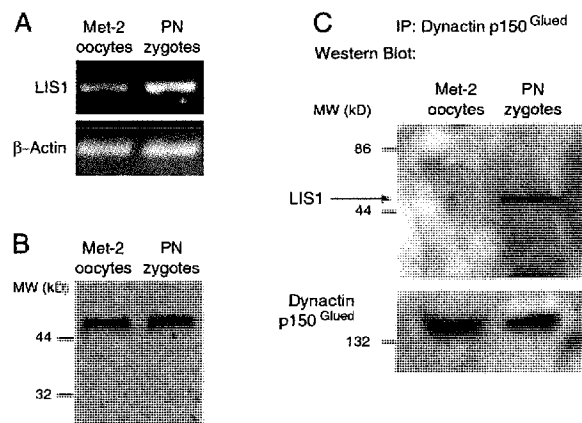


Figure 4.2. LIS1 RNA expression, protein expression and co-immunoprecipitation with dynactin. (A) RNA from 5 meiotically arrested (Met-2) bovine oocytes or 5 pronucleate (PN) bovine zygotes was isolated, reverse transcribed, and amplified for each RT-PCR reaction. Lis1 and control β -actin products were electrophoresed, imaged and quantified. Semi-quantitative comparison between the levels of Lis1 products in oocytes and zygotes and the normalized standards of β -actin products suggests that Lis1 transcription may occur upon fertilization. (B) Protein from bovine Met-2 oocytes and PN zygotes was extracted, resolved by SDS-PAGE, and subjected to Western blot analysis using anti-LIS1 antibodies. Single 45-kD bands are detected in both oocytes and zygotes. (C) SDS-PAGE and Western blot analysis following immunoprecipitation (IP) of dynactin p150^{Glued} from bovine Met-2 oocytes and PN zygotes. LIS1 is enriched in the dynactin immunoprecipitate prepared from zygotes, but not from oocytes. Dynactin p150^{Glued} is detected in both samples.

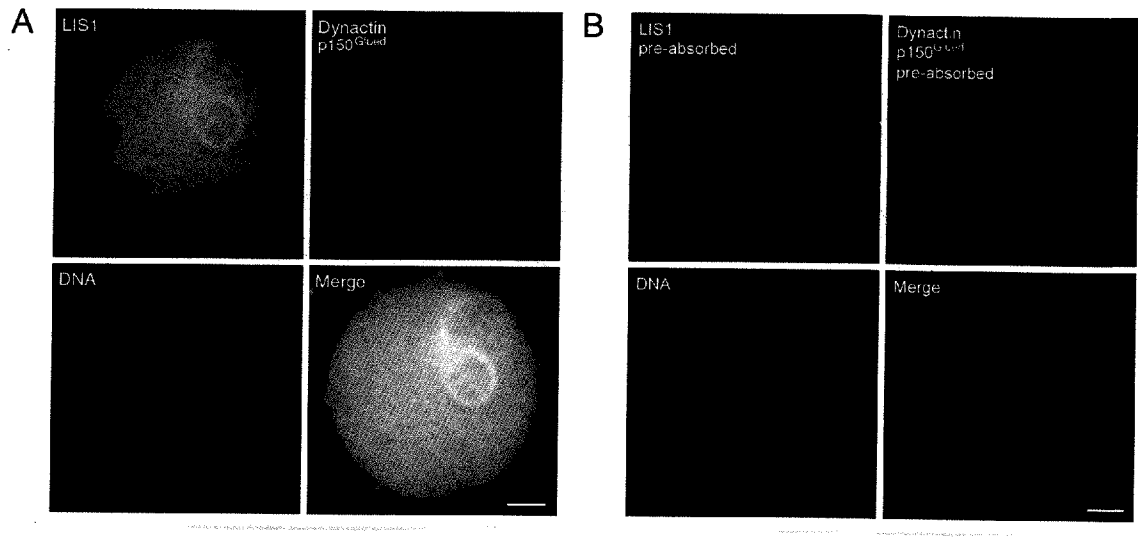


Figure 4.3. LIS1 and dynactin co-localize around the pronuclear surfaces in zygotes. (A) Pronucleate-stage bovine zygote shows both LIS1 (green) and Dynactin p150^{Glued} (red) concentrated around the two pronuclei (DNA; blue). Co-localization is detected in the three-channel overlay (Merge). (B) Pre-absorption of anti-LIS1 antibodies with their antigens and pre-incubation of anti-p150^{Glued} antibodies with human endothelial cell lysates result in a loss of LIS1 and dynactin detection in zygotes. Scale bar = 10 μ m.

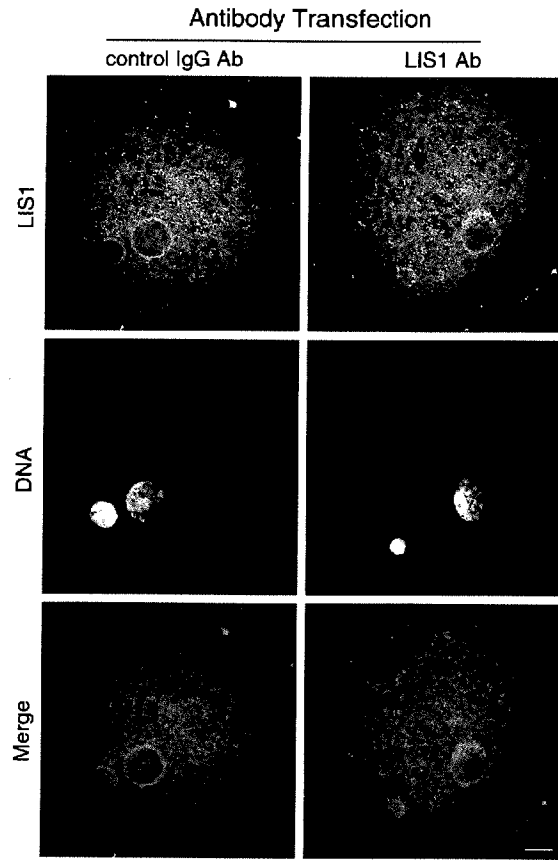


Figure 4.4. LIS1 is required for pronuclear apposition. (Left panel) Normal inter-pronuclear distances are observed when control IgG antibodies are transfected into bovine zygotes. LIS1 concentrates around the two pronuclei, with additional punctate cytoplasmic foci. (Right panel) Transfection using anti-LIS1 antibodies inhibits pronuclear apposition, while the distribution of LIS1 resembles control conditions. Scale bar = 10 μ m.

Chapter 5

Golgi Dynamics During Meiosis Are Distinct From Mitosis and Are Coupled to Endoplasmic Reticulum Dynamics Until Fertilization

Christopher Payne^{1,2} and Gerald Schatten²

¹ Program in Molecular and Cellular Biosciences, Department of Cell and Developmental Biology, Oregon Health and Science University, Portland, Oregon 97201

² Pittsburgh Development Center, Magee-Womens Research Institute, Departments of Obstetrics, Gynecology and Reproductive Sciences, and Cell Biology and Physiology, University of Pittsburgh School of Medicine, Pittsburgh, Pennsylvania 15213

Accepted for publication in *Developmental Biology* (2003). In press.

Summary

One current theory of the Golgi apparatus views its organization as containing both a matrix fraction of structural proteins and a reservoir of cycling enzymes. During mitosis, the putative matrix protein GM130 is phosphorylated and relocated to spindle poles. When the secretory pathway is inhibited during interphase, GM130 redistributes to regions adjacent to vesicle export sites on the endoplasmic reticulum (ER). Strikingly, meiotic maturation and fertilization in non-rodent mammalian eggs presents a unique experimental environment for the Golgi apparatus, because secretion is inhibited until after fertilization, and because the centrosome is absent until introduced by the sperm. Here we test the hypothesis that phosphorylated GM130 associates not with meiotic spindle poles, but with ER clusters in the mature bovine oocyte. At the germinal vesicle stage, phosphorylated GM130 is observed as fragments dispersed throughout the cytoplasm. During meiotic maturation, GM130 reorganizes into punctate foci that associate near the ER-resident protein calreticulin, and is notably absent from the meiotic spindle. GM130 co-localizes with Sec23, a marker for ER vesicle export sites, but not with *Lens culinaris* agglutinin, a marker for cortical granules. Because disruption of vesicle transport has been shown to block meiotic maturation and embryonic cleavage in some species, we also test the hypothesis that fertilization and cytokinesis are inhibited with membrane trafficking disruptor brefeldin A (BFA). Despite Golgi fragmentation after BFA treatment, pronuclei form and unite, and embryos cleave and develop through the eight-cell stage. We conclude that while the meiotic phosphorylation cycle of GM130 mirrors that of mitosis, absence of a maternal centrosome precludes Golgi association

with the meiotic spindle. Fertilization introduces the sperm centrosome that can reorganize Golgi proteins, but neither fertilization nor cytokinesis prior to compaction requires a functional Golgi apparatus.

Introduction

Upon resumption of meiosis, mammalian oocytes in prophase I proceed through germinal vesicle breakdown (GVBD), undergo genomic reduction through the extrusion of the first polar body, and arrest in metaphase II (Gosden et al., 1997). Sperm penetration activates the oocyte, leading to the emission of a second polar body and the formation, migration, and apposition of the two pronuclei (Aitken, 1997). Successful genomic union then completes the fertilization process. These events are highly dynamic, involving the active reorganization of the chromatin, cytoskeleton, membrane organelles, and other structural components within the oocyte (Albertini, 1992; Perreault, 1992). Genomic reduction during meiosis is accompanied by centrosome reduction in most mammalian species, including bovine, rhesus monkey, and human (Schatten, 1994). Rodent oocytes, in contrast, retain their centrosomes throughout meiotic maturation (Schatten et al., 1986). Bovine is an ideal model species for studying oocyte maturation and fertilization because, as in rhesus and human oocytes, the centrosome is not present until sperm entry (Sathananthan et al., 1991; Navara et al., 1994; Schatten, 1994; Sutovsky et al., 1996).

The dynamics of Golgi membranes during meiosis and fertilization in mammals are not entirely known. Mouse, rhesus, and bovine GV oocytes contain dispersed fragments of Golgi that vesiculate following GVBD (Calarco et al., 1972; Wassarman and Josefowicz, 1978; Hyttel et al., 1986; McGaughey et al., 1990; Assey et al., 1994; Moreno et al., 2002), yet the distribution and modification of these vesicles following polar body extrusion and insemination have not been fully examined and warrant further study. Brefeldin A (BFA), a fungal metabolite that inhibits protein secretion by disrupting ER-to-Golgi vesicle transport (Lippincott-Schwartz et al., 1989), blocks meiotic maturation in mouse oocytes and prevents cell division in *C. elegans* zygotes and embryos (Moreno et al., 2002; Skop et al., 2001). It is unclear, however, whether Golgi disruption with BFA inhibits the fertilization process that occurs between meiosis and cytokinesis. While primarily dependent on the cytoskeleton to unite the pronuclei and initiate cleavage, fertilization and cell division both involve extensive membrane organelle transport (Terasaki and Jaffe, 1991; Rouvière et al., 1994; Danilchik et al., 1998; Skop et al., 2001). These trafficking events include the intermingling of pronuclear envelopes with ER and Golgi membranes along microtubules during fertilization (Terasaki and Jaffe, 1991; Rouvière et al., 1994), as well as the delivery of Golgi membrane-derived vesicles to cleavage furrows during cytokinesis (Danilchik et al., 1998; Skop et al., 2001). BFA has been shown to inhibit pronuclear movement in parthenogenetically activated oocytes (Clayton et al., 1995), raising the possibility that BFA might also inhibit pronuclear migration in zygotes during fertilization.

Golgi structure has been theorized to contain both matrix proteins and resident enzymes (Slusarewicz et al., 1994; Nakamura et al., 1995; Lippincott-Schwartz et al.,

2000). Putative matrix proteins, such as GM130, become phosphorylated and associate with spindle poles during mitosis, while resident enzymes are reabsorbed into the ER (Lowe et al., 1998; Jesch and Linstedt, 1998; Zaal et al., 1999; Seemann et al., 2002). Phosphorylation of GM130 occurs during prophase and coincides with the fragmentation and partitioning of Golgi proteins into daughter cells (Lowe et al., 2000). Cyclin B-Cdc2 kinase phosphorylates GM130 on serine 25, while PP2A phosphatase dephosphorylates the residue during telophase (Lowe et al., 1998; Lowe et al., 2000). Because mammalian oocytes contain large stockpiles of cyclin B1, cyclin B2, cdc2, and PP2A mRNA and protein (Kubiak et al., 1993; Smith et al., 1998; Ledan et al., 2001), it is possible that these molecules act upon Golgi proteins during meiosis to partition the organelle.

In this report we examine whether GM130 becomes phosphorylated during meiosis, and whether it associates with spindle poles or ER vesicle export sites in mature bovine oocytes. Fertilized oocytes were then treated with BFA to examine whether fertilization and cytokinesis are inhibited when membrane trafficking is disrupted. Our findings show that phosphorylated GM130 localizes to ER vesicle export sites and not to meiotic spindle poles, and that neither fertilization nor cell division to the eight-cell stage requires trafficking through the secretory pathway. These results suggest that the Golgi apparatus is organized by a mechanism independent of the centrosome and unique to meiotic maturation, but that the structure and function of the Golgi are not essential for initial embryonic development.

Results

Golgi protein GM130 disperses to clusters of endoplasmic reticulum and not to meiotic spindle poles during oocyte maturation

To determine whether the putative Golgi matrix relocates to spindle poles or to ER membranes during meiotic maturation, we examined the distribution of GM130 and ER-resident protein calreticulin in both GV and metaphase II-arrested (Met-2) oocytes. At the GV stage, the majority of oocytes (81%; 116/143) show GM130 dispersed throughout the ooplasm as fragments (Figure 5.1A). This pattern is similar to the distribution of Golgi markers giantin and BODIPY-ceramide recently characterized in mouse and rhesus GV oocytes (Moreno, et al., 2002). Like these other markers, the GM130 staining concentrates around the GV surface in the interior of the oocyte, but unlike those markers, it is reduced near the cortex and is absent from the oocyte surface. The GM130 staining is distinct from calreticulin, which both concentrates around the GV surface in a punctate distribution and localizes near the cortex in diffuse patches (Figure 5.1B). No co-localization is detected between the Golgi and the ER in GV oocytes (Figure 5.1C).

Following GVBD, completion of first meiosis and arrest at Met-2, 86% of oocytes (134/155) show punctate foci of GM130 localized in specific ooplasmic domains (Figure 5.1D). Strikingly, these domains correspond to regions of concentrated staining for calreticulin (Figure 5.1E), showing a distribution of punctate Golgi proteins near ER clusters (Figure 5.1F). This pattern resembles somatic cells treated with either BFA or dominant-negative Sar1p protein, in which putative matrix proteins appear to associate

with vesicle export sites on the ER (Ward, et al., 2001; Miles, et al., 2001). GM130 does not preferentially localize to meiotic spindle poles in Met-2 oocytes (Figure 5.1D, asterisks), unlike the observed distribution of GM130 to mitotic spindle poles in somatic cells (Seemann, et al., 2002).

GM130 reorganizes around the pronuclei during fertilization

Upon the insemination of oocytes and the formation of pronucleate-stage (PN) zygotes, GM130 once again appears fragmented and dispersed around the male and female pronuclei in the majority of oocytes (92%; 167/182; Figure 5.1G). The staining pattern for calreticulin in zygotes resembles that observed in Met-2 oocytes, with clusters of ER distributed throughout the cytoplasm (Figure 5.1H). No preferential accumulation or distribution of ER proteins is detected around the two pronuclei. Like in GV oocytes, no co-localization is detected between GM130 and calreticulin in PN zygotes (Figure 5.1I).

Following the first mitotic division, 2-cell embryos show a juxtanuclear distribution of GM130 within each of the blastomeres (Figure 5.1J). The dispersed Golgi fragments observed in GV oocytes and PN zygotes are no longer seen. Either a single Golgi or several Golgi clusters are detected in 83% of embryos at the 2-cell stage (81/98). Calreticulin, meanwhile, distributes more diffusely throughout the cytoplasm, with less concentrated staining observed near the cortex (Figure 5.1K). Co-distribution of the Golgi and ER is also seen, with an increased localization of calreticulin detected in the regions enriched with GM130 (Figure 5.1L). The staining patterns of the Golgi and ER in 2-cell embryos, therefore, more closely resemble those observed in somatic cells.

COP II vesicle component Sec23 co-localizes with GM130 during meiotic maturation

Golgi proteins were recently shown to redistribute to vesicle export sites on the ER following the inhibition of the ER-to-Golgi transport pathway by BFA or mutant Arf1 (Ward et al., 2001). A marker for these sites is Sec23, a component of the COP II coat that mediates vesicle budding from regions of transitional smooth ER (Barlowe et al., 1994; Kuge et al., 1994; Paccaud et al., 1996). Because foci of GM130 localize near clusters of calreticulin in Met-2 oocytes, we decided to examine the distribution of GM130 with respect to Sec23 in both Met-2 oocytes and PN zygotes. The majority of Met-2 oocytes (95%; 72/76) show a striking co-localization between punctate foci of GM130 and Sec23 dispersed throughout the cytoplasm (Figure 5.2A-C). Neither protein distributes to the meiotic spindle poles (Figure 5.2A, asterisks). While Sec23 foci are also seen in PN zygotes, GM130 predominantly and distinctly reorganizes around the pronuclei, and co-localization is now limited to regions of reticulated distribution near the cortex (Figure 5.2D-F). This staining pattern is observed in 78% of zygotes (63/81). It appears that GM130 relocates during meiotic maturation to associate with Sec23 at ER export sites, then redistributes again during fertilization to localize to the apposed pronuclei.

The distribution of GM130 near the oocyte cortex suggests that Golgi proteins may also associate with cortical granules, membrane-bound organelles which secrete a variety of enzymes during fertilization to block polyspermy (Wessel et al., 2001). Cortical granules release their contents upon sperm activation to modify the extracellular

environment of the oocyte, and can be labeled in Met-2 oocytes with FITC-conjugated *Lens culinaris* agglutinin (LCA), a lectin isolated from lentils (Cherr et al., 1988; Ducibella et al., 1988a; Wang et al., 1997). When Met-2 oocytes are double labeled for GM130 and LCA, the Golgi proteins and cortical granules distribute as distinct foci (Figure 5.2G-I), with no-colocalization detected in any of the oocytes examined (68/68). Thus, while GM130 associates with Sec23 and ER export sites during meiotic maturation, it does not associate with either meiotic spindle poles or cortical granules.

GM130 is phosphorylated during oocyte maturation and dephosphorylated during fertilization

The fragmentation, dispersion, and reorganization of the Golgi apparatus observed between GVBD and PN apposition raise the possibility that GM130 might be phosphorylated in the oocyte during this time. Therefore, to characterize the condition of this protein in GV and Met-2 arrested oocytes, PN zygotes, and 2-cell embryos, we used an antibody that specifically recognizes the phosphorylated form of GM130 (Lowe, et al., 2000).

At the GV and Met-2 stages, the majority of oocytes (90%; 114/127) contain almost all of their GM130 protein in a phosphorylated state, revealed through double labeling with anti-GM130 antibodies (Figure 5.3A-F). Since GV oocytes are in prophase of first meiosis and Met-2 oocytes are in metaphase of second meiosis, the phosphorylation of GM130 appears to persist throughout meiotic maturation. Following insemination and pronuclear formation, all observed zygotes (92/92) contain GM130 in a dephosphorylated state, since no signal is detected with anti-phospho-GM130 antibodies

(Figure 5.3G-I). When 2-cell embryos are examined shortly after cytokinesis, the majority of GM130 is dephosphorylated and juxtannuclear (85%; 76/89). A narrow band of GM130, however, is phosphorylated and resides near the cleavage furrow in some of the embryos (Figure 5.3J-L).

Brefeldin A disrupts a functionally active Golgi apparatus but does not inhibit development during fertilization

By assessing the motility of energy-dependent vesicles coated with β -coatamer (β -COP) and the sensitivity of meiotic maturation to brefeldin A (BFA), it was recently shown that Golgi fragments are functionally active in mouse GV oocytes (Moreno, et al., 2002). COP I vesicles, which are comprised of β -COP, participate in anterograde and retrograde membrane transport in the ER and Golgi (Lowe and Kreis, 1998). While the Golgi fragments disperse during meiotic maturation, they relocalize around the two pronuclei during fertilization. Therefore, we questioned whether β -COP distribution and BFA sensitivity are also exhibited during the fertilization process.

Control-treated zygotes show β -COP protein dispersed around the male and female pronuclei in a pattern that resembles GM130 distribution (Figure 5.4A). The majority of zygotes treated with 5 μ g/ml BFA, however, display a severe disruption in β -COP staining (89%; 39/44). Punctate β -COP redistributes throughout the cytoplasm under these conditions (Figure 5.4B). Despite the disruption and redistribution of β -COP, however, pronuclear union appears unaffected. The surface-to-surface internuclear distances of the pronuclei do not differ greatly between control and BFA treatment conditions (Table 2). All distances are <10 μ m, the average diameter of a pronucleus.

Successful pronuclear migration and apposition occur despite the fragmentation of the Golgi apparatus, measured by examining the distribution of GM130 (Figure 5.4C,D), cis/medial Golgi enzyme mannosidase II (Figure 5.4E,F), and COP I vesicle protein giantin (Figure 5.4G,H). All of the BFA-treated zygotes stained for these Golgi markers contain pronuclei that are $<10\ \mu\text{m}$ apart, identical to controls (Table 2). An intact Golgi apparatus, therefore, does not appear to be necessary for the microtubule-dependent mechanism of pronuclear migration in the zygote. We wondered, however, whether BFA would affect subsequent mitosis and cytokinesis.

Brefeldin A does not inhibit cytokinesis in the pre-compacted embryo

Embryos treated with $5\ \mu\text{g/ml}$ BFA show no significant differences in developmental rates when compared to control-treated embryos; approximately the same number of pre-compacted eight-cell embryos forms (48.7% control vs. 44.5% BFA-treated; Table 3). Similar numbers of embryos arrest at the 1-cell, 2-cell, and 3/4-cell stages under both culture conditions. Higher concentrations of BFA induce cell cycle arrest in the zygote, causing death prior to first mitosis (data not shown). When compared to controls, zygotes treated with BFA form 2-cell embryos that display normal outward appearance, showing well-formed cleavage furrows and evenly distributed cytoplasm (Figure 5.5A,B). Under BFA treatment, development to the 3/4-cell stage is also achieved (Figure 5.5D), although the cleavage furrows are not as clearly defined between all blastomeres as they are in controls (Figure 5.5C). By the time eight-cell embryos form, those treated with BFA show an increase in misshapen blastomeres and blebbing, in addition to poorly defined cleavage furrows (Figure 5.5F). Despite these anomalies,

individual blastomeres can still be discerned. However, unlike the control embryos, development arrests at this stage and these embryos fail to compact (Figure 5.5E; shown as pre-compacted embryos).

Discussion

We have examined the potential roles of a putative Golgi matrix protein during bovine oocyte maturation, fertilization, and cytokinesis. Our results provide new insights into Golgi function during meiosis as compared to mitosis, and during the cell cycles of fertilization and early embryonic development. The finding that Golgi protein GM130 localizes to ER vesicle export sites during meiotic maturation suggests that meiosis may follow a unique set of requirements that could be facilitated by the absence of a centrosome. GM130 phosphorylation coincides with Golgi fragmentation, and might ensure correct partitioning within the oocyte. While a functional secretory pathway is ultimately necessary for embryo compaction, it appears not to be required for either fertilization or subsequent cell division.

ER-resident proteins redistribute during oocyte maturation but do not reorganize during fertilization

Previous studies using mouse and hamster oocytes have shown that a dramatic reorganization and concentration of membrane vesicles and inositol 1,4,5-triphosphate (IP₃) receptors occurs near the cortex during meiotic maturation (Ducibella et al., 1988b;

Mehlmann et al., 1995; Shiraishi et al., 1995). IP₃ receptors, which mediate Ca²⁺ release from the ER during fertilization, become sensitized during the maturation process (Kline, 2000). It is thought that the formation of cortical ER clusters facilitates the generation of repetitive Ca²⁺ waves upon oocyte activation (Kline et al., 1999). Our current observations of ER rearrangements in bovine, shifting from irregular masses at the GV stage to ordered clusters at Met-2 arrest, resemble the redistribution previously detected in hamster (Shiraishi et al., 1995). ER membranes initially concentrated around the GV and in patches near the cortex disperse to form clusters positioned at periodic intervals that are absent from the region surrounding the meiotic spindle.

When oocyte activation and sperm entry trigger Ca²⁺ release during fertilization, sperm aster microtubules form, pronuclei develop, and Golgi membranes reorganize. Like the observations made in activated mouse oocytes (Kline et al., 1999), we note here that the cortical ER clusters do not reorganize in bovine zygotes. This stable organization may be required for the generation of Ca²⁺ oscillations that occurs following oocyte activation in mammals (Kline, 2000). This differs from events observed in other phyla: sea urchin zygotes contain ER membranes that reorganize and redistribute to the centrosome attached to the male pronucleus (Terasaki and Jaffe, 1991). Such rearrangements correspond to a single Ca²⁺ transient (Eisen et al., 1984). ER dynamics at fertilization, therefore, may depend upon whether Ca²⁺ release is singular or oscillatory (Kline et al., 1999).

In the 2-cell bovine embryo, cortical ER clusters are no longer detected. The redistribution of membrane to a more diffuse network surrounding the nucleus reflects an organization similar to that found in somatic cells. Observations in mouse embryos have

shown that IP₃ receptors are downregulated after fertilization (Parrington et al., 1998), suggesting that ER reorganization may correspond to these changes. Our results indicate that structural alterations of the ER, including a loss of clusters, occur following the zygotic cell cycle. These changes may reflect a shift in ER structure and function required by multicellular embryos.

Phosphorylated GM130 localizes to the ER but not the meiotic spindle in the mature oocyte

We have shown that throughout oocyte meiosis, as in somatic cell mitosis, Golgi protein GM130 is in a phosphorylated state. Both the clustered Golgi fragments at the GV stage and the dispersed Golgi foci at Met-2 arrest are recognized by the phospho-specific antibody PS25. GM130 becomes dephosphorylated following sperm incorporation, with PP2A previously identified as the phosphatase that acts upon the serine residue (Lowe et al., 2000). Interestingly, PP2A has been shown to localize to the Met-2 spindle (Lu et al., 2002), a region to which GM130 does not redistribute. The majority of GM130 is dephosphorylated in 2-cell embryos, except for a small band of phosphorylated protein at the site of the cleavage furrow (Figure 5.3G,H). Perhaps this retention is important for the cytokinesis process in the early embryo.

Immunofluorescence detection of the Golgi apparatus, fragmenting during meiotic maturation and reorganizing around the pronuclei during fertilization and early embryogenesis, is consistent with previous ultrastructural reports (Hyttel et al., 1986; Hyttel et al., 1988; Hyttel et al., 1989; Assey et al., 1994; Plante and King, 1994). Transmission electron microscopy has shown that the Golgi changes from well-

developed complexes at the GV stage to highly dispersed fragments at Met-2 arrest (Hyttel et al., 1986; Assey et al., 1994). In PN zygotes, the Golgi appears once again as defined complexes, or flattened stacks of lamellae, that often associate near the pronuclear membranes (Hyttel et al., 1988; P. Sutovsky, personal communication). The dynamics of GM130 observed here, together with the phosphorylated state of GM130 detected in GV and Met-2 oocytes, suggests that the fragmentation and dispersion of GM130 may accompany its phosphorylation.

Somatic cells treated with BFA show redistribution of GM130 to structures adjacent to ER domains (Ward et al., 2001). This evidence supports the view of the Golgi apparatus as a dynamic structure, the maintenance of which depends upon membrane recycling to and from the ER (Lippincott-Schwartz et al., 2000). An alternative view is that the Golgi is an autonomous organelle with stable components, capable of providing a template for its own growth and division (Shorter and Warren, 2002). Supporting evidence for this model is provided by mitotic cells, in which ER markers distribute as a fine reticulum that is excluded from areas near the spindle poles. Golgi markers - including GM130 - localize under these conditions as tiny vesicles that are enriched at the centrosome regions of the spindle (Jesch and Linstedt, 1998; Seemann et al., 2002). This association of the Golgi with the mitotic spindle is thought to ensure accurate partitioning of Golgi proteins into the daughter cells. We find here that GM130 co-localizes with the ER vesicle export site marker Sec23 and not with the meiotic spindle in Met-2 oocytes. Perhaps this preferential distribution ensures that the majority of Golgi protein remains in the oocyte and does not get expelled along with the chromosomes in either the first or

second polar bodies. Because the polar bodies are destined for degeneration, partitioning the Golgi into their cytoplasm would not be developmentally advantageous.

Interestingly, GM130 localization to ER vesicle export sites in bovine oocytes contrasts with giantin distribution to spindle poles observed in mouse oocytes (Moreno et al., 2002). This differential distribution of Golgi proteins could be attributed to the presence of a maternal centrosome in mouse oocytes and its absence in bovine (Schatten, 1994). Given that the mature bovine oocyte is acentrosomal, and because the secretory pathway is inhibited during meiotic maturation, the reorganization of Golgi during meiosis might naturally follow the mechanism of redistribution to ER export sites after BFA or nocodazole treatment. This condition would contrast with the distribution of Golgi to the spindle poles during mitosis. Conversely, the centrosome in mouse oocytes might promote Golgi localization to the meiotic spindle to partition Golgi proteins in a process distinct to rodents. Further experiments will be needed to clarify these associations, and to address the role of the centrosome in organizing the Golgi during meiotic maturation.

Pronuclear formation, migration and apposition do not require a functional secretory pathway

Because the Golgi apparatus reorganizes around the pronuclei as they unite during fertilization, membrane trafficking along microtubules might establish a physical connection between the Golgi and pronuclear membranes. This could allow the Golgi to “drag” the female pronucleus towards the centrosome attached to the male pronucleus. Treatment of pronucleate-stage zygotes with BFA, however, allowed us to determine that

neither an intact Golgi apparatus nor a functional secretory pathway is necessary for successful pronuclear migration and apposition. Golgi components on COP I vesicles (β -COP, giantin), on putative cis-matrix (GM130), and in the enzymatic pathway (mannosidase II) are all disrupted when exposed to BFA, yet the male and female pronuclei unite as in controls (Figure 5.4; Table 2). Specifically, the female pronucleus migrates along microtubules towards the male pronucleus that is usually positioned near the center of the egg (Schatten, 1994). These results contrast with previous observations using a Ca^{2+} ionophore to parthenogenetically activate mouse oocytes, in which BFA prevented female pronuclei from migrating to the center as in controls (Clayton et al., 1995). We attribute this discrepancy to different activation methods and divergent centrosome inheritance strategies between mouse and bovine (Schatten, 1994).

Golgi membranes are organized by the centriole pair and pericentriolar material of the centrosome that focuses the Golgi to a juxtannuclear position in many somatic cells (Thyberg and Moskalewski, 1999). Bull sperm, like rhesus and human, introduces the centrosome to the egg cytoplasm, resulting in centrosome attachment to the male pronucleus. Movement of Golgi membranes along microtubules could therefore accompany the migration of the female pronucleus towards the centrosome. Indeed, the dynamics of giantin and β -COP, which redistribute in meiotic mouse oocytes, identifies the likelihood of vesicle trafficking. Curiously, while BFA treatment arrests in vitro maturation (Moreno et al., 2002), it does not inhibit in vitro fertilization, highlighting a significant difference between the two events.

Cytokinesis in pre-compacted embryos may proceed in the absence of a functional Golgi apparatus

It has been shown in *Xenopus* and *C. elegans* embryos undergoing cytokinesis that new membrane is delivered to and inserted within the region of the cleavage furrow (Danilchik et al., 1998; Skop et al., 2001). This vesicle trafficking involves microtubules and is accompanied by the secretion of a variety of proteins (Straight and Field, 2000). When *C. elegans* embryos are treated with BFA, cytokinesis fails after an initial, well-formed cleavage furrow regresses (Skop et al., 2001). This failure is attributed to impaired secretion and the absence of membrane accumulation. Mouse embryos, in contrast, do not show cytokinesis failure when exposed to BFA, since activated oocytes cleave to the 2-cell stage despite an inhibited secretory pathway (Clayton et al., 1995). Our finding that bovine zygotes complete cytokinesis and divide through the eight-cell stage in the presence of BFA agrees with those observations in mouse, and suggests that mammalian embryos might not require a functional secretory pathway for cytokinesis prior to compaction.

The differential effects of BFA on cytokinesis observed in *C. elegans*, mouse, and bovine embryos might, however, be attributed to the varying concentrations of drug used in the different studies. It was noted that 15 $\mu\text{g/ml}$ BFA consistently induced cytokinesis failures in *C. elegans* without impacting cell viability, while lower concentrations did not reproduce the phenotype (Skop et al., 2001). Studies on mouse, and here using bovine, expose embryos to 5 $\mu\text{g/ml}$ BFA which, despite failing to inhibit cytokinesis, completely disrupts the Golgi apparatus and prevents the surface expression of the secretory protein E-cadherin (Figure 5.4; Clayton et al., 1995). Cytokinesis failure might therefore require

a higher concentration of BFA than that which is sufficient to disrupt the Golgi and inhibit secretion. We noted, however, that BFA concentrations higher than 5 $\mu\text{g/ml}$ were often detrimental to bovine cell cycle progression.

Loss of E-cadherin from the surface of mouse embryos impairs the cell-cell adhesion of blastomeres (Clayton et al., 1995). The process of compaction requires a significant increase in intercellular adhesion and polarization, and relies upon the preservation and maintenance of secretion. Morphological observations of bovine embryonic development in the presence of BFA suggest that both the shape and definition of the blastomeres are affected by this exposure, and that the inhibition of compaction could be due to an impaired secretory pathway. These findings raise the possibility that, while the Golgi apparatus is necessary for the expression of essential proteins on the cell surface and secretion of factors into the extracellular milieu, perhaps it is not required for cytokinesis progression in early mammalian embryos. Further studies will be needed to address these important questions concerning the role of Golgi proteins during early embryonic development.

Meiotic maturation prepares the oocyte for fertilization through a dramatic reorganization and partitioning of chromatin and cytoplasmic components. Putative Golgi matrix proteins likely associate with clusters of ER and vesicle export sites to ensure their retention for embryogenesis. Unlike mitosis, the outcome of meiosis is not an equal distribution of cytoplasmic content into daughter cells. The absence of the Golgi on the meiotic spindle reduces the likelihood of Golgi partitioning into polar bodies. Interestingly, once fertilization is underway, processes as distinct as nuclear trafficking and cytokinesis do not depend upon a functional Golgi apparatus. These results suggest

that the secretory pathway may not be essential for embryonic development prior to compaction, and that both oocyte maturation and fertilization provide unique environments in which to study Golgi protein structure and function.

Table 2

Distance between pronuclei in 1-cell zygotes:

condition of zygote	$\geq 10\ \mu\text{m}$ apart	$< 10\ \mu\text{m}$ apart
control	0% (0/127)	100% (127/127)
+ brefeldin A	0% (0/131)	100% (131/131)

Table 3**Effect of brefeldin A (BFA) on bovine embryonic development *in vitro*:**

Number of fertilized eggs at the 1-, 2-, 3/4-, 8-cell stage 90 hours after sperm addition					% of embryos at the 8-cell stage
<u>control</u>	<u>1-cell</u>	<u>2-cell</u>	<u>3/4-cell</u>	<u>8-cell</u>	
234	50	13	57	114	114/234 (48.7%)
<u>BFA-treated</u>	<u>1-cell</u>	<u>2-cell</u>	<u>3/4-cell</u>	<u>8-cell</u>	
218	48	24	49	97	97/218 (44.5%)

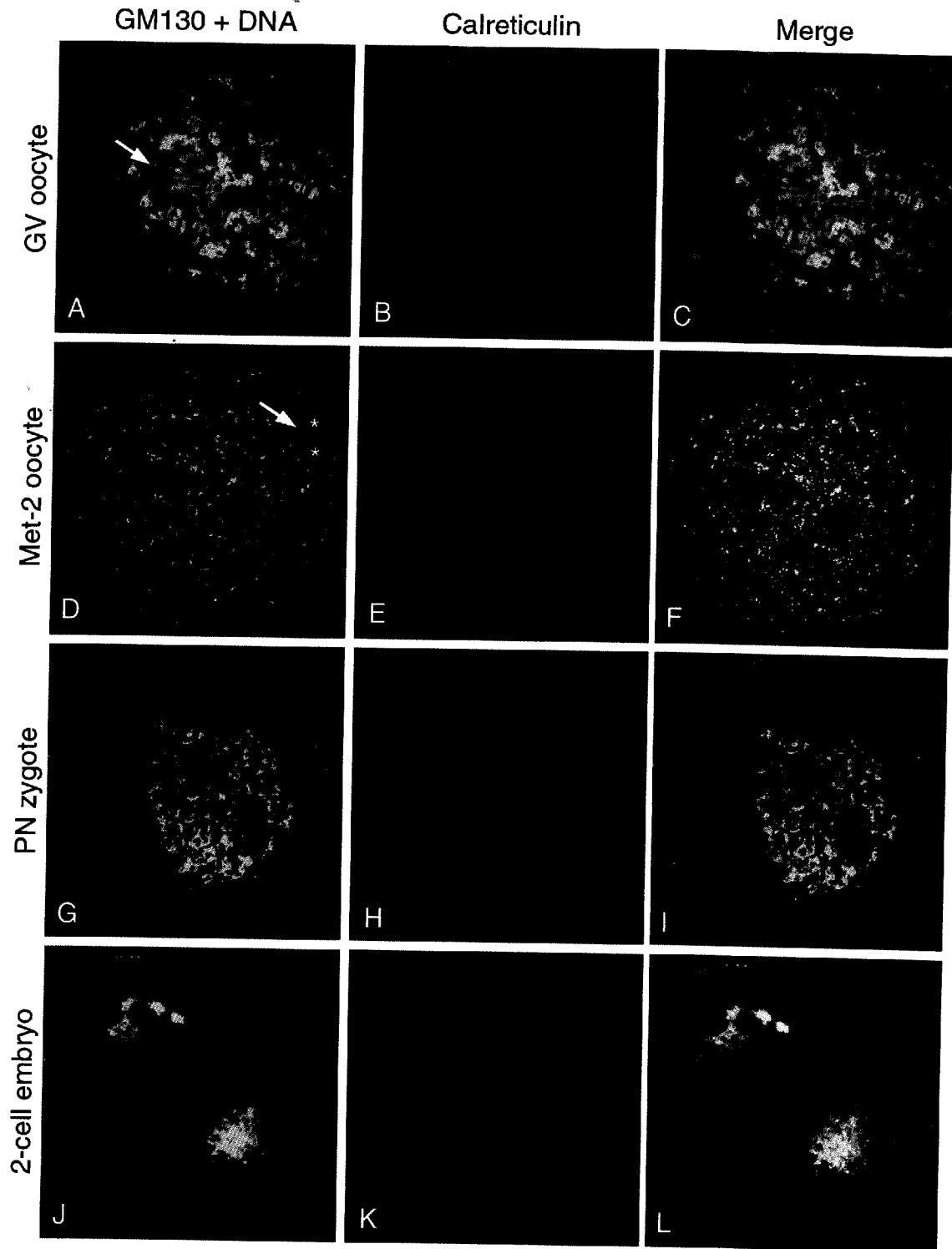


Figure 5.1. Golgi and ER dynamics during oocyte in vitro maturation, in vitro fertilization and early embryonic development. (A) GV oocytes show Golgi protein GM130 (green) dispersed in fragments throughout the ooplasm; arrow denotes GV DNA (blue). (B) ER marker calreticulin (red) localizes in a

reticulated pattern around the GV and distributes in patches near the cortex. Distinct patterns of GM130 and calreticulin are detected when the channels are merged (C). Following in vitro maturation and Met-2 arrest (D), GM130 is localized to specific ooplasmic domains in the form of punctate foci; arrow denotes Met-2 DNA and asterisks mark the meiotic spindle poles. (E) Calreticulin is now enriched in clusters throughout the cytoplasm; these clusters are detected in the same regions as the GM130 foci when the channels are merged (F). In vitro fertilization induces oocyte activation and pronuclear (PN) formation, migration and apposition (G), with GM130 dispersed once again as fragments that localize around the pronuclei. (H) Calreticulin distributes predominantly as clusters throughout the cytoplasm. Distinct patterns of GM130 and calreticulin are detected when the channels are merged (I). Following the first mitotic division and formation of 2-cell embryos (J), GM130 shows both juxtannuclear localization and cytoplasmic aggregation within the blastomeres. (K) Calreticulin distribution is enriched near the nuclei, with additional diffuse staining throughout the cytoplasm that is absent from much of the cortical region. (L) Merge of the channels shows extensive co-localization between the Golgi and the ER.

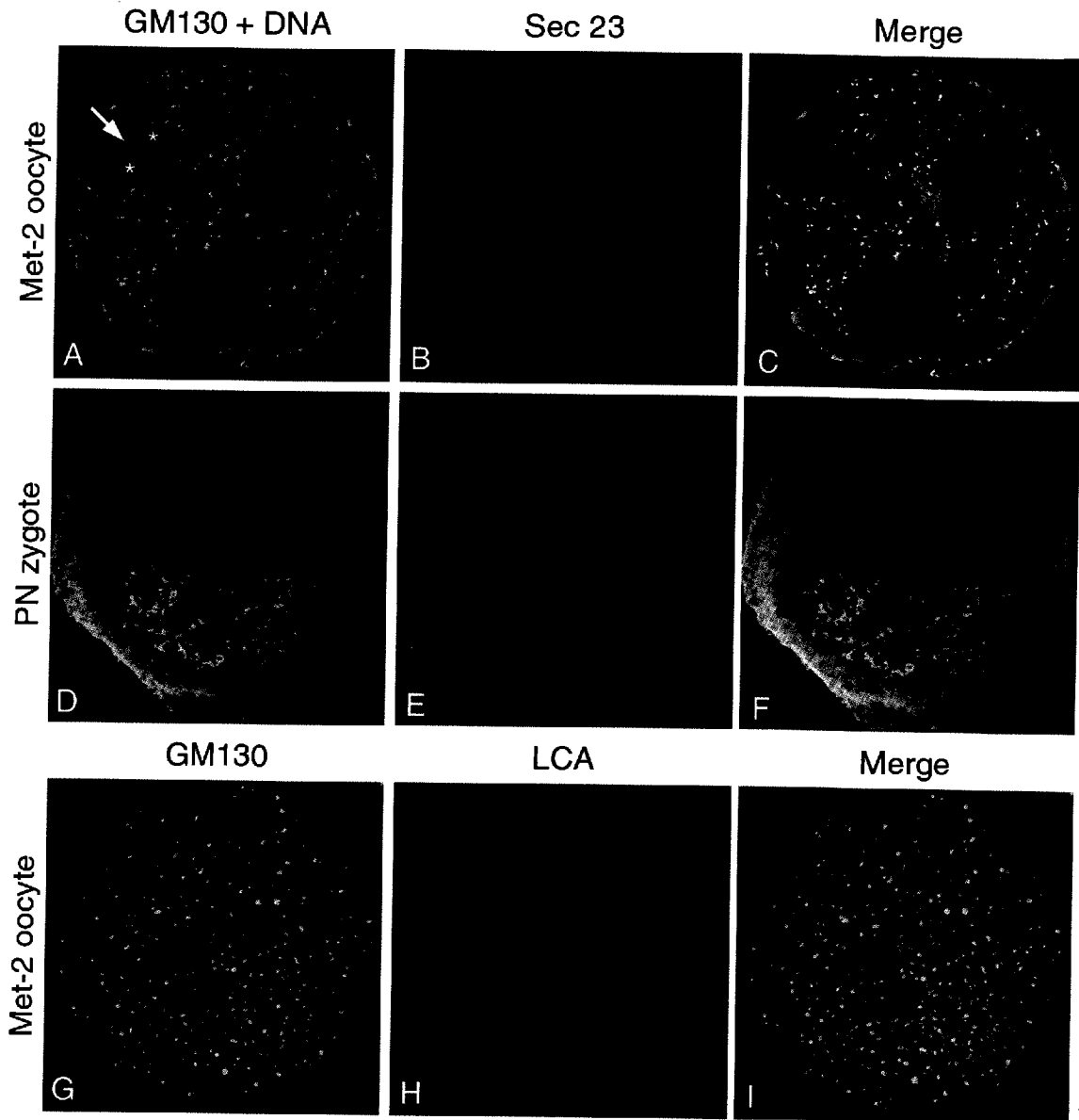


Figure 5.2. GM130 co-localizes with Sec23 at ER vesicle export sites but not with LCA at cortical granules. (A-C) Met-2 oocytes show GM130 (green) and Sec23 (red), a marker for ER vesicle export sites, co-localizing as punctate foci throughout the cytoplasm when the channels are merged (C); arrow denotes Met-2 DNA (blue) and asterisks mark the meiotic spindle poles. In pronucleate-stage (PN) zygotes (D-F), GM130 reorganizes as fragments that localize around the pronuclei. An additional band of GM130 appears near the cortex (D). Sec23 continues to distribute in the cytoplasm as punctate foci (E); co-localization between GM130 and Sec23 is now limited to the reticulated band near the cortex when the channels are merged (F). (G-I) Cortical sections of Met-2 oocytes show distinct distribution patterns for GM130 and

FITC-conjugated *Lens culinaris* agglutinin (LCA), a marker for cortical granules. No co-localization is observed when the channels are merged (I). [Note: GM130 was originally detected in (G) with 568 nm excitation (red), while LCA was detected in (H) with 488 nm excitation (green); colors were then reversed using Adobe Photoshop software.]

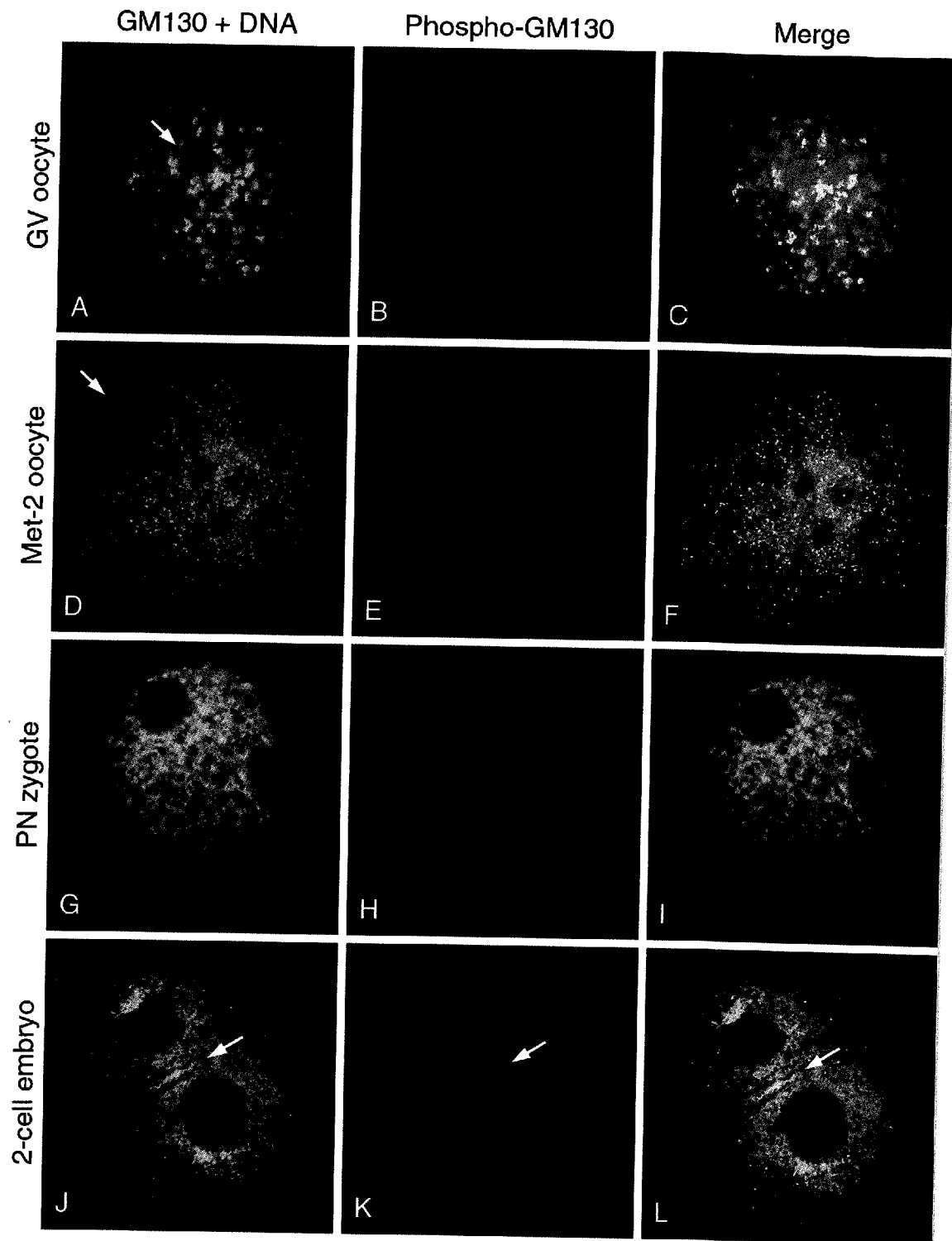


Figure 5.3. Phosphorylation cycle of GM130 during oocyte in vitro maturation, in vitro fertilization and early embryonic development. (A-C) GV oocytes show Golgi protein GM130 (green; detected with

antibody clone 35) in a phosphorylated state (red; detected with phospho-specific polyclonal antibody PS25) at prophase of meiosis I; arrow denotes GV DNA (blue). Nearly identical GM130 staining is observed when the channels are merged (C). In Met-2 arrested oocytes (D-F), the punctate GM130 is phosphorylated, with similar distribution patterns for both antibodies detected when the channels are merged (F); arrow denotes Met-2 DNA. During pronuclear (PN) migration in zygotes (G-I), GM130 is dephosphorylated, as no PS25 labeling is detected (H). In 2-cell embryos (J-L), the majority of GM130 is dephosphorylated, except for a narrow band of protein at the cleavage furrow (arrows).

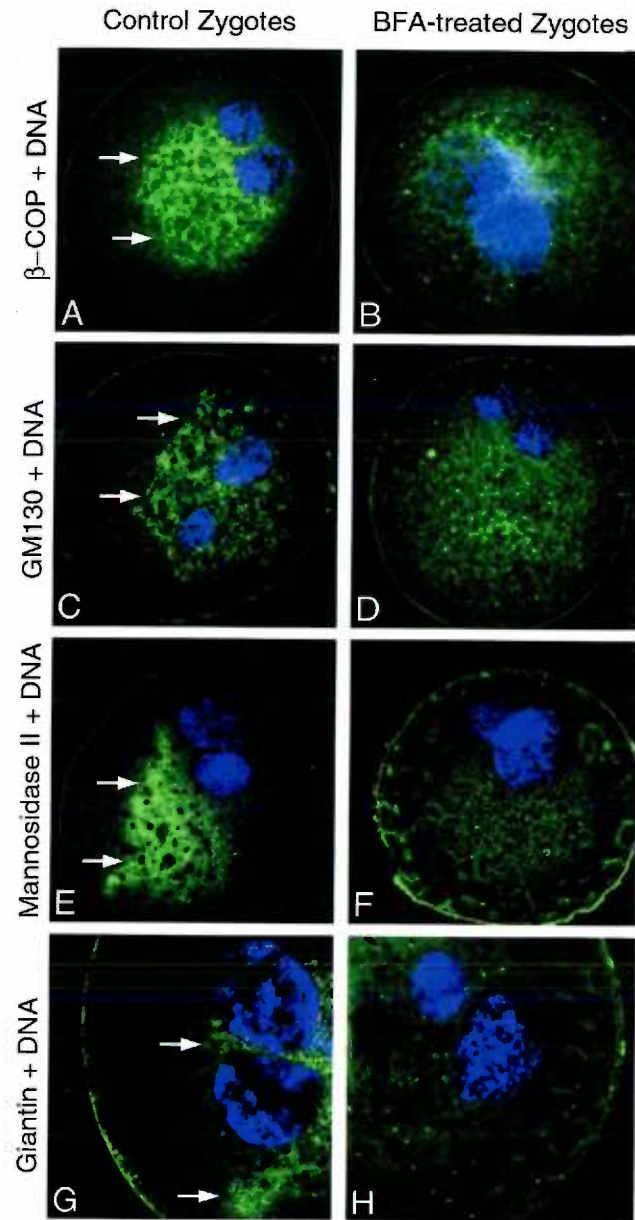


Figure 5.4. Brefeldin A (BFA) disrupts the Golgi apparatus but does not inhibit pronuclear apposition in zygotes. (A) COP I vesicle coatomer protein β -COP localizes to a region surrounding the two apposing pronuclei in control zygotes; arrows indicate the edge of the staining region. In BFA-treated zygotes (B), β -COP distributes diffusely within the cytoplasm, with additional punctate staining. Pronuclear apposition is not inhibited, however, despite nearly 20 h of exposure to BFA. In control zygotes, Golgi proteins GM130 (C), mannosidase II (E) and giantin (G) localize to regions surrounding the apposing pronuclei; arrows indicate edges of the staining regions. BFA-treatment alters the distribution of these

Golgi proteins, with punctate GM130 (D) dispersed throughout the cytoplasm, and both mannosidase II (F) and giantin (H) enriched in clusters near the cortex and dispersed as punctate foci. Despite the disruption caused to Golgi membranes, BFA does not inhibit pronuclear apposition, with all pronuclei showing surface-to-surface internuclear distances of $<10\ \mu\text{m}$. The average diameter of a pronucleus is $10\ \mu\text{m}$.

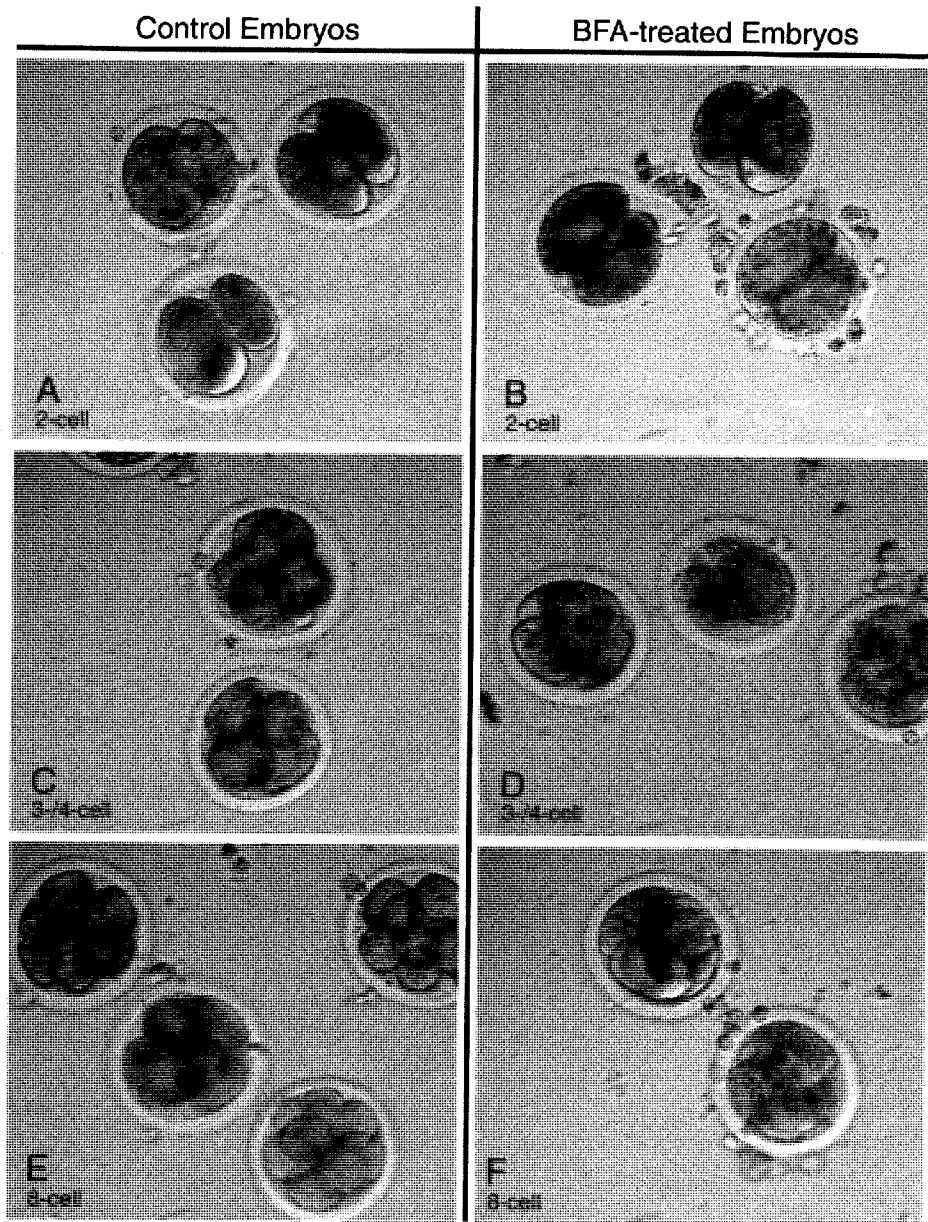


Figure 5.5. Effect of Brefeldin A (BFA) on development in early embryos. In vitro fertilized oocytes were cultured for 90 h under control conditions or in the presence of BFA. (A, B) 2-cell embryos develop from zygotes in both control (A) and BFA-treated groups (B), with the latter displaying normal outward appearance and defined cleavage furrows. The formation of 3-cell and 4-cell embryos occurs under BFA conditions (D), though outward appearance is slightly diminished and cleavage furrows are not as clearly defined as in controls (C). Eight-cell embryos develop normally in the control (E), but not the BFA-treated

group (F), in which embryos display poorly shaped blastomeres, ill-defined cleavage furrows and increased blebbing. Compaction occurs in the control embryos, but not in those treated with BFA.

Chapter 6

Summary and Conclusions

This thesis details our efforts to understand the molecular mechanisms that underlie the extensive reorganization of microtubule motor proteins, sperm-derived and oocyte-derived nuclear components, and endomembranes within the fertilized mammalian egg. Cytoplasmic dynein and its cofactor dynactin have been proposed to mediate pronuclear migration because of the direction of female pronuclear movement to the minus ends of microtubules, anchored at the sperm centrosome at the male pronucleus (Schatten, 1994, Reinsch and Karsenti, 1997; Reinsch and Gönczy, 1998). During these motility events, the Golgi apparatus reappears as flattened stacks of lamellae that often associate near the pronuclear membranes (Hyttel et al., 1988; P. Sutovsky, personal communication). It has not been clear, however, from which structures in the unfertilized oocyte these Golgi proteins are reorganizing – the endoplasmic reticulum or the meiotic spindle poles. We hypothesized that studies examining the roles and interactions of molecular motors with nuclear and cytoplasmic components during meiosis and fertilization would reveal potential molecular mechanisms that might facilitate the remarkable dynamics during these stages in development.

Dynactin Association with Dynein, LIS1 and Nuclear Pore Complexes Mediates Female Pronuclear Migration

We have shown that dynactin localizes around both the male and female pronuclei, and that it co-localizes and co-immunoprecipitates with dynein, nucleoporins and vimentin (Payne et al., 2003). Dynein, meanwhile, concentrates around only the female pronucleus, and is dependent upon the sperm aster for its localization. These results are the first identification of specific interactions between microtubule motors and the nuclear pore complex (NPC), and provides a mechanism of how the female pronucleus might physically attach to sperm aster microtubules. Dynein-dynactin association with NPCs has previously been suggested as a candidate interaction to explain other processes like nuclear envelope breakdown (Salina et al., 2002; Lénárt and Ellenberg, 2003), and is consistent with in vitro data showing that ‘artificial nuclei’ lacking nuclear membranes do not move on stabilized microtubules in the presence of dynein (Reinsch and Karsenti, 1997). Our data suggest the possibility that the dynein-dynactin complex interacts with NPCs through its association with vimentin, which is both an NPC-associated protein and a binding partner to the motor (Cronshaw et al., 2002; Helfand et al., 2002).

The preferential distribution of dynein to the female pronucleus depends upon the presence of an organized sperm aster (Payne et al., 2003). We conclude from this result that dynein might be delivered to the female pronuclear surface on the plus ends of the astral microtubules. Recent evidence in *S. cerevisiae* shows that dynein is delivered to the cell cortex on the plus ends of polymerizing astral microtubules, and that dynein accumulates at these plus ends in the absence of dynactin (Sheeman et al., 2003). This differential localization of dynein and dynactin could ensure that female pronuclear

motility is properly regulated. Centrosome-anchored microtubules in fibroblasts do not accumulate dynein at their minus ends until after entering S-phase, the cell cycle stage during which pronuclear migration begins in mammalian zygotes (Quintyne and Schroer, 2002). Proximity of the centrosome to the male pronucleus might preclude dynein from associating with the male pronuclear surface until after female pronuclear migration has begun.

One of the proteins that interacts with the dynein-dynactin complex and is necessary for neuronal migration is LIS1 (Faulkner et al., 2000; Tai et al., 2002). We have shown in this thesis that LIS1 co-localizes and co-immunoprecipitates with dynactin, and is necessary for pronuclear migration (Payne et al., unpublished data). LIS1 concentrates around the two pronuclei in the zygote, and appears to have increased mRNA and protein levels when compared to the oocyte. It is likely that LIS1 interacts with the motor complex at the pronuclear surface to facilitate motility. Chariot™ transfection of zygotes with antibodies raised against LIS1, dynein, dynactin, nucleoporins, and vimentin results in the inhibition of pronuclear union (Payne et al., 2003). The transfection of these antibodies does not disrupt sperm aster organization, however, and anti-Golgi and anti-ER antibodies transfected into zygotes do not inhibit pronuclear apposition.

Given the data accumulated from our immunolocalization, immunoprecipitation, and antibody transfection experiments, we propose a model to explain how a dynein-dynactin-LIS1 complex might regulate nuclear motility during fertilization (Figure 6.1). The formation of pronuclei likely recruits LIS1 to pronuclear surfaces, where dynactin, vimentin, and NPCs are localized. Growth of the sperm aster outward from the

centrosome would extend microtubule plus ends away from the male pronucleus, some of which reach the female pronuclear surface. These microtubule plus ends could deliver dynein to the female pronucleus, allowing dynein to bind to a LIS1-dynactin complex with NPCs and vimentin at nuclear pores. The dynein-dynactin-LIS1 complex would then be able to transport the female pronucleus along the sperm aster to the microtubule minus ends. This movement culminates with pronuclear apposition.

Golgi Proteins Do Not Associate with Meiotic Spindle Poles, But Re-Distribute Around the Pronuclei During Fertilization

We have examined the roles and interactions of Golgi protein GM130 during meiosis, fertilization, and cytokinesis, and our results provide new insights into the fate of the Golgi during meiosis as compared to mitosis, as well as during the cell cycles of fertilization and early embryonic development. In this thesis, we have shown that GM130 disperses into cytoplasmic foci during oocyte meiotic maturation, and that it associates with ER vesicle export sites but not meiotic spindle poles at Met-2 arrest (Payne and Schatten, 2003). This finding differs from the observations made in mitotic cells, in which GM130 localizes to the spindle and is enriched at the poles (Seemann et al., 2002). Instead, the Met-2 association of GM130 with ER domains resembles the interaction that occurs in somatic cells following BFA treatment (Ward et al., 2001). Because the Met-2 oocyte of most mammalian species lacks centrioles at the meiotic spindle poles, we

conclude that the absence of a maternal centrosome precludes Golgi association with the meiotic spindle.

Following sperm entry, oocyte activation, and pronuclear formation, GM130 reorganizes around the two pronuclei and appears in much larger fragments that no longer associate with clusters of ER (Payne and Schatten, 2003). The ER dynamics in bovine zygotes resemble those observed in mouse (Kline et al., 1999), with very little reorganization of the cortical clusters until mitosis. Both the Golgi apparatus and the ER distribute to more traditional locations in 2-cell embryos: focused near the nucleus and extended throughout the cytoplasm, respectively. GM130 shows nearly identical phosphorylation patterns during meiosis as compared to mitosis, however, with the serine 25 residue phosphorylated in GV and Met-2 oocytes and dephosphorylated in zygotes and the majority of 2-cell embryos (Lowe et al., 2000; Payne and Schatten, 2003).

While Golgi membranes distribute around the two pronuclei, they do not appear to influence pronuclear motility. We have shown that neither pronuclear apposition nor cytokinesis prior to compaction is inhibited following BFA treatment (Payne and Schatten, 2003). These experiments were performed in response to observations made in mouse oocytes and *C. elegans* zygotes, in which BFA appeared to inhibit nuclear migration and cell division, respectively (Clayton et al., 1995; Skop et al., 2001). The difference in our findings is perhaps due to a difference in BFA treatment conditions, or a difference in drug sensitivity between species, but we conclude that neither fertilization nor early embryonic cleavage requires a functional Golgi apparatus.

We conclude that successful meiotic maturation, fertilization and early embryonic cell division in mammals depend upon the exquisite choreography of motor proteins, endomembranes and nuclear components, all interacting within the oocyte and zygote in spatio-temporal harmony. The absence of a maternal centrosome likely influences Golgi dynamics during oocyte meiotic maturation, while the presence of a sperm centrosome likely directs motor protein dynamics of the dynein-dynactin-LIS1 complex during mammalian fertilization.

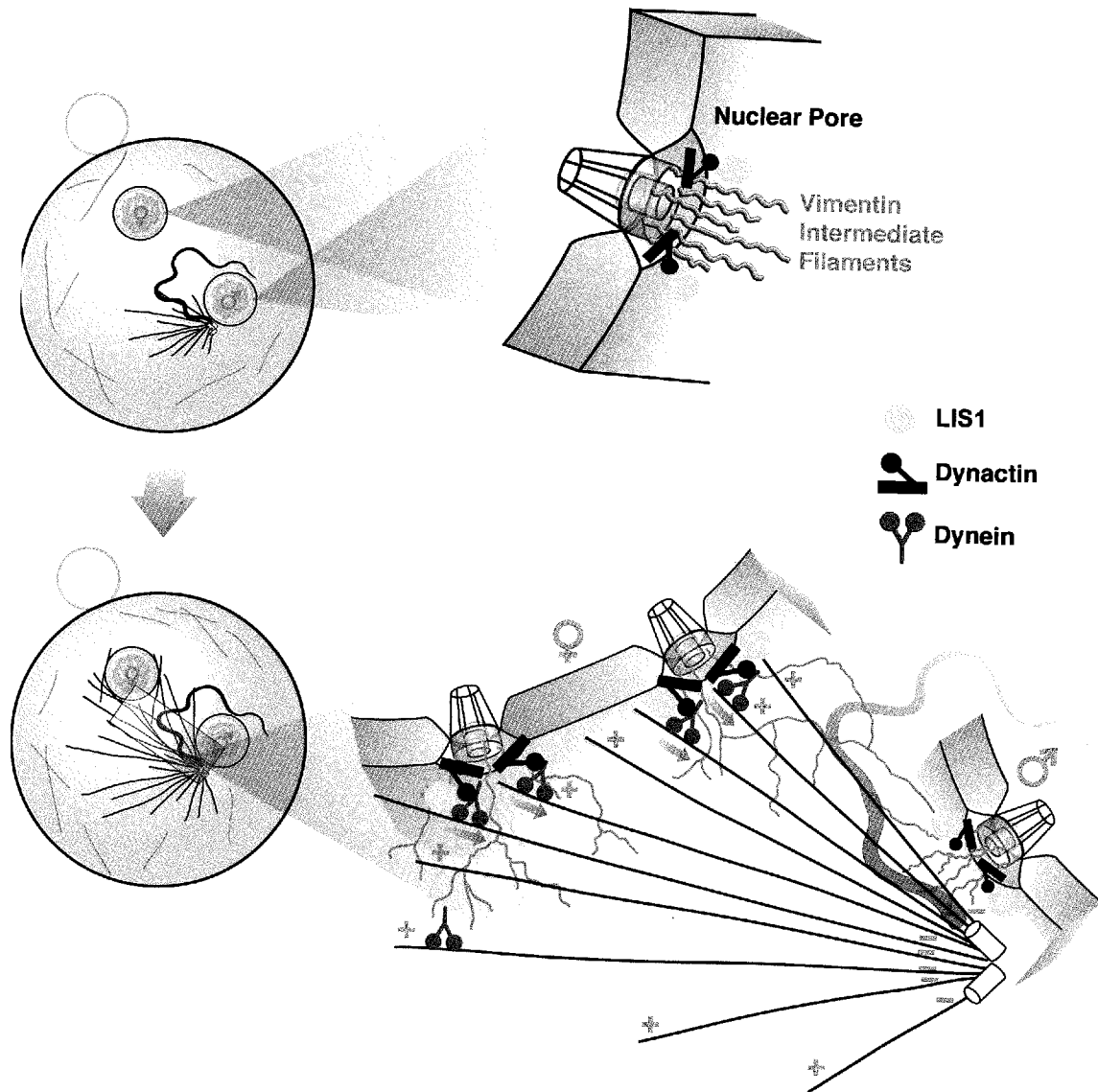


Figure 6.1. A model for nuclear motility regulated by a dynein-dynactin-LIS1 complex during fertilization. Modification of Figure 3.8. **Top:** Formation of pronuclei is likely to recruit LIS1 (yellow circle) to the cytoplasmic face of the nuclear pore complex (basket structure), where dynactin (black rectangle with side arm) and vimentin filaments (green squiggly lines) are localized. **Bottom:** Growth of sperm aster microtubules, nucleated by the centrosome attached to the male pronucleus, extends microtubule plus ends away from the male pronucleus, some of which then reach the female pronuclear surface. These microtubule plus ends could deliver dynein (red wishbone) preferentially to the surface of the female pronucleus, allowing dynein to bind to a dynactin-LIS1 complex and vimentin at nuclear pores.

The dynein-dynactin-LIS1 complex would then be able to transport the female pronucleus to microtubule minus ends along the sperm aster.

Appendix 1

Biparental Inheritance of γ -Tubulin During Human Fertilization: Molecular Reconstitution of Functional Zygotic Centrosomes in Inseminated Human Oocytes and in Cell-Free Extracts Nucleated by Human Sperm

Calvin Simerly¹, Sara S. Zoran¹, Chris Payne¹, Tanja Dominko¹, Peter Sutovsky¹,
Christopher S. Navara¹, Jeffery L. Salisbury² and Gerald Schatten¹

¹ Departments of Cell-Developmental Biology and Obstetrics-Gynecology, Oregon Health Sciences University, and the Oregon Regional Primate Research Center, Portland, Oregon 97006

² Department of Biochemistry and Molecular Biology, Mayo Clinic Foundation, Rochester, Minnesota 55905

Published in *Molecular Biology of the Cell* (1999) **10**, 2955-2969.

Summary

Human sperm centrosome reconstitution and the parental contributions to the zygotic centrosome are examined in mammalian zygotes and after exposure of spermatozoa to *Xenopus laevis* cell-free extracts. The presence and inheritance of the conserved centrosomal constituents γ -tubulin, centrin, and MPM-2 (which detects phosphorylated epitopes) are traced, as is the sperm microtubule-nucleating capability on reconstituted centrosomes. γ -Tubulin is biparentally inherited in humans (maternal >> than paternal): Western blots detect the presence of paternal γ -tubulin. Recruitment of maternal γ -tubulin to the sperm centrosome occurs after sperm incorporation in vivo or exposure to cell-free extract, especially after sperm "priming" induced by disulfide bond reduction. Centrin is found in the proximal sperm centrosomal region, demonstrates expected Ca^{2+} sensitivity, but appears absent from the zygotic centrosome after sperm incorporation or exposure to extracts. Sperm centrosome phosphorylation is detected after exposure of primed sperm to egg extracts as well as during the early stages of sperm incorporation after fertilization. Finally, centrosome reconstitution in cell-free extracts permits sperm aster microtubule assembly in vitro. Collectively, these results support a model of a blended zygotic centrosome composed of maternal constituents attracted to an introduced paternal template after insemination.

Introduction

Although the molecular characterization of the centrosome is progressing swiftly (see reviews by Brinkley et al., 1980; Schliwa et al., 1982; Kuriyama et al., 1986; McIntosh and Koonce, 1989; Rose et al., 1993; see also Davis, 1997; Stearns and Winey, 1997; Doxsey, 1998; Zimmerman et al., 1999), the precise manner in which the conserved proteins interact to form a fully functional centrosome capable of duplication is still largely unclear. γ -Tubulin appears to be an essential, invariant centrosomal protein serving both to nucleate microtubules and to define the microtubule's intrinsic polarity (Oakley and Oakley, 1989; Horio et al., 1991; Stearns et al., 1991; Zheng et al., 1991; Joshi et al., 1992; Palacios et al., 1993). In lower vertebrates such as *Xenopus* and in mice, γ -tubulin appears to be strictly acquired from the maternal cytoplasm after insemination, being lost from the mature spermatozoa probably during the latter stages of spermatogenesis (Gard, 1994; Stearns and Kirschner, 1994; Manandhar et al., 1998). Centrin, a ubiquitous, Ca^{2+} -sensitive, biparentally contributed centrosomal component, has been reported to sever axonemal microtubules from their associated basal bodies and may also be involved in centrosome duplication (Baum et al., 1986; Sanders and Salisbury, 1989, 1994; Biggins and Rose, 1994; Stearns and Kirschner, 1994; reviewed by Salisbury, 1995). Phosphorylation of centrosomal components during meiosis or mitosis is a well-conserved mechanism for regulating centrosome activity, as observed in studies in a variety of cell types with the phosphoprotein mAb MPM-2 (Davis et al., 1983; Vandr  et al., 1986).

Centrosome reconstitution during fertilization, an essential process for the initiation of development, is a unique model for exploring the molecular components necessary to determine centrosome parental origin and function (reviewed by Schatten, 1994). Classic studies (Boveri, 1901) suggested that the sperm in most animals contributes the dominant centrosome structure, because a sperm aster composed of a radial array of microtubules is focused on the cytoplasmic site adjacent to the sperm pronucleus during monospermic fertilization. Although the presence of multiple sperm asters during polyspermy supports the hypothesis that the centrosome is of paternal origin, studies on parthenogenesis and murine fertilization demonstrate that oocytes possess mechanisms to reconstitute a maternal centrosome that is capable of duplication and of forming a functional bipolar mitotic spindle (Schatten et al., 1986, 1991; reviewed by Schatten, 1994).

The cell-free system to explore the molecular events leading to centrosome reconstitution and microtubule assembly has been developed using demembranated *Xenopus laevis* sperm exposed to *X. laevis* cytostatic factor (CSF) arrested egg extracts (Doxsey et al., 1994; Félix et al., 1994; Stearns and Kirschner, 1994). These studies demonstrated that frog sperm have centrin but no detectable quantities of γ -tubulin or the phosphorylated epitopes recognized by the mAb MPM-2. After exposure to egg extracts, γ -tubulin is bound to the sperm centrosome; this binding is independent of microtubule or microfilament assembly (Stearns and Kirschner, 1994). The sperm exposed to egg extracts also became immunoreactive for MPM-2, suggesting that a phosphorylation reaction occurred. Moreover, these centrosomes were competent for nucleating microtubule growth into sperm asters.

This study explores centrosomal molecules in human and bovine gametes to understand the molecular basis of zygotic centrosomal reconstitution during nonrodent mammalian fertilization. The experimental approaches used provide a means to identify the inheritance characteristics of conserved centrosomal proteins and their fates after either in vitro fertilization or exposure to CSF-arrested *Xenopus* cell-free extracts. Surprisingly, γ -tubulin is observed to be biparentally inherited in nonrodent mammalian gametes: both human and bovine mature sperm retain γ -tubulin, as detected by Western blots. Paternal γ -tubulin is largely inaccessible in the mature spermatozoa, however, until after disulfide bond reduction. Exposure of disulfide-reduced sperm to egg cytoplasm dramatically increases γ -tubulin detection at the sperm centrosome and is a principal step in sperm aster formation in vitro. Centrin is detected in both human and bovine gametes, as demonstrated by immunostaining in mature spermatozoa and Western blots of bovine oocytes. Centrin localization at the neck region in spermatozoa is Ca^{2+} sensitive and consistently modified upon exposure to oocyte cytoplasm, either after fertilization or after exposure to cell-free extracts. Centrin is predicted to be important in the reorganization of the sperm centrosomal complex after insemination and perhaps in the subsequent splitting of the early zygotic centrosome. The phosphorylation of the human and bovine sperm centrosome is apparent after cytoplasmic exposure, as detected by the MPM-2 antibody. Taken together, the results of this work help to characterize the parental origins of specific centrosomal molecules, the process of reconstitution, and the microtubule-organizing ability of the reconstituted sperm centrosome in vitro.

Results

Exposure of lysolecithin-permeabilized *Xenopus* sperm to CSF-arrested cell-free extract leads to the accumulation of γ -tubulin at the sperm centrosome, as previously reported (Doxsey et al., 1994; Félix et al., 1994; Stearns and Kirschner, 1994; our unpublished results). In mature human sperm permeabilized with lysolecithin and fixed in methanol, <5% of the sperm demonstrated XG-1-4 γ -tubulin immunostaining at the centrosomal region by indirect immunofluorescence (Figure A1.1A,B, and A1.1L, left bar). Similar low levels of detectable γ -tubulin staining at the base of the sperm head were observed after permeabilized sperm were treated with 5 mM DTT, which reduces disulfide bonds and permits sperm nuclear decondensation in cell-free extracts (Figure A1.1C,D, arrows, and A1.1L, middle bar). However, exposure of permeabilized human sperm to CSF-arrested extract significantly increased XG-1-4 γ -tubulin detection at the sperm centrosome, especially after priming with 5 mM DTT (Figure A1.1E,F, and A1.1L, right bar). The majority of γ -tubulin observed at the base of permeabilized, DTT-treated human sperm appears to be maternally derived, in that immunodepletion of the CSF extract with the XG-1-4 γ -tubulin antibody before sperm addition did not demonstrate γ -tubulin at the base of the sperm head after anti- γ -tubulin immunofluorescence staining (Figure A1.1G,H). Similar evidence of the acquisition of maternal γ -tubulin in bovine sperm was also seen (Figure A1.1I,J).

Interestingly, a 55-kDa band was detected in Western blots of *Xenopus*, bovine, and human sperm using XG-1-4 γ -tubulin antibody (Figure A1.1K: *Xenopus* sperm, lane 1; bull sperm, lanes 2 and 3; human sperm, lane 4). Purified α - and β -tubulin protein (Figure A1.1K, lane 5) was not detected with the XG-1-4 antibody in Western blots.

Human and bovine sperm probed with antibodies against centrin are shown in Figure A1.2. The centrin antibody 20H5 bound preferentially to the centrosomal region in human sperm after permeabilization and methanol fixation, with sperm typically demonstrating one or two punctate spots (Figure A1.2A,B, arrows, and A1.2J, first bar). This staining pattern was not affected in lysolecithin-permeabilized sperm containing 2 mM CaCl_2 (Figure A1.2C,D, arrows, and A1.2J, second bar).

After 5 mM DTT treatment, sperm decondensation ensued (Figure A1.2F) and centrin antibody localization was retained at the base of the sperm head (Figure A1.2E, arrow, and A1.2J, third bar). Occasionally, the sperm heads and tails separated during this DTT priming step and centrin antibody localization remained exclusively with the sperm tails, further demonstrating that the paternal centrin protein resides within the pericentriolar region in human and bull spermatozoa. In contrast to 5 mM DTT treatment alone, however, DTT-primed sperm subsequently exposed to 2 mM CaCl_2 lost detectable centrin immunostaining at the sperm centrosome (Figure A1.2G, arrow, and A1.2J, fourth bar). Identical results were found with bovine sperm (our unpublished results).

Bull and human DTT-primed sperm subjected to Western blot analysis with the centrin mAb 20H5 and the use of techniques designed for the transfer of low-molecular-mass Ca^{2+} -binding proteins (Hulen et al., 1991) demonstrated distinct proteins migrating at ~20 kDa (Figure A1.2I: lane 1, bovine; lane 3, human). The bands observed in bovine and human sperm were similar in molecular mass to that observed after 20H5 anti-centrin immunoblotting of bacterially expressed centrin protein (Figure A1.2I, lane 4; immunoblotted with the polyclonal antibody 24/14-1). A Western blot of DTT-primed bovine sperm exposed to 2 mM CaCl_2 showed the loss of 20H5 detection, suggesting that

high external Ca^{2+} removes paternal centrin from the sperm centrosome (Figure A1.2I, lane 2).

Electron micrographs of mature nonrodent mammalian sperm often showed the presence of an intact proximal centriole but only a remnant of the distal centriole (Zamboni and Stefanini, 1971). Control immunogold labeling with anti- β -tubulin antibody demonstrated extensive decoration of the proximal centriole (Figure A1.3A,B, asterisks) and microtubule outer doublets (Figure A1.3A, arrowheads) in bovine sperm. In contrast, immunogold labeling with 20H5 anti-centrin antibody demonstrated centrin association with the ends of the centriolar cylinder in the proximal centriole only (Figure A1.3C,D, arrows and asterisks). Human sperm labeled with secondary antibody alone showed no immunogold labeling of the implantation fossa, including the proximal centriole (Figure A1.3E,F, asterisks).

Human and bovine lyssolecithin-permeabilized sperm exposed to 5 mM DTT treatment and CSF-arrested cell-free extracts demonstrated a significant reduction in the detection of 20H5 antibody labeling at the sperm centrosome after 1 h of incubation (Figures A1.3G,H, arrows, and A1.2J, fifth bar). Similar observations were made after immunolabeling with 13A1 and 3C10 mouse anti-centrin mAbs, indicating that the centrin was either lost or masked after exposure to egg cytoplasm. These observations are in agreement with human sperm centrin immunolabeling after in vitro fertilization (see Figure A1.6C, inset).

MPM-2, which recognizes phosphorylated epitopes (Davis et al., 1983), has been used successfully to demonstrate that *Xenopus* sperm centrosomes are phosphorylated after exposure to *Xenopus* egg extracts (Figure A1.4A,B) (Doxsey et al., 1994; Félix et

al., 1994; Stearns and Kirschner, 1994). The centrosomes from human and bovine sperm displayed a similar response. Only 3% of human sperm permeabilized in lysolecithin and fixed in methanol demonstrated positive MPM-2 immunostaining at the base of the sperm head (Figure A1.4C,D, arrows, and A1.4M, first bar). In contrast, more than half of the human sperm permeabilized in lysolecithin and subsequently incubated for 1 h in CSF-arrested extract were found to be positive for MPM-2 labeling (Figure A1.4E,F, arrows, and A1.4M, second bar). Priming sperm first by 5 mM DTT treatment did not increase the detection of MPM-2 staining at the base of the human sperm (Figure A1.4G,H, arrows, and A1.4M, third bar) until after CSF-arrested extract exposure (Figure A1.4I,J, arrows, and A1.4M, fourth bar). Although a punctate MPM-2 immunostaining pattern of the sperm head, midpiece, and principal piece of the sperm tail was sometimes observed in mature spermatozoa, the immunostaining pattern was clearly more pronounced at the junction between the sperm head and tail after extract exposure. This observation was in good agreement with the pronounced MPM-2 decoration of the sperm centrosomal area after bovine sperm incorporation in vivo (Figures 6.4K,L, arrows, and 6.6D, arrow).

Microtubule nucleation and assembly into the sperm aster, using human or bovine centrosomes as templates, is demonstrated in Figure A1.5. *Xenopus* sperm, permeabilized in lysolecithin and incubated in a CSF-arrested extract containing rhodamine-conjugated tubulin, assembled microtubules in vitro after a 10-min incubation at room temperature (Figure A1.5A, red). In both human and bovine sperm, in vitro microtubule assembly was observed at the base of the sperm head, but only after membrane permeabilization with lysolecithin, 5 mM DTT treatment, and exposure to CSF-arrested egg extract for up to 1 h (Figure A1.5B,C, red). Extended incubation periods of human or bovine sperm resulted

in extensive random microtubule polymerization and stabilization onto the decondensing nuclei, as observed by Ohsumi et al. (1986). However, the possibility of unanchored microtubules assembling and secondarily associating with the sperm chromatin was not observed in these CSF extracts, because very few free microtubules were assembled within 1 h of extract treatment (note the background of Figure A1.5) (Verde et al., 1990; Stearns and Kirschner, 1994). Exposure of permeabilized, DTT-treated human sperm to rhodamine tubulin in Pipes buffer without previous CSF extract treatment did not lead to microtubule assembly in vitro from the sperm centrosome (Figure A1.5D, arrow).

The sperm aster, a radially symmetrical array of microtubules nucleated from the sperm centrosome, assembles within hours of sperm entry in bovine (Navara et al., 1994) and human (Simerly et al., 1995) oocytes. Astral microtubules (Figure A1.6A, red) emanated from the base of the incorporated, decondensed bovine sperm head (Figure A1.6A, blue; M, male pronucleus; F, female pronucleus), which coincided with γ -tubulin immunoreactivity (Figure A1.6A, arrow, green). Similar microtubule and γ -tubulin immunostaining patterns have been observed in early human zygotes (Simerly et al., 1995).

In a dispermic human oocyte at first mitotic metaphase (Figure A1.6B, blue), each sperm axoneme terminated at one pole of the bipolar mitotic spindle (Figure A1.6B, red, arrows). γ -Tubulin was detected as four bright punctate sources, two at each of the spindle poles (Figure A1.6B, green). In contrast to fertilized oocytes, however, γ -tubulin was undetectable at meiotic spindle poles in mature human or bovine oocytes (not shown), although a prominent 55-kDa band was observed on Western blots using unfertilized bovine oocytes (Figure A1.6E).

Consistent with the observation that centrin immunostaining is reduced at the base of the human sperm head after exposure to cell-free extracts in vitro (Figure A1.3G,H), 20H5 centrin antibody localization (Figure A1.6C, inset) was not observed in microtubule-containing asters (Figure A1.6C, red, arrows; incorporated sperm tail, arrowhead) of a pronucleate-stage human zygote (Figure A1.6C, blue; M, male pronucleus; F, female pronucleus).

In inseminated bovine oocytes, MPM-2 immunostaining of two bright dots (Figure A1.6D, green, arrow) within the developing sperm aster (Figure A1.6D, red) was observed after sperm incorporation (Figure A1.6D, blue; M, male pronucleus; F, female pronucleus), consistent with the observation that zygotic centrosomal phosphorylation occurs during the early stage of sperm aster formation in vivo.

Discussion

This study explores the gametic centrosomal contributions to the zygote and the process by which they form a complete, functional, and replicative microtubule-organizing center during fertilization. Although each gamete contributes equal amounts of genetic information at fertilization, the egg provides the stockpiles of proteins and the energy, cellular machinery, and environment needed for the initial phase of embryonic development. Among the crucial events necessary for early development is the reconstitution of the sperm centrosome (Schatten, 1994). The “procentrosome” (Stearns, 1995) of the mature nonrodent mammalian sperm is the paternally contributed component that must attract and organize maternal centrosomal proteins capable of

microtubule nucleation and duplication into the zygotic centrosome. The implication is that each gamete contains critical, complementary protein components but does not possess a fully functional centrosome without gametic union. A reconstituted zygotic centrosome, composed of a blend of maternal and paternal centrosomal proteins, has additional functions unique from somatic cell centrosome functions: it must choreograph the union of the parental genomes and establish the initial cleavage axis, thereby greatly influencing the distribution of organelles, cytoplasm, and all subsequent cell divisions.

Questions might be posed as to the relevance of extracts prepared from *Xenopus* oocytes as a reliable indicator for exploring early fertilization events in mammalian oocytes. Concerns regarding the use of frog cell-free extracts might include intracellular species specificity for the mammalian zygotic centrosome reconstitution, including the inability of maternal centrosomal proteins from *Xenopus* to associate with the human sperm centrosome, as well as the presence of disulfide bonds in the mammalian sperm heads. However, centrosomal fractions from diverse species such as sea urchins and *Tetrahymena* will nucleate asters after microinjection into *Xenopus* eggs (Heidermann and Kirschner, 1975; Maller et al., 1976; Karsenti et al., 1984). In addition, a high degree of evolutionary conservation of centrosomal proteins, such as γ -tubulin, centrin, and pericentrin, argue against this concern (Oakley, 1992; Zimmerman et al., 1999). Both human and *Xenopus* sperm added to extracts simultaneously result in both sperm centrosomes attracting γ -tubulin.

Past studies have shown that cycling frog extracts mimic many aspects of the cell cycle in vivo, including events such as semiconservative DNA replication, nuclear envelope breakdown and reformation, cell cycle alterations in microtubule dynamics, and

membrane vesicle fusion (Murray, 1991). Recent evidence has also shown that the human sperm genome can be completely replicated in *Xenopus* extracts (Xu et al., 1998). Both *Xenopus* and mammalian oocytes are arrested at metaphase of second meiosis by cytostatic factor, and both species are fertilized at this stage. At fertilization, sperm fusion with the oocyte induces an increase in intracytoplasmic Ca^{2+} that presumably inactivates both CSF and maturation-promoting factor, allowing these oocytes to pass from metaphase II arrest into interphase. The first mitotic cycle in frogs is only 75 min, whereas those of primate and bovine oocytes are 24–36 h, and *Xenopus* egg cytoplasm does not efficiently reduce the cysteine-rich disulfide bonds in protamines in mature mammalian sperm (Brown et al., 1987; Lohka and Maller, 1988). Nevertheless, this study is focused only on the very early events occurring in CSF-arrested frog extracts that permit the assembly of the zygotic centrosome, including the ability to bind maternal γ -tubulin, the Ca^{2+} sensitivity of centrin localized to the sperm proximal centriole, and the phosphorylation of centrosomal epitopes in M-phase extracts as might occur during the early stages of sperm penetration in mammalian oocytes.

Immunofluorescence and Western blotting with human, bovine, and *Xenopus* sperm suggest that paternally derived γ -tubulin is present in modest amounts before exposure to egg cytoplasm (Figure A1.1), albeit at concentrations nearing detection thresholds (Félix et al., 1994; Stearns and Kirschner, 1994). The variability in detection of γ -tubulin in mature spermatozoa by immunofluorescence suggests that paternal γ -tubulin may be largely inaccessible until after cytoplasmic exposure. In addition, the presence of any paternal γ -tubulin in the mature spermatozoa is not sufficient to assemble microtubules in vitro without previous exposure to cytoplasmic extract (Figure A1.5D).

The introduced paternal γ -tubulin may be necessary for attracting larger amounts of maternal γ -tubulin protein to the centrosome, a step critical for nucleation of a small sperm astral array. The unveiling of γ -tubulin at the sperm centrosome may be a direct consequence of sperm head decondensation, in which the loosening of the tightly compacted implantation fossa is linked to the loosening of the tightly compacted sperm chromatin by disulfide bond reduction. Alternatively, disulfide bond reduction may directly unfold the highly condensed procentrosomal structure, thereby exposing hidden γ -tubulin and γ -tubulin-binding sites. This would enable the reconstituting zygotic centrosome to acquire additional maternal γ -tubulin for nucleation of microtubules, which, in turn, would promote the attraction of yet more maternal γ -tubulin for building the microtubule sperm astral array. Support for this sequence of events is provided by the detection of γ -tubulin in mature bovine oocytes in Western blots (Figure A1.6E) and by the finding that the mature *Xenopus* oocyte is enriched in γ -tubulin in the cortical region (Gard, 1994), suggesting that any newly incorporated sperm has immediate access to an oocyte's centrosomal protein pool. The nature of the γ -tubulin-binding protein's effect on the sperm centrosome is unknown, although it may be linked to the presence of the γ -tubulin ring complexes (Moritz et al., 1995; Zheng et al., 1995). If this model is correct, there are serious clinical implications for patients being treated for infertility by intracytoplasmic sperm injection, in which, typically, a single spermatozoan is microinjected deep into the oocyte's center rather than into the cell cortical region.

Centrin is a paternal centrosomal component in human and bovine sperm that appears to reside in the proximal centriole (Figure A1.3). Interestingly, centrin is also strongly detected by Western blots in bovine oocytes, although no centrin is detected in

the assembled sperm asters by immunofluorescence in either human (Figure A1.6C, inset) or bovine (our unpublished results) zygotes. This observation agrees with cellular fractionation experiments, which demonstrate that the vast majority of cytoplasmic centrin is not associated with the centrosome (Paoletti et al., 1996). Three human centrin genes, *Hcen1p*, *Hcen2p*, and *Hcen3p*, have recently been cloned (Lee and Huang, 1993; Errabolu et al., 1994; Middendorp et al., 1997) and are localized in several cell types with the anti-centrin mAb 20H5. Although *Hcen2p* and *Hcen3p* stain the centrosomes of ciliated and nonciliated cell types, *Hcen1p* stains only the centriolar region of ciliated cells (Salisbury, 1995). Perhaps the *Hcen2* and *Hcen3* gene products are found in both gametes, whereas the *Hcen1* gene product is exclusively parceled to the sperm, so that the epitope recognized by 20H5 more closely resembles that of a specific region on the *Hcen1* gene product, thereby explaining the differential staining between gametes. Alternatively, centrin could be functionally and immunologically hidden within the oocyte by forming complexes with other proteins. Although no 20H5 centrin detection has been observed in early zygotes, egg activation events could induce a disassembly of this complex and result in the liberation of centrin for participation in later mammalian embryonic development after the first cell cycle.

Centrin has been localized to the stellate fibers of the transition zone between the basal body and the axoneme (Sanders and Salisbury, 1989; Baron et al., 1992) and to the distal lumen of the centrioles in animal cells (Paoletti et al., 1996; Middendorp et al., 1997). Indirect and direct evidence implicates centrin as a Ca^{2+} -binding protein that undergoes ultrastructural and distributional changes upon alteration of Ca^{2+} levels (Sanders and Salisbury 1989, 1994; Baron et al., 1994; Errabolu et al., 1994). In

Chlamydomonas, it has been suggested that Ca^{2+} induces centrin proteins to “contract” and exert shear force and torsional load on the axonemal doublets, resulting in flagellar severing (Sanders and Salisbury, 1994). In human and bovine sperm, centrin also displays a Ca^{2+} sensitivity after DTT priming and exposure to >1 mM CaCl_2 , as observed by both immunofluorescence (Figure A1.2G) and Western blots (Figure A1.2I). Fertilization is also accompanied by an increase in intracellular Ca^{2+} (reviewed by Whitaker and Swann, 1993). One of the proposed functions for an increase in intracellular Ca^{2+} might be a centrin-induced uncoupling of the sperm tail axoneme from the basal body, although clearly the sperm axoneme is not severed from the proximal centriole in the human or bovine sperm during the first cell cycle. This loosening of the sperm centrosomal region might initiate a functional and structural conversion of the sperm basal body to that of a mature centriole. Perhaps the increase in intracellular Ca^{2+} also aids in breaking the tether between mother and daughter centrioles before replication (Bornens et al., 1987) or in the separation of centrioles at anaphase. In frogs, the microinjection of recombinant heterologous centrin into one blastomere of a two-cell frog embryo impaired early amphibian development by disrupting cytoplasmic microtubules, nuclear segregation, and cytokinesis (Paoletti et al., 1996).

This study suggests that the human sperm centrosome contains γ -tubulin, albeit inaccessible as a result of centrosomal protein folding or compaction induced by disulfide bond formation. The oxidation state of mammalian sperm has also been well characterized. It has been reported that the oxidation of sulfhydryl groups occurs in sperm heads and tails as they mature during their passage through the epididymis (Calvin et al., 1973; Kosower and Kosower, 1987; Shalgi et al., 1989). Mammalian sperm chromatin, in

contrast to that from *X. laevis*, contains cysteine-rich protamines in the oxidized state that become reduced by endogenous reductases shortly after sperm penetration, allowing for the exchange of protamines for histones (Rodman et al., 1981; Perreault et al., 1984, 1987; Ward and Coffey, 1991; Bellvé et al., 1993). The reducing environment of the mammalian oocyte also provides the means for breaking disulfide bonds and allowing pronuclear decondensation, centrosomal exposure, and possibly centrosomal decondensation. Oxidizing and reducing compounds will affect microtubule stability, presumably by acting on the centrosome (Mazia and Zimmerman, 1958; Mellon and Rebhun, 1976; Oliver et al., 1976). Interestingly, these observations on the oxidative cycles in mammalian gametes are supported by research into thiol cycles, which have been shown to correspond precisely with other cell cycle events, such as DNA decondensation, and the state of centrosomal condensation during mitotic spindle formation (Mazia and Zimmerman, 1958; Mazia, 1961). It is interesting to speculate that these cyclical changes in the centrosome oxidation state could account for the expansion and contraction observed in this structure as it progresses through the cell cycle.

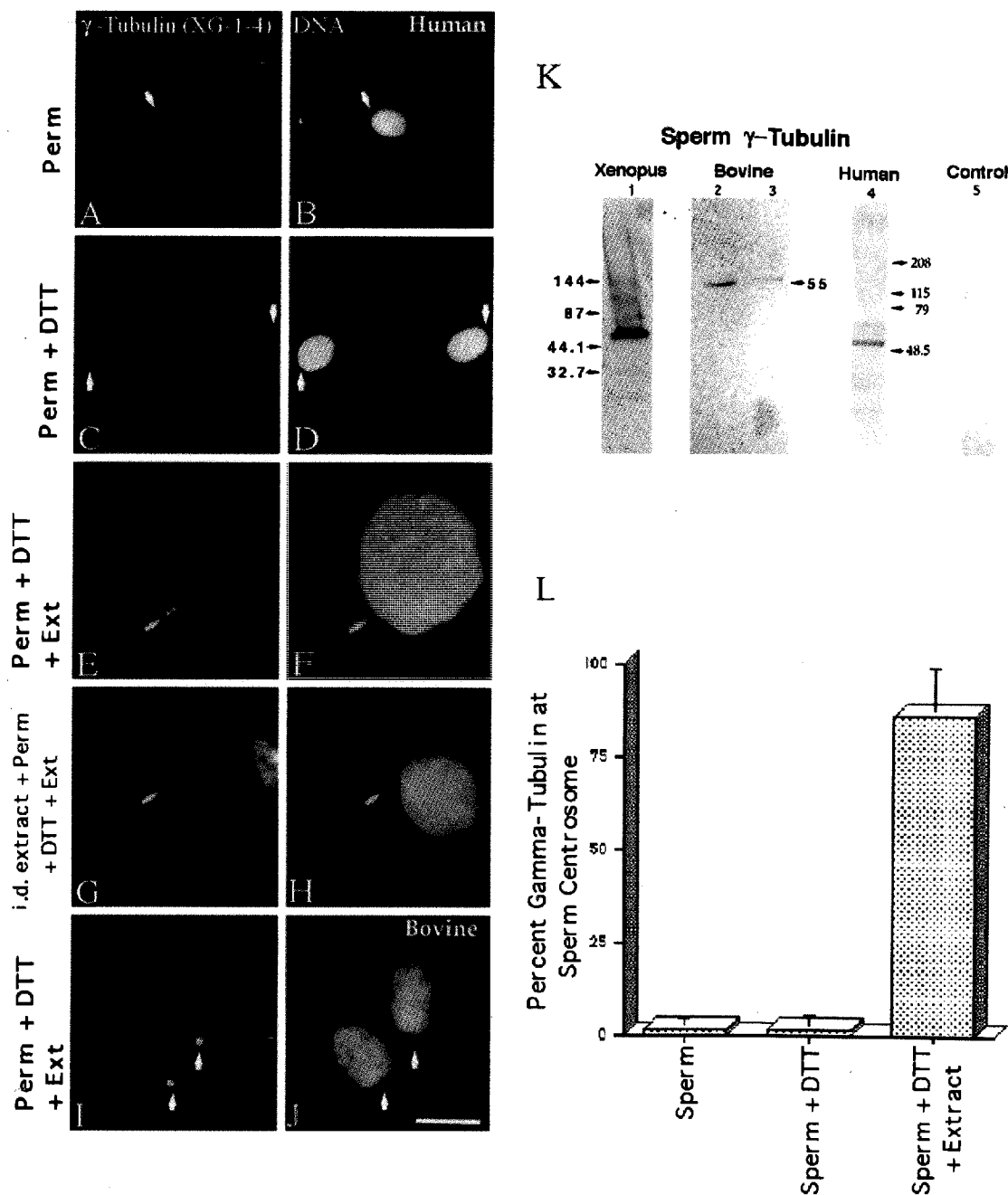
The MPM-2 results reported in this study differ slightly from the observations of Pinto-Correia et al. (1994) and Long et al. (1997). In those studies, the phosphoprotein antibody was detected in bull, rabbit, boar, and mouse sperm in the outer dense fibers and connecting piece within the neck region before insemination. Dephosphorylation of these midpiece components occurred after the Ca^{2+} -induced maturation-promoting factor decline associated with sperm penetration, resulting in sperm aster microtubule assembly in vivo. Although we occasionally observed MPM-2 punctate staining in the head, midpiece, and principal piece in bovine and human spermatozoa, a positive detection of

MPM-2 antibody at the sperm centrosome was found in <5% of the mature spermatozoa, whether permeabilized or exposed to disulfide bond reduction (Figure A1.4M). However, a significant increase in phosphorylation of the human sperm centrosomal region occurred after exposure to CSF-arrested egg extract, which is in agreement with the detection of MPM-2 in the decondensing sperm head after rabbit fertilization in vitro (Pinto-Correia et al., 1994). In addition, we also observed MPM-2 immunostaining at the sperm centrosome during early bovine sperm incorporation after in vitro fertilization (Figure A1.4L) and during the early stages of sperm aster formation in vivo (Figure A1.6D).

Many kinases are present and functional in CSF-arrested *X. laevis* egg extracts, including p34cdc2 and MAPKs (reviewed by Murray and Hunt, 1993). In mammalian oocytes, sperm incorporation and sperm aster formation overlap with the completion of second meiosis. Maturation-promoting factor activity, as measured by H1 kinase activity, decreases after sperm incorporation, although microtubule and chromatin configurations remain in a metaphase-like configuration for several hours after oocyte activation, probably as a result of high MAPK activity (Choi et al., 1991; Verlhac et al., 1994). This unique transition period between the completion of second meiosis and the first interphase in mammals may be important for sperm nuclear remodeling events, including reconstitution of the zygotic sperm centrosome. Nevertheless, pronuclear migration occurs strictly during interphase, requiring continued microtubule nucleation, organization, and interaction with chromatin or nuclear envelopes (Harrouk and Clarke, 1993; Steffen-Zoran et al., 1993). For this degree of microtubule dynamics, some kinase activity would be expected.

Centrosome reconstitution appears to be a multistep process occurring between the end of second meiosis and the transition into interphase of the first cell cycle. Microtubule nucleation and organization capabilities must function properly and quickly to form the sperm aster, the structure responsible for pronuclear migration. After pronuclear apposition, the centrosomes must replicate and split to provide the correct number of microtubule organizing centers necessary to form the bipolar mitotic spindle apparatus. Analysis of human and bovine sperm in cell-free extracts has provided clues to the milestones that must be reached before a zygotic centrosome is functional to organize microtubules in vitro. In lower animals such as amphibians, zygotic centrosome formation is microtubule and microfilament independent but egg extract and ATP dependent (Stearns and Kirschner, 1994). Mammalian sperm, exposed to increased levels of Ca^{2+} and with the plasma membrane destabilized, must be treated to disulfide bond reduction to extricate the sperm mitochondria, outer dense fibers, and fibrous sheath structures. This may expose the sperm centrosome to the maternal cytoplasmic environment, and, concomitant with the onset of pronuclear decondensation also initiated by disulfide bond reduction, the sperm centrosome unveils γ -tubulin and other centrosomal protein-binding sites. A large, cortically derived maternal γ -tubulin pool, which can accumulate into spindle poles during parthenogenesis, is typically attracted and bound to the sperm procentrosome after insemination and, with phosphorylation, shifts the microtubule dynamics to a state of nucleation and polymerization (reviewed by Schatten, 1994). Although speculative, this study characterizes the presence of centrin, γ -tubulin, and the state of centrosomal phosphorylation in nonrodent gametes, demonstrating steps in the normal sequence of events that transform the mature

mammalian sperm into an active participant in the zygote, i.e., the intracellular priming of the sperm centrosome induced by endogenous disulfide bond reduction within the mammalian oocyte's cytoplasm.



Very similar observations have been observed in bovine spermatozoa treated in exactly the same manner. However, both human (E and F) and bovine (I and J) spermatozoa treated with 5 mM DTT followed by CSF-arrested cell-free extract exposure demonstrated extensive DNA decondensation after 1 h (F and J) and XG-1-4 γ -tubulin immunolocalization at the sperm centrosomal regions (E and I; arrows point to the sperm centrosomal region). Immunodepletion of γ -tubulin from the CSF-arrested extracts by the XG-1-4 γ -tubulin abolishes detection of γ -tubulin at the base of permeabilized, DTT-treated human spermatozoa, demonstrating that the vast majority of γ -tubulin is maternally derived (G and H). (K) Western blot analysis of *Xenopus*, human, and bovine sperm demonstrates prominent bands at ~55 kDa with the XG-1-4 antibody, indicating the presence of paternal γ -tubulin in these sperm. Lane 1, *Xenopus* sperm, 1.25×10^6 sperm per lane; lane 2, bovine sperm subjected to Percoll density centrifugation, at $\sim 2.6 \times 10^6$ sperm per lane; lane 3, washed bovine sperm without Percoll separation, at $\sim 2.6 \times 10^6$ sperm per lane; lane 4, human sperm subjected to Percoll density separation and labeled with XG-1-4 γ -tubulin antibody, $\sim 2.5 \times 10^6$ sperm per lane; lane 5, 0.5 μ g of purified α - and β -tubulin, demonstrating no cross-reactivity of these tubulin superfamily members with the XG-1-4 γ -tubulin antibody. (L) Graphic representation of permeabilized human spermatozoa immunostained with γ -tubulin XG-1-4 antibody after permeabilization, DTT priming, and CSF-arrested cell-free extract. By immunofluorescence, very little paternal γ -tubulin is observed in permeabilized human sperm (left bar) or permeabilized human sperm primed by exposure to 5 mM DTT (middle bar). However, a significant increase in the detection of γ -tubulin is observed when permeabilized and primed sperm are treated with CSF-arrested cell-free extract (right bar). All images were double labeled for γ -tubulin and Hoechst DNA. (Arrows) Sperm centrosomal region as observed with phase or differential interference contrast optics. Bar in J, 10 μ m.

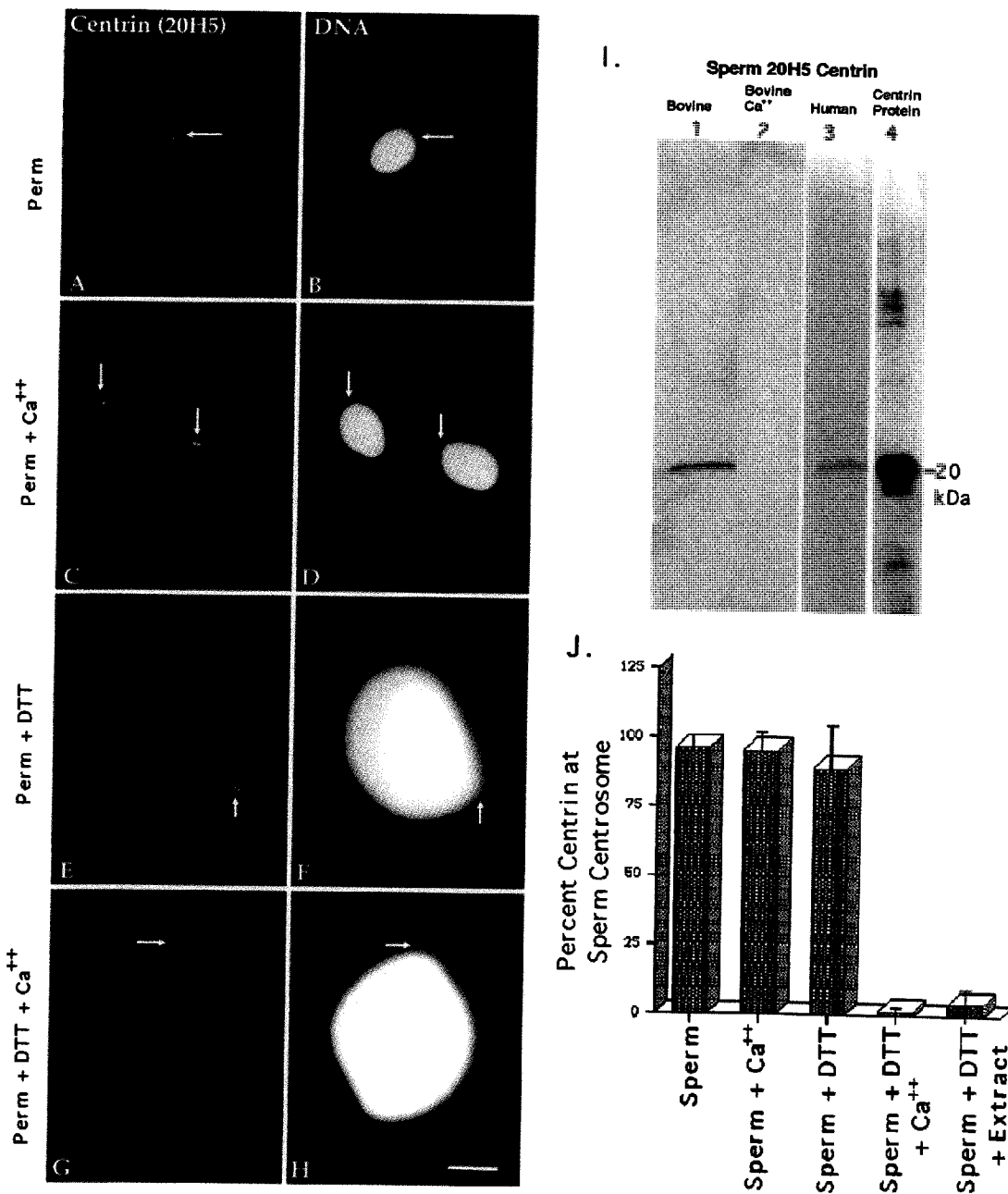
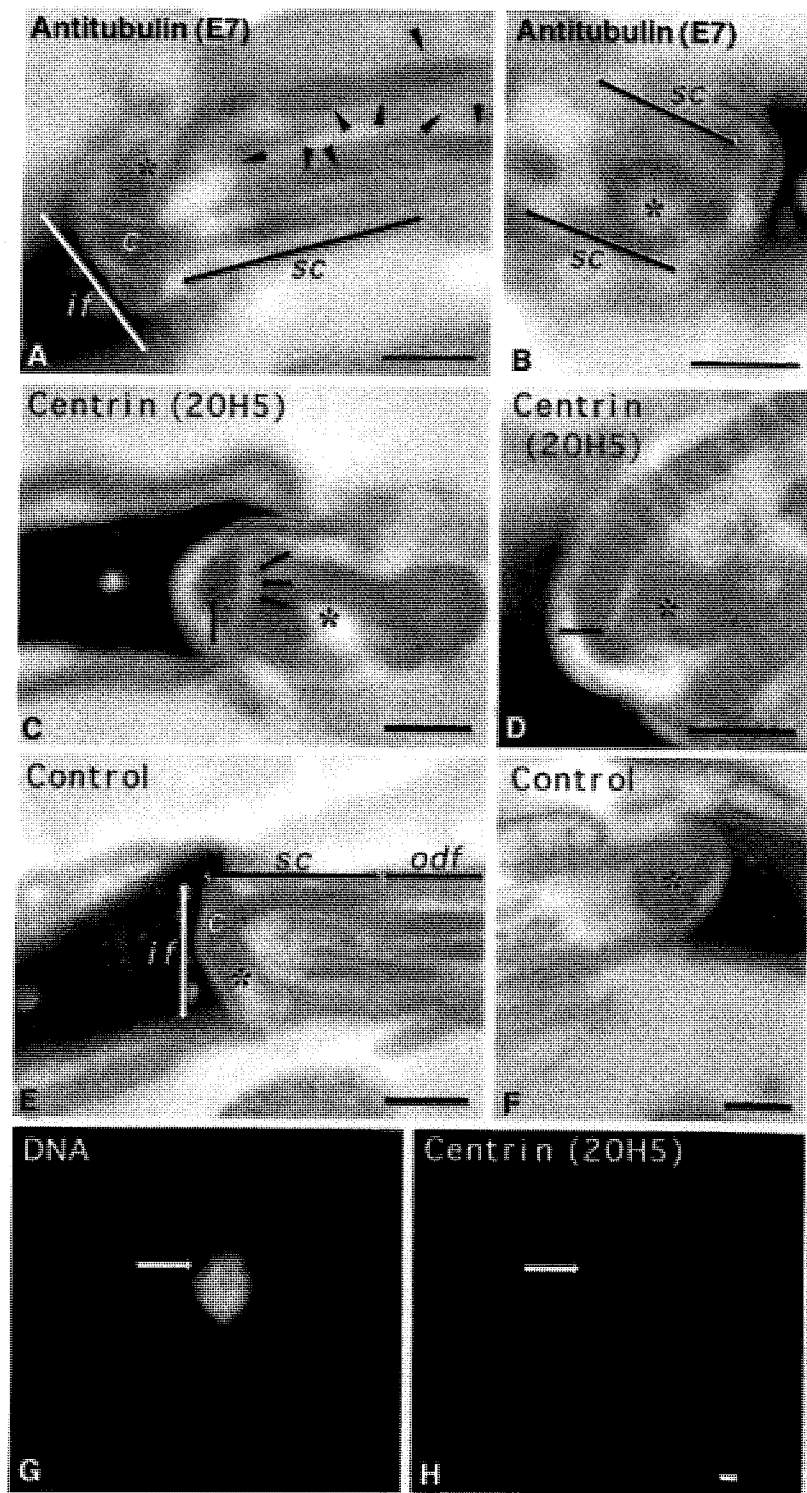


Figure A12. Centrin in human sperm centrosomes. Centrin is localized exclusively as either a pair of punctate sources or a single spot (depending on orientation) at the centrosome in permeabilized human sperm (A, centrin antibody 20H5; B, DNA) or permeabilized spermatozoa exposed to 2 mM CaCl_2 (C and D). This staining is not dependent on Ca^{2+} exposure. Sperm exposed to 5 mM DTT (E and F) for 40 min show no change in the centrin-staining pattern from controls. However, spermatozoa exposed to DTT and 2 mM CaCl_2 show a dissipation of centrin staining (G and H). Arrows indicate the point of tail attachment to

the sperm head as observed with phase or differential interference contrast optics. Identical results were found with bovine sperm. (I) Western blots of bovine and human sperm, demonstrating a single band at ~20 kDa that co-migrates with bacterially expressed centrin and the Ca^{2+} sensitivity of sperm centrosomal centrin. Lane 1, DTT-primed bovine sperm (60 μg of total protein per lane); lane 2, DTT-primed bovine sperm treated for 30 min with 2 mM CaCl_2 , showing the loss in 20H5 centrin detection after high external Ca^{2+} treatment (43 μg of total protein per lane); lane 3, human sperm, immunoprecipitated with 20H5 anti-centrin and immunostained with anti-centrin serum 24/14-1; lane 4, purified bacterially expressed centrin protein immunostained with anti-centrin serum 24/14-1. (J). Graphic representation of human spermatozoa immunostained with 20H5 centrin after permeabilization, DTT priming, and elevated external Ca^{2+} exposure. Analysis reveals that DTT-primed spermatozoa treated with either high external Ca^{2+} (fourth bar) or CSF-arrested extract (fifth bar) demonstrate a significant reduction in the detection of centrin at the sperm centrosome. Bar in H, 10 μm .



FigureA1.3. Ultrastructural detection of centrin in the bovine mature sperm centrosome and its sensitivity to CSF-arrested cell-free extract. (A and B) Immunogold labeling of mature bovine

spermatozoa with anti- β -tubulin antibody, demonstrating extensive immunolabeling of the sperm proximal centriole (asterisks) and outer microtubule doublets of the sperm axoneme (A, arrowheads). (C and D) Immunogold labeling of mature bovine sperm with anti-centrin antibody 20H5. In C, a longitudinal section of proximal centriole in the sperm tail connecting piece is observed, with centrin localized to its capitulum-attached end (arrows). (D) Oblique sections of the proximal centriole demonstrating centrin detection in an area of the centriole adjacent to the striated columns of the connecting piece. (E and F) Control bovine spermatozoa immunolabeled with colloidal gold-conjugated secondary antibody only. No labeling is observed in the connecting piece structures (E, longitudinal section of the centriole) or in the proximal centriole (F, cross-section). (G and H) Human permeabilized spermatozoa treated sequentially with 5 mM DTT and CSF-arrested cell-free extract and then immunostained with the 20H5 centrin antibody. The primed sperm has begun to decondense in the presence of egg extract (G), but 20H5 centrin is no longer detected at the base of the sperm head (H, arrow). if, implantation fossa; c, capitulum; sc, striated columns; odf, outer dense fibers; asterisks, proximal centriole. Bars in A, B, D, E, and F, 0.2 μm ; bar in C, 0.5 μm ; bar in H, 1 μm .

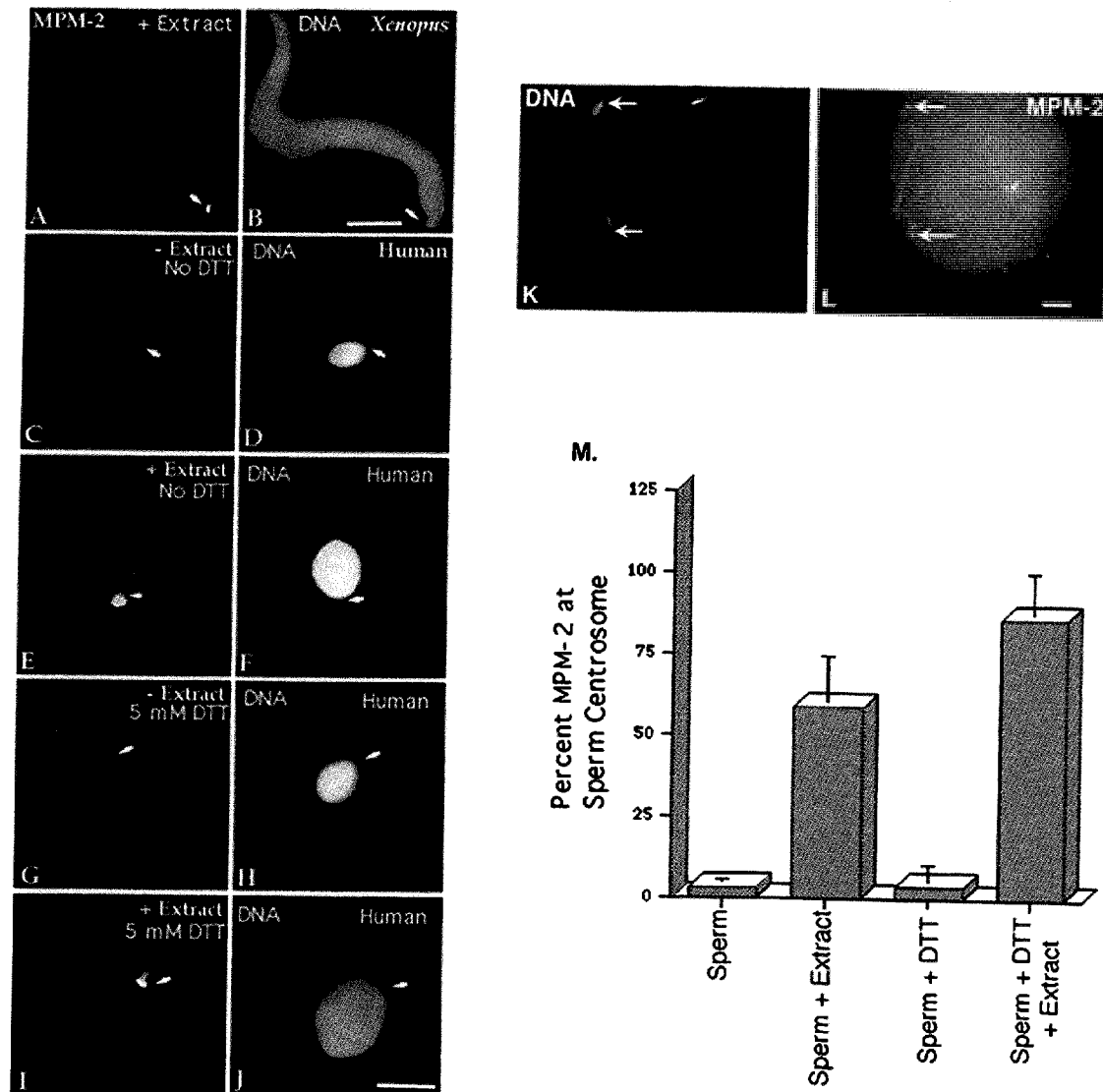


Figure A14. MPM-2 detection in human sperm and early bovine sperm penetration. *X. laevis* sperm become phosphorylated after incubation in *X. laevis* CSF-arrested cell-free extract (A, MPM-2; B, DNA). The mature human sperm centrosome does not immunostain with MPM-2 antibody after methanol fixation (C, MPM-2; D, DNA), although punctate staining is occasionally observed in the head, midpiece, and principal sperm tailpiece (not shown). Human spermatozoa permeabilized in lysolecithin and exposed to CSF-arrested cell-free extract demonstrate MPM-2 immunostaining at the sperm centrosomal region (E, MPM-2; F, DNA). Sperm priming with 5 mM DTT does not significantly increase the detection of centrosome phosphorylation (G, MPM-2; H, DNA) until after exposure to CSF-arrested cell-free extract (I,

MPM-2; J, DNA). Arrows depict sperm tail attachment to the sperm head as observed with phase or differential interference contrast optics. Similar results were observed in mature bovine sperm exposed to CSF-arrested extracts. (K and L) Dispermic penetration in a bovine oocyte after in vitro fertilization (8 h after insemination). MPM-2 phosphorylation of the sperm centrosomes (L, arrows) is observed, suggesting that the positive MPM-2 staining of the assembling zygotic centrosome observed after exposure to frog extracts is mimicked in vivo. (M) Graphic representation of human spermatozoa immunostained with MPM-2 antibody after permeabilization, DTT treatment, and exposure to cell-free extract. The analysis demonstrates that significant MPM-2 immunostaining at the sperm centrosome is observed only when permeabilized or DTT-primed spermatozoa are exposed to CSF-arrested cell-free extract (second and fourth bars). Bars in B, J, and L, 10 μ m.

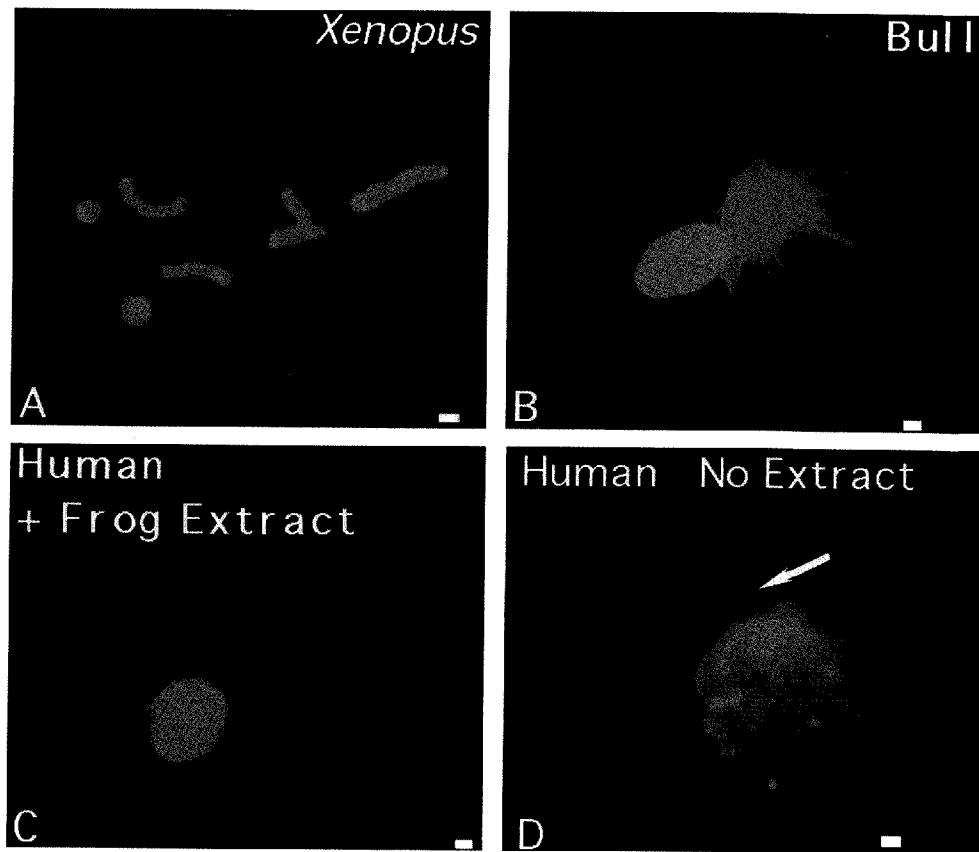


Figure A1.5. Microtubule assembly in vitro nucleated by *X. laevis*, human, and bovine sperm. (A) Lysolecithin-permeabilized *Xenopus* sperm incubated in CSF-arrested cell-free extract containing 0.08 mg/ml rhodamine-conjugated bovine brain tubulin. Microtubule assembly (red) is radially symmetric and tightly focused at the sperm centrosome (blue, DNA). Bull (B) and human (C) sperm (blue), exposed to 5 μ M ionomycin and primed with 5 mM DTT, also demonstrate assembly of microtubules in vitro (red) from the centrosomal region after 40–60 min of incubation in CSF-arrested cell-free extract. No free asters or assembled microtubules are present in the background, suggesting that microtubule nucleation, as opposed to microtubule capture, has occurred. Primed human sperm (blue) that was not exposed to CSF extract did not nucleate microtubules when exposed to rhodamine-conjugated bovine brain tubulin in Pipes buffer alone (D, red; arrow points to sperm axoneme). Bar in A, 30 μ m; bars in B, C, and D, 1 μ m.

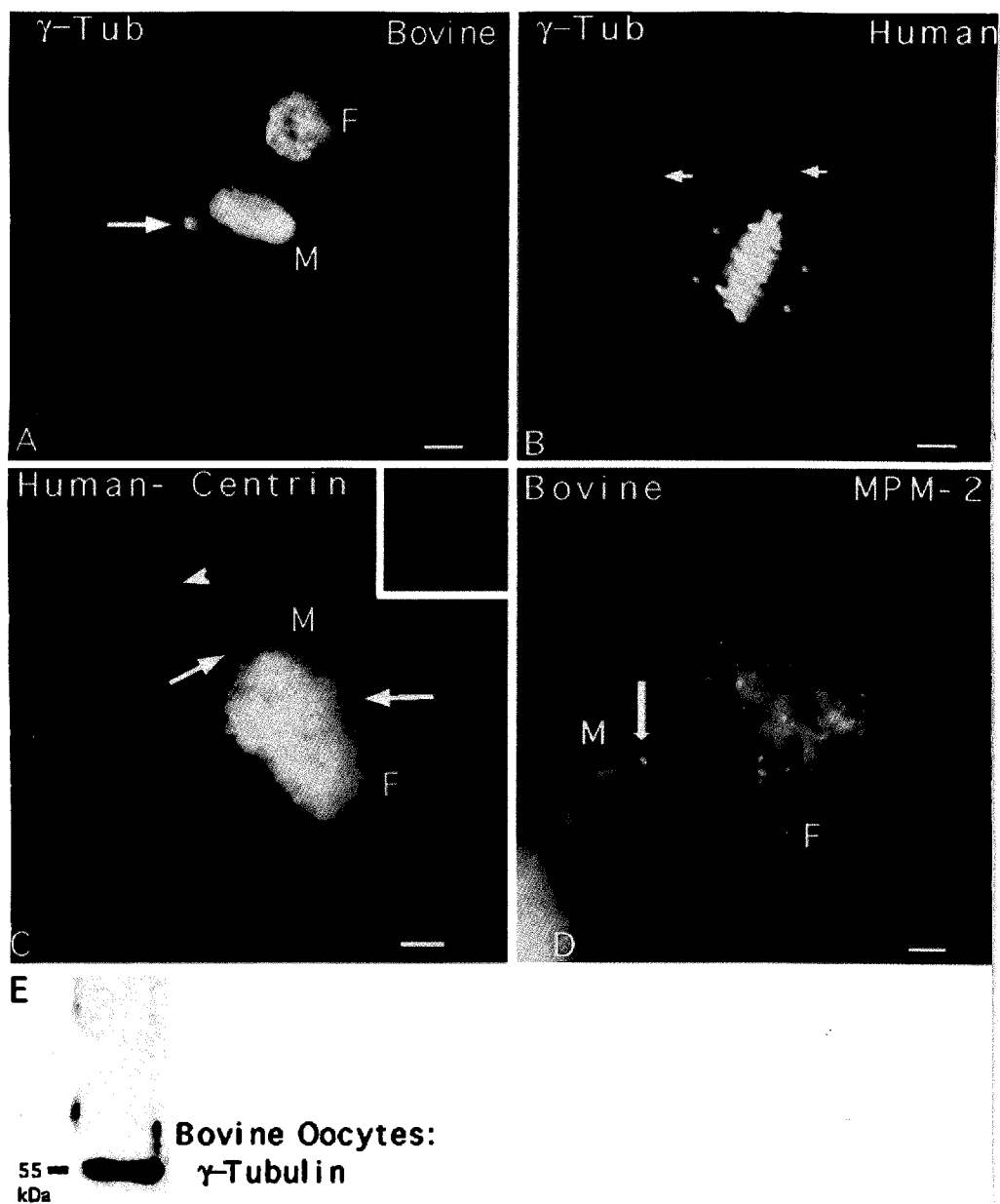


Figure A16. γ -Tubulin, centrin, and MPM-2 detection in human and bovine zygotes. (A) Fertilized bovine oocyte fixed 12 h after insemination and immunostained with γ -tubulin antibody (red), XG-1-4 γ -

tubulin antibody (green), and Hoechst DNA (blue). The sperm aster is a radially symmetrical array of microtubules emanating from the base of the sperm head (M). γ -Tubulin is detectable as a bright dot at the focal point of the sperm aster (arrow). (B) A dispermic human zygote fixed 26.5 h after insemination and triple labeled for microtubules (red, co-stained with β -tubulin and acetylated α -tubulin antibodies), XG-1-4 γ -tubulin antibody (green), and Hoechst DNA (blue). Each pole of the bipolar mitotic spindle has a sperm axoneme (red, arrows). γ -Tubulin is detected as four bright dots at the spindle poles (green), two of which are associated with the incorporated sperm axonemes (red, arrows). (C) An arrested, monospermically inseminated human oocyte fixed 48 h after insemination and immunostained with antibodies to microtubules (red, glutamate α -tubulin antibody), 20H5 mAb to centrin (inset), and Hoechst DNA (blue). A replicated and split centrosome, indicated by the two small microtubule asters (red, arrows) around the adjacent male (M) and female (F) pronuclei, is shown. The incorporated sperm axoneme (arrowhead) is associated with one of the two microtubule asters, but no centrin is detected at the centrosome (inset). (D) A bovine oocyte fertilized in vitro and fixed 10 h after insemination demonstrating sperm aster formation (red) and a pair of MPM-2 immunoreactive foci within the assembled astral microtubules (green). After activation of bovine oocytes, cortical microtubule assembly increases (red) and other cytoplasmic MPM-2 reactive foci (green) can be seen within this polymerizing array. (E) A 55-kDa band is prominently detected in 50 mature bovine oocytes after Western blotting with the rabbit polyclonal XG-1-4 antibody, indicating the presence of abundant maternal γ -tubulin protein. All images were triple labeled for microtubules (red), γ -tubulin, centrin, or MPM-2 (green), and DNA (blue). Bars, 10 μ m.

Appendix 2

Non-Random Chromosome Positioning in Human Sperm and Sex Chromosome Anomalies Following Intracytoplasmic Sperm Injection

Craig Marc Luetjens, Christopher Payne and Gerald Schatten

Departments of Obstetrics & Gynecology and Cell & Developmental Biology, Oregon Health Sciences University, and Oregon Regional Primate Research Center, Beaverton, Oregon 97006, USA

Published in *The Lancet* (1999) **353**, 1240.

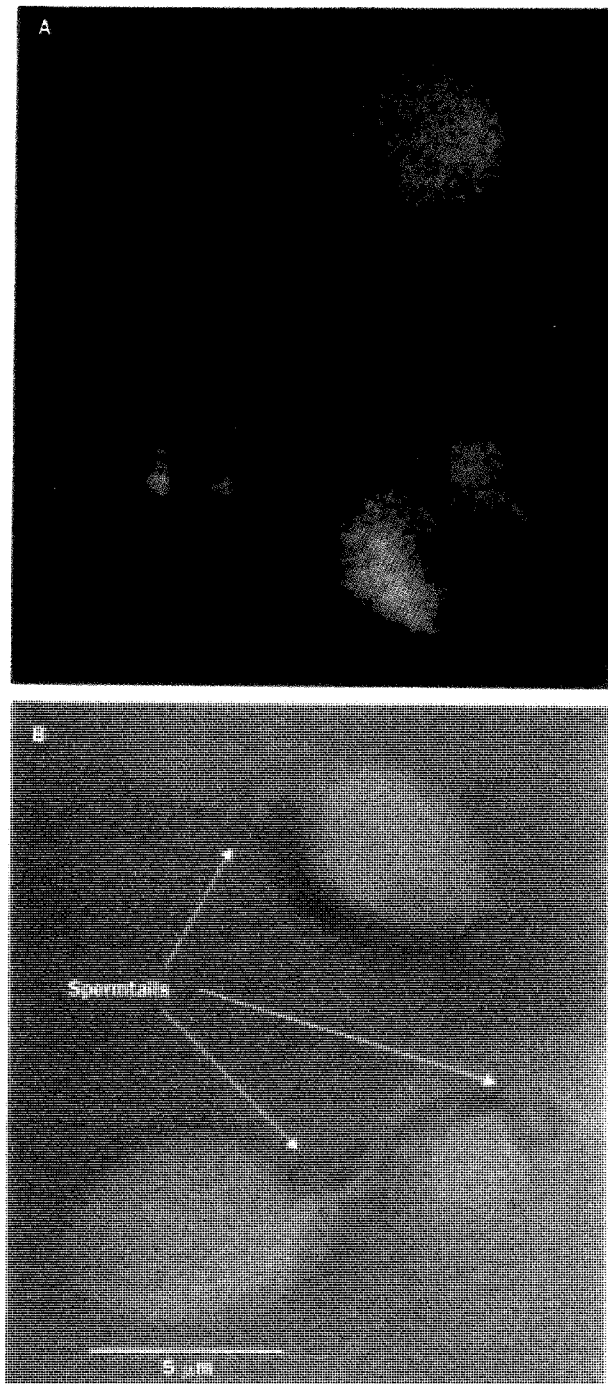
Although intracytoplasmic sperm injection (ICSI) has been used successfully in the treatment of male infertility, there are reports of increased sex chromosome anomalies in children conceived after ICSI (Bonduelle et al., 1998). Inheritance of chromosome anomalies from the parents alone cannot explain the higher incidence of aneuploidy due to mitotic errors after fertilization. Because sperm nuclear decondensation is atypical after ICSI (Bourgain et al., 1998; Hewitson et al., 1996), with the apical region remaining condensed for longer than the basal region, we investigated whether this delay might result in the retardation of X chromosome decondensation. The apical tip of the sperm nucleus adjacent to the perinuclear theca remains condensed until the remnants of the acrosome are removed. These structures are lost uniformly at the egg cortex during in vitro fertilization. Chromosome anomalies could be related to this delay, which may not allow the complete decondensation of all the chromosomes and which may lead to asymmetrical segregation at first mitosis.

Sperm chromosomes are positioned non-randomly in marsupials and hamsters, and the centromeres and telomeres of human sperm chromosomes have been shown to be non-randomly positioned (Zalensky, 1998). If the chromosomes of sperm nuclei have preferred positions in the sperm head, perhaps the delayed decondensation of the apical tip of the sperm contributes to chromosome anomalies in ICSI children.

We used chromosome paints (Oncor Inc, USA) to identify the X chromosome and chromosome 18. To preserve the three-dimensional structure of the chromosomes and ensure that chromosome paints had access to the DNA, the sperm were gently permeabilized and decondensed in mitotic *Xenopus* egg extracts, an in vitro system that closely mimics an in vivo environment (Ohsumi et al., 1988).

Chromosome paint for chromosome 18 hybridized in more than 80% (190/234) of sperm examined, and chromosome paint for X chromosome hybridized in just over 40% (230/553). The sperm tail was used as a reference to identify apical or basal position (Figure A2.1B, arrows; DNA, blue). Chromosome 18 was found near the sperm tail in almost 60% of the sperm (113/190; Figure A2.1A, red), while the X chromosome was found near the sperm tail in less than 40% (88/230; Figure A2.1A, green). This shows that chromosome 18 is preferentially located in the basal region of the sperm nucleus, while the X chromosome is preferentially located in the apical region.

The placement of chromosomes within the sperm nucleus may have implications for assisted reproductive technologies (ART), and may help explain the apparent increase in sex chromosome aberrations in ICSI offspring. This increase could be due to the fact that the X chromosome in sperm nuclei preferentially localizes in the apical region. In such nuclei, the S-phase of the cell cycle may be delayed due to the decreased rate of nuclear decondensation in the apical region of the sperm head, hindering progression to the onset of first mitosis in the zygote. This may lead to mitotic errors in the distribution of the X chromosome during first cleavage, implying that such positioning of the sex chromosome could lead to the increase in sex chromosome anomalies following ICSI.



FigureA21. Human sperm after in vitro decondensation and chromosome painting. A: X chromosome (green), chromosome 18 (red); B: DIC image overlaid with a fluorescence image stained for DNA with Hoechst 33342 (blue).

Appendix 3

Molecular Correlates of Primate Nuclear Transfer Failures

Calvin Simerly¹, Tanja Dominko², Christopher Navara¹, Christopher Payne¹, Saverio Capuano¹, Gabriella Gosman¹, Kowit-Yu Chong¹, Diana Takahashi¹, Crista Chace¹, Duane Compton³, Laura Hewitson¹ and Gerald Schatten¹

¹ Pittsburgh Development Center, Magee-Womens Research Institute, Departments of Obstetrics-Gynecology-Reproductive Sciences & Cell Biology-Physiology, University of Pittsburgh School of Medicine, Pittsburgh, PA 15213

² CellThera, Worcester, MA 01605

³ Department of Biochemistry, Dartmouth Medical School, Hanover, NH 03755

Published in *Science* (2003) **300**, 297.

Somatic cell nuclear transfer (SCNT) (Wilmut, 2002) in nonhuman primates could accelerate medical research by contributing identical animals for research and clarifying embryonic stem cell potentials (Thomson et al., 1998). Although rhesus embryos begin development after embryonic cell nuclear transfer (ECNT) (Meng et al., 1997; Dominko et al., 1999; Mitalipov et al., 2002), there has only been one report of rhesus births after ECNT (Meng et al., 1997), and that report has not been replicated.

Here, molecular obstacles were identified using 716 rhesus oocytes in four experimental studies: set A, SCNT [rhesus cumulus, umbilical cord blood, epithelial-derived fibroblasts, and inner cell mass-derived precursor embryonic stem cells; 193 oocytes; 62.8% nuclear transfer (NT) success assayed by interphase nucleus formation], and set B, ECNT from dissociated 16- to 32-cell stage embryos (381 oocytes; 97.2% NT success), because ECNT success is greater than SCNT (Wilmut, 2002). Because meiotic spindle removal appeared to be responsible for these NT failures, we performed two additional experiments in which either we did not remove the spindle (set C) or we removed and reinserted it (set D). In set C, NTs into concurrently fertilized oocytes generated tetraploids (55 oocytes; 54.4% success), whereas in set D, fertilization of reconstituted oocytes (that had previously been enucleated and then renucleated) generated diploids (95 oocytes; 67.1% success).

Rhesus NTs look superficially normal, yet no pregnancies resulted from 33 embryos transferred into 16 surrogates (compared with seasonably variable 28 to 66% pregnancy rates by assisted reproduction) (Hewitson et al., 1999). DNA and microtubule imaging showed disarrayed mitotic spindles with misaligned chromosomes (Figure A3.1A; all 116 ECNTs and all 30 SCNTs examined displayed aberrant spindles). Despite

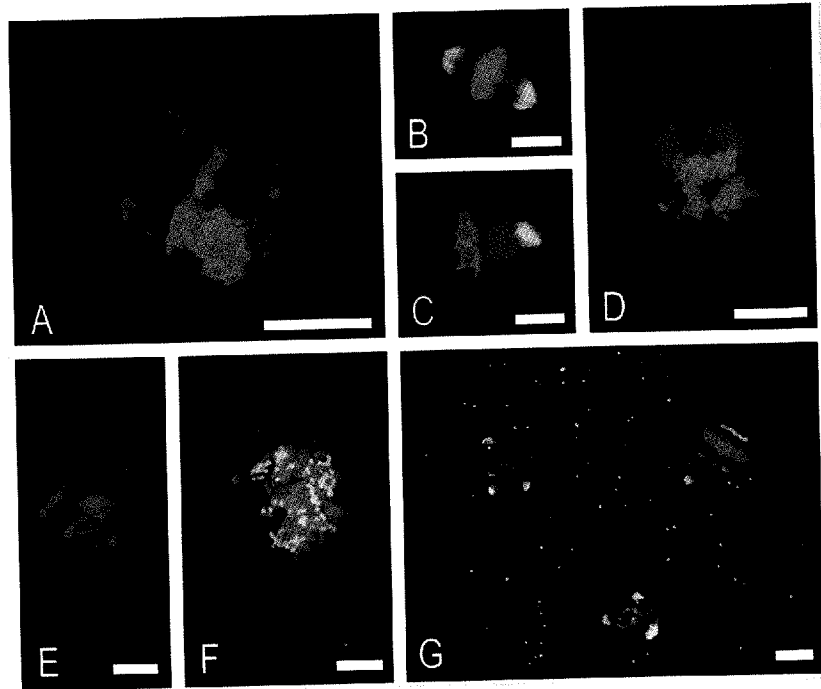
these defects, cleavages continue, but unequal chromosome segregations produce aneuploid embryos.

NuMA (Nuclear-Mitotic Apparatus), a matrix protein responsible for spindle pole assembly (Mountain et al., 1999), concentrates at centrosomes in unfertilized meiotic (Figure A3.1B) and fertilized mitotic cells (Figure A3.1C). After NT, NuMA is not detected on the abnormal mitotic spindles (Figure A3.1D) or in enucleated oocytes. HSET and Eg5 are mitotic kinesin motors (Mountain et al., 1999; Blangy et al., 1995). HSET, found during meiosis and mitosis, is not detected in NT spindles (Figure A3.1E). Eg5 detects centromere pairs at meiosis and mitosis, including misaligned ones on NT spindles (Figure A3.1F). Thus, meiotic spindle removal depletes the ooplasm of NuMA and HSET, both vital for mitotic spindle pole formation.

Normal spindles found in tetraploids suggest meiotic spindle removal as the source of NT anomalies. In tetraploids, chromosomes aligned properly on bipolar spindles with centrosomal NuMA (Figure A3.1G). NT mitotic spindles could be distinguished from the fertilized spindle by the sperm tail. Similarly, fertilization of reconstituted oocytes resulted in apparently normal divisions. Thus, manipulation of the embryos alone was not the cause of the problem, and proper mitotic spindles can be organized around somatic chromosomes if the meiotic spindle is left intact.

Primate NT appears to be challenged by stricter molecular requirements for mitotic spindle assembly than in other mammals. In cattle, the somatic centrosome is transferred during NT (Navara et al., 1994), whereas mice rely on the oocyte's maternal centrosome (Schatten, 1994). Also, NuMA and HSET are not exclusively concentrated on the meiotic spindle in mammals other than primates (Mountain et al., 1999). With

current approaches, NT to produce embryonic stem cells in nonhuman primates may prove difficult - and reproductive cloning unachievable.



FigureA31. Faulty mitotic spindles produce aneuploid embryos after primate nuclear transfer. (A) Defective NT mitotic spindle with misaligned chromosomes. Centrosomal NuMA at meiosis **(B)** and mitosis **(C)**, but not in mitotic spindles after NT **(D)**. The centrosomal kinesin HSET is also missing after NT **(E)**, but not centromeric Eg5 **(F)**. Bipolar mitotic spindles with aligned chromosomes and centrosomal NuMA after NT into fertilized eggs **(G)**. DNA, microtubule, NuMA, and kinesin imaging: Blue, DNA; red, β -tubulin; green, NuMA in **(B)**, **(C)**, **(D)**, and **(G)**; HSET in **(E)**; and Eg5 in **(F)**. Scale bar, 10 μ m.

References

- Aitken, R.J. (1997). The cell biology of fertilization. *Adv. Exp. Med. Biol.* **424**, 291-299.
- Albertini, D.F. (1992). Cytoplasmic microtubular dynamics and chromatin organization during mammalian oogenesis and oocyte maturation. *Mutat. Res.* **296**, 57-68.
- Allen, T.D., Cronshaw, J.M., Bagley, S., Kiseleva, E., and Goldberg, M.W. (2000). The nuclear pore complex: mediator of translocation between nucleus and cytoplasm. *J. Cell Sci.* **113**, 1651-1659.
- Aris, J.P., and Blobel, G. (1989). Yeast nuclear envelope proteins cross react with an antibody against mammalian pore complex proteins. *J. Cell Biol.* **108**, 2059-2067.
- Asch, R., Simerly, C., Ord, T., Ord, V.A., and Schatten, G. (1995). The stages at which human fertilization arrests: microtubule and chromosome configurations in inseminated oocytes which failed to complete fertilization and development in humans. *Hum. Reprod.* **10**, 1897-1906.
- Assey, R.J., Hyttel, P., Greve, T., and Purwantara, B. (1994). Oocyte morphology in dominant and subordinate follicles. *Mol. Reprod. Dev.* **37**, 335-344.
- Baguisi, A., Behboodi, E., Melican, D.T., Pollock, J.S., Destrempe, M.M., Cammuso, C., Williams, J.L., Nims, S.D., Porter, C.A., Midura, P., et al. (1999). Production of goats by somatic cell nuclear transfer. *Nat. Biotechnol.* **17**, 456-461.
- Barlowe, C., Orci, L., Yeung, T., Hosobuchi, M., Hamamoto, S., Salama, N., Rexach, M.F., Ravazzola, M., Amherdt, M., and Schekman, R. (1994). COPII: a membrane coat formed by Sec proteins that drive vesicle budding from the endoplasmic reticulum. *Cell* **77**, 895-907.

- Baron, A.T., Greenwood, T.M., Bazinet, C.W., and Salisbury, J.L. (1992). Centrin is a component of the pericentriolar lattice. *Biol. Cell* **76**, 383–388.
- Baron, A.T., Suman V.J., Nemeth, E., and Salisbury, J.L. (1994). The pericentriolar lattice of PtK2 cells exhibits temperature and Ca^{2+} -modulated behavior. *J. Cell Sci.* **107**, 2993–3003.
- Baum, P., Furlong, C., and Byers, B. (1986). Yeast gene required for spindle pole body duplication: homology of its product with Ca^{2+} -binding proteins. *Proc. Natl. Acad. Sci. USA* **83**, 5512–5516.
- Bavister, B.D., Leibfried, M.L., and Lieberman, G. (1983). Development of preimplantation embryos of the golden hamster in a defined culture medium. *Biol. Reprod.* **28**, 235–247.
- Beaudouin, J., Gerlich, D., Daigle, N., Eils, R., and Ellenberg, J. (2002). Nuclear envelope breakdown proceeds by microtubule-induced tearing of the lamina. *Cell* **108**, 83–96.
- Bellvé, A.R., Zheng, W., and Martinova, Y.S. (1993). Recovery, capacitation, acrosome reaction, and fractionation of sperm. *Methods Enzymol.* **225**, 113–136.
- Biggins, S., and Rose, M.D. (1994). Direct interaction between yeast spindle pole body components: Kar1p is required for Cdc31p localization to the spindle pole body. *J. Cell Biol.* **125**, 843–852.
- Blangy, A., Lane, H.A., d'Herin, P., Harper, M., Kress, M., and Nigg, E.A. (1995). Phosphorylation by p34cdc2 regulates spindle association of human Eg5, a kinesin-related motor essential for bipolar spindle formation in vivo. *Cell* **83**, 1159–1169.

- Boatman, D.E., and Bavister, B.D. (1984). Stimulation of rhesus monkey sperm capacitation by cyclic nucleotide mediators. *J. Reprod. Fertil.* **71**, 357-366.
- Bonduelle, M., Aytoz, A., Van Assche, E., Devroey, P., Liebaers, I., and Van Steirteghem, A. (1998). Incidence of chromosomal aberrations in children born after assisted reproduction through intracytoplasmic sperm injection. *Hum. Reprod.* **13**, 781-782.
- Bornens, M., Paintrand, M., Berges, J., Marty, M.C., and Karsenti, E. (1987). Structural and chemical characterization of isolated centrosomes. *Cell Motil. Cytoskeleton* **8**, 238-249.
- Bourgain, C., Nagy, Z.P., de Zutter, H., van Ranst, H., Nogueira, D., and van Steirteghem, A.C. (1998). Ultrastructure of gametes after intracytoplasmic sperm injection. *Hum. Reprod.* **13** (suppl. 1), 107-116.
- Boveri, T. (1901). *Zellen-studien: Über die Natur der Centrosomen, Vol. IV*. Jena, Germany: Fisher.
- Bowen, J.R., Gibson, F.L., Leslie, G.I., and Saunders, D.M. (1998). Medical and developmental outcome at 1 year for children conceived by intracytoplasmic sperm injection. *Lancet* **351**, 1529-1534.
- Brinkley, B.R., Cox, S.M., and Fistel, S. (1980). Organizing centers for cell processes. *Neurosci. Res. Program Bull.* **19**, 108-124.
- Brown, D.B., Blake, E.J., Wolgemuth, D.J., Gordon, K., and Ruddle, F.H. (1987). Chromatin decondensation and DNA synthesis in human sperm activated in vitro by using *Xenopus laevis* egg extracts. *J. Exp. Zool.* **242**, 215-231.

- Burkhardt, J.K., Echeverri, C.J., Nilsson, T., and Vallee, R.B. (1997). Overexpression of the dynamitin (p50) subunit of the dynactin complex disrupts dynein-dependent maintenance of membrane organelle distribution. *J. Cell Biol.* **139**, 469-484.
- Busson, S., Dujardin, D., Moreau, A., Dompierre, J., and De Mey, J.R. (1998). Dynein and dynactin are localized to astral microtubules and at cortical sites in mitotic epithelial cells. *Curr. Biol.* **8**, 541-544.
- Cahana, A., and Reiner, O. (1999). LIS1 and platelet-activating factor acetylhydrolase (Ib) catalytic subunits, expression in the mouse oocyte and zygote. *FEBS Lett.* **451**, 99-102.
- Calarco, P.G., Donahue, R.P., and Szollosi, D. (1972). Germinal vesicle breakdown in the mouse oocyte. *J. Cell Sci.* **10**, 369-385.
- Calvin, H.I., Yu, C.C., and Bedford, J.M. (1973). Effects of epididymal maturation, zinc (II) and copper (II) on the reactive sulfhydryl content of structural elements in rat spermatozoa. *Exp. Cell Res.* **81**, 333-341.
- Cherr, G.N., Drobnis, E.Z., and Katz, D.F. (1988). Localization of cortical granule constituents before and after exocytosis in the hamster egg. *J. Exp. Zool.* **246**, 81-93.
- Chesne, P., Adenot, P.G., Viglietta, C., Baratte, M., Boulanger, L., and Renard J.P. (2002). Cloned rabbits produced by nuclear transfer from adult somatic cells. *Nat. Biotechnol.* **20**, 366-369.
- Choi, T., Aoki, F., Mori, M., Yamashita, M., Nagahama, Y., and Kohmoto, K. (1991). Activation of p34cdc2 protein kinase activity in meiotic and mitotic cell cycles in mouse oocytes and embryos. *Development* **113**, 789-795.

- Clayton, L., McConnell, J.M.L., and Johnson, M.H. (1995). Control of the surface expression of uvomorulin after activation of mouse oocytes. *Zygote* **3**, 177-189.
- Colman, A., Jones, E.A., and Heasman, J. (1985). Meiotic maturation in *Xenopus* oocytes: a link between the cessation of protein secretion and the polarized disappearance of Golgi apparatus. *J. Cell Biol.* **101**, 313-318.
- Coquelle, F.M., Caspi, M., Cordelieres, F.P., Dompierre, J.P., Dujardin, D.L., Koifman, C., Martin, P., Hoogenraad, C.C., Akhmanova, A., Galjart, N., De Mey, J.R., and Reiner, O. (2002). LIS1, CLIP-170's key to the dynein/dynactin pathway. *Mol. Cell Biol.* **22**, 3089-3102.
- Cronshaw, J.M., Krutchinsky, A.N., Zhang, W., Chait, B.T., and Matunis, M.J. (2002). Proteomic analysis of the mammalian nuclear pore complex. *J. Cell Biol.* **158**, 915-927.
- Danilchik, M.V., Funk, W.C., Brown, E.E., and Larkin, K. (1998). Requirement for microtubules in new membrane formation during cytokinesis of *Xenopus* embryos. *Dev. Biol.* **194**, 47-60.
- Davis, F.M., Tsao, T.Y., Fowler, S.K., and Rao, P.N. (1983). Monoclonal antibodies to mitotic cells. *Proc. Natl. Acad. Sci. USA* **80**, 2926-2930.
- Davis, L.I., and Blobel, G. (1987). Nuclear pore complex contains a family of glycoproteins that includes p62: glycosylation through a previously unidentified cellular pathway. *Proc. Natl. Acad. Sci. USA* **84**, 7552-7556.
- Davis, T.N. (1997). The centrosome on center stage. *Trends Cell Biol.* **7**, 508-510.

- Dawe, A.L., Caldwell, K.A., Harris, P.M., Morris, N.R., and Caldwell, G.A. (2001). Evolutionarily conserved nuclear migration genes required for early embryonic development in *Caenorhabditis elegans*. *Dev. Genes Evol.* **211**, 434-441.
- Dean, B., Chang, S., Stevens, J., Thomas, P.E., and King, C. (2002). Isolation and characterization of a UDP-glucuronosyltransferase (UGT1A01) cloned from female rhesus monkey. *Arch. Biochem Biophys.* **402**, 289-295.
- Dobyns, W.B., Reiner, O., Carrozzo, R., and Ledbetter, D.H. (1993). Lissencephaly: a human brain malformation associated with deletion of the LIS1 gene located at chromosome 17p13. *JAMA* **270**, 2838-2842.
- Dominko, T., Ramalho-Santos, J., Chan, A., Moreno, R.D., Luetjens, C.M., Simerly, C., Hewitson, L., Takahashi, D., Martinovich, C., White, J.M., and Schatten, G. (1999). Optimization Strategies for Production of Mammalian Embryos by Nuclear Transfer. *Cloning* **1**, 143-152.
- Doxsey, S. (1998). The centrosome: a tiny organelle with big potential. *Nat. Genet.* **20**, 104-106.
- Doxsey, S. (2001). Re-evaluating centrosome function. *Nat. Rev. Mol. Cell Biol.* **2**, 688-698.
- Doxsey, S.J., Stein, P., Evans, L., Calarco, P.D., and Kirschner, M. (1994) Pericentrin, a highly conserved centrosome protein involved in microtubule organization. *Cell* **76**, 639-650.
- Ducibella, T., Anderson, E., Albertini, D.F., Aalberg, J., and Rangarajan, S. (1988a). Quantitative studies of changes in cortical granule number and distribution in the mouse oocyte during meiotic maturation. *Dev. Biol.* **130**, 184-197.

- Ducibella, T., Rangarajan, S., and Anderson, E. (1988b). The development of mouse oocyte cortical reaction competence is accompanied by major changes in cortical vesicles and not cortical granule depth. *Dev. Biol.* **130**, 789-792.
- Echeverri, C.J., Paschal, B.M., Vaughan, K.T., and Vallee, R.B. (1996). Molecular characterization of the 50-kD subunit of dynactin reveals function for the complex in chromosome alignment and spindle organization during mitosis. *J. Cell Biol.* **132**, 617-633.
- Eid, L.N., Lorton, S.P., and Parrish, J.J. (1994). Paternal influence on S-phase in the first cell cycle of the bovine embryo. *Biol. Reprod.* **51**, 1232-1237.
- Eisen, A., Kiehart, D.P., Wieland, S.J., and Reynolds, G.T. (1984). Temporal sequence and spatial distribution of early events of fertilization in single sea urchin eggs. *J. Cell Biol.* **99**, 1647-1654.
- Errabolu, R., Sanders, M.A., and Salisbury, J.L. (1994). Cloning of a cDNA encoding human centrin, an EF-hand protein of centrosomes and mitotic spindle poles. *J. Cell Sci.* **107**, 9-16.
- Ewald, A., Zunkler, C., Lourim, D., and Dabauvalle, M.C. (2001). Microtubule-dependent assembly of the nuclear envelope in *Xenopus laevis* egg extract. *Eur. J. Cell Biol.* **80**, 678-691.
- Faulkner, N.E., Dujardin, D.L., Tai, C.Y., Vaughan, K.T., O'Connell, C.B., Wang, Y., and Vallee, R.B. (2000). A role for the lissencephaly gene LIS1 in mitosis and cytoplasmic dynein function. *Nat. Cell Biol.* **2**, 784-791.

- Félix, M.A., Antony, C., Wright, M., and Maro, B. (1994). Centrosome assembly in vitro: role of γ -tubulin recruitment in *Xenopus* sperm aster formation. *J. Cell Biol.* **124**, 19–31.
- Fujitani, Y., Higaki, S., Sawada, H., and Hirose, K. (1989). Quick-freeze, deep-etch visualization of the nuclear pore complex. *J. Electron Microsc.* **38**, 34–40.
- Gagnon, C. (1995). Regulation of sperm motility at the axonemal level. *Reprod. Fertil. Dev.* **7**, 847–855.
- Gard, D.L. (1994). γ -Tubulin is asymmetrically distributed in the cortex of *Xenopus* oocytes. *Dev. Biol.* **161**, 131–140.
- Geiser, J.R., Schott, E.J., Kingsbury, T.J., Cole, N.B., Totis, L.J., Bhattacharyya, G., He, L., and Hoyt, M.A. (1997). *Saccharomyces cerevisiae* genes required in the absence of the CIN8-encoded spindle motor act in functionally diverse mitotic pathways. *Mol. Biol. Cell* **8**, 1035–1050.
- Gibbons, I.R. (1995). Dynein family of motor proteins: present status and future questions. *Cell. Motil. Cytoskeleton* **32**, 136–144.
- Gilbert, S.F. (1997). *Developmental Biology*, 5th Edition. Sinauer Associates, Inc.
- Gönczy, P., Pichler, S., Kirkham, M., and Hyman, A.A. (1999). Cytoplasmic dynein is required for distinct aspects of MTOC positioning, including centrosome separation, in the one cell stage *Caenorhabditis elegans* embryo. *J. Cell Biol.* **147**, 135–150.
- Gosden, R., Krapez, J., and Briggs, D. (1997). Growth and development of the mammalian oocyte. *Bioessays* **19**, 875–882.

- Harlow, E., and Lane, D. (1988). *Antibodies: a laboratory manual*. Cold Spring Harbor Laboratory Press.
- Harrouk, W., and Clarke H.J. (1993). Sperm chromatin acquires an activity that induces microtubule assembly during residence in the cytoplasm of metaphase oocytes of the mouse. *Chromosoma* **102**, 279–286.
- Heidermann, S.R., and Kirschner, M.W. (1975). Aster formation in egg of *Xenopus laevis*. *J. Cell Biol.* **67**, 105–117.
- Helfand, B.T., Mikami, A., Vallee, R.B., and Goldman, R.D. (2002). A requirement for cytoplasmic dynein and dynactin in intermediate filament network assembly and organization. *J. Cell Biol.* **157**, 795-806.
- Hewitson, L., Dominko, T., Takahashi, D., Martinovich, C., Ramalho-Santos, J., Sutovsky, P., Fanton, J., Jacob, D., Monteith, D., Neuringer, M., Battaglia, D., Simerly, C., and Schatten, G. (1999). Unique checkpoints during the first cell cycle of fertilization after intracytoplasmic sperm injection in rhesus monkeys. *Nat. Med.* **5**, 431-433.
- Hewitson, L., Simerly, C., Dominko, T., and Schatten, G. (2000a). Cellular and molecular events after in vitro fertilization and intracytoplasmic sperm injection. *Theriogenology* **53**, 95-104.
- Hewitson, L., Simerly, C., and Schatten, G. (2000b). Cytoskeletal aspects of assisted fertilization. *Semin. Reprod. Med.* **18**, 151-159.
- Hewitson, L.C., Simerly, C.R., Tengowski, M.W., Sutovsky, P., Navara, C.S., Haavisto, A.J., and Schatten, G. (1996). Microtubule and chromatin configurations during

- Rhesus* intracytoplasmic sperm injection: successes and failures. *Biol. Reprod.* **55**, 271–280.
- Hewitson, L., Takahashi, D., Dominko, T., Simerly, C., and Schatten, G. (1998). Fertilization and embryo development to blastocysts by intracytoplasmic sperm injection in the rhesus monkey. *Hum. Reprod.* **13**, 2786–2790.
- Hirotsune, S., Fleck, M.W., Gambello, M.J., Bix, G.J., Chen, A., Clark, G.D., Ledbetter, D.H., McBain, C.J., and Wynshaw-Boris, A. (1998). Graded reduction of *Pafah1b1* (*Lis1*) activity results in neuronal migration defects and early embryonic lethality. *Nat. Genet.* **19**, 333–339.
- Holleran, E.A., Karki, S., and Holzbaur, E.L.F. (1998). The role of the dynactin complex in intracellular motility. *Int. Rev. Cytol.* **182**, 69–109.
- Holzbaur, E.L.F., Mikami, A., Paschal, B.M., and Vallee, R.B. (1994). Molecular characterization of cytoplasmic dynein. In: *Microtubules*. Wiley-Liss, Inc., 251–267.
- Horio, T., Uzawa, S., Jung, M.K., Oakley, B.R., Tanaka, K., and Yanagida, M. (1991). The fission yeast γ -tubulin is essential for mitosis and is localized at microtubule organizing centers. *J. Cell Sci.* **99**, 693–700.
- Hulen, D., Baron, A., Salisbury, J., and Clarke, M. (1991). Production and specificity of monoclonal antibodies against calmodulin from *Dictyostelium discoideum*. *Cell Motil. Cytoskeleton* **18**, 113–122.
- Hyttel, P., Callesen, H., and Greve, T. (1986). Ultrastructural features of preovulatory oocyte maturation in superovulated cattle. *J. Reprod. Fertil.* **76**, 645–656.

- Hyttel, P., Greve, T., and Callesen, H. (1988). Ultrastructure of in vivo fertilization in superovulated cattle. *J. Reprod. Fertil.* **82**, 1-13.
- Hyttel, P., Greve, T., and Callesen, H. (1989). Ultrastructural aspects of oocyte maturation and fertilization in cattle. *J. Reprod. Fertil. Suppl.* **38**, 35-47.
- In't Veld, P., Brandenburg, H., Verhoeff, A., Dhont, M., and Los, F. (1995). Sex chromosomal abnormalities and intracytoplasmic sperm injection. *Lancet* **346**, 773.
- Jaenisch, R., Eggan, K., Humpherys, D., Rideout, W., and Hochedlinger, K. (2002). Nuclear cloning, stem cells, and genomic reprogramming. *Cloning Stem Cells* **4**, 389-396.
- Jesch, S.A., and Linstedt, A.D. (1998). The Golgi and endoplasmic reticulum remain independent during mitosis in HeLa cells. *Mol. Biol. Cell* **9**, 623-635.
- Jones, J.C.R., Goldman, A.E., Steinert, P.M., Yuspa, S., and Goldman, R.D. (1982). Dynamic aspects of the supramolecular organization of intermediate filament networks in cultured epidermal cells. *Cell Motility* **2**, 197-213.
- Joshi, H.C., Palacios, M.J., McNamara, L., and Cleveland, D.W. (1992). γ -Tubulin is a centrosomal protein required for cell cycle-dependent microtubule nucleation. *Nature* **356**, 80-83.
- Karki, S., and Holzbaur, E.L.F. (1995). Affinity chromatography demonstrates a direct binding between cytoplasmic dynein and the dynactin complex. *J. Biol. Chem.* **270**, 28806-28811.
- Karki, S., and Holzbaur, E.L.F. (1999). Cytoplasmic dynein and dynactin in cell division and intracellular transport. *Curr. Opin. Cell Biol.* **11**, 45-53.

- Karsenti, E., Newport, J., Hubble, R., and Kirschner, M. (1984). Interconversion of metaphase and interphase microtubule arrays as studied by the injection of centrosomes and nuclei into *Xenopus* eggs. *J. Cell Biol.* **98**, 1730–1745.
- Kato, Y., Tani, T., Sotomaru, Y., Kurokawa, K., Kato, J., Doguchi, H., Yasue, H., and Tsunoda, Y. (1998). Eight calves cloned from somatic cells of a single adult. *Science* **282**, 2095–2098.
- Kellogg, D.R., Moritz, M., and Alberts, B.M. (1994). The centrosome and cellular organization. *Annu. Rev. Biochem.* **63**, 639–674.
- Kline, D. (2000). Attributes and dynamics of the endoplasmic reticulum in mammalian eggs. *Curr. Topics Dev. Biol.* **50**, 125–154.
- Kline, D., Mehlmann, L., Fox, C., and Terasaki, M. (1999). The cortical endoplasmic reticulum (ER) of the mouse egg: localization of ER clusters in relation to the generation of repetitive Ca^{2+} waves. *Dev. Biol.* **215**, 431–442.
- Kosower, N.S., and Kosower, E.M. (1987). Thiol labeling with bromobimanes. *Methods Enzymol.* **143**, 76–84.
- Kubiak, J.Z., Weber, M., de Pennart, H., Winston, N.J., and Maro, B. (1993). The metaphase II arrest in mouse oocytes is controlled through microtubule-dependent destruction of cyclin B in the presence of CSF. *EMBO J.* **12**, 3773–3778.
- Kuge, O., Dascher, C., Orci, L., Rowe, T., Amherdt, M., Plutner, H., Ravazzola, M., Tanigawa, G., Rothman, J.E., and Balch, W.E. (1994). Sar1 promotes vesicle budding from the endoplasmic reticulum but not Golgi compartments. *J. Cell Biol.* **125**, 51–65.

- Kuntziger, T., and Bornens, M. (2000). The centrosome and parthenogenesis. *Curr. Top. Dev. Biol.* **49**, 1-25.
- Kuriyama, R., Borisy, G.G., and Masui, Y. (1986). Microtubule cycles in oocytes of the surf clam, *Spisula solidissima*: an immunofluorescence study. *Dev. Biol.* **114**, 151–160.
- Lamb, D.J. (1999). Debate: is ICSI a genetic time bomb? Yes. *J. Androl.* **20**, 23-33.
- Laurinčík, J., Hyttel, P., Baran, V., Eckert, J., Lucas-Hahn, A., Pivko, J., Niemann, H., Brem, G., and Schellander, K. (1998). A detailed analysis of pronucleus development in bovine zygotes in vitro: cell-cycle chronology and ultrastructure. *Mol. Reprod. Dev.* **50**, 192-199.
- Ledan, E., Polanski, Z., Terret, M.E., and Maro, B. (2001). Meiotic maturation of the mouse oocyte requires an equilibrium between cyclin B synthesis and degradation. *Dev. Biol.* **232**, 400-413.
- Lee, V.D., and Huang, B. (1993). Molecular cloning and centrosomal localization of human caltractin. *Proc. Natl. Acad. Sci. USA* **90**, 11039–11043.
- LeMaire-Adkins, R., Radke, K., and Hunt, P.A. (1997). Lack of checkpoint control at the metaphase/anaphase transition: a mechanism of meiotic nondisjunction in mammalian females. *J. Cell Biol.* **139**, 1611-1619.
- Lénárt, P., and Ellenberg, J. (2003). Nuclear envelope dynamics in oocytes: from germinal vesicle breakdown to mitosis. *Curr. Opin. Cell Biol.* **15**, 88-95.
- Lippincott-Schwartz, J., Roberts, T.H., and Hirschberg, K. (2000). Secretory protein trafficking and organelle dynamics in living cells. *Annu. Rev. Cell Dev. Biol.* **16**, 557-589.

- Lippincott-Schwartz, J., Yuan, L.C., Bonifacino, J.S., and Klausner, R.D. (1989). Rapid redistribution of Golgi proteins into the ER in cells treated with brefeldin A: evidence for membrane cycling from Golgi to ER. *Cell* **56**, 801-813.
- Lo Nigro, C., Chong, C.S., Smith, A.C., Dobyns, W.B., Carrozzo, R., and Ledbetter, D.H. (1997). Point mutations and an intragenic deletion in LIS1, the lissencephaly causative gene in isolated lissencephaly sequence and Miller-Dieker syndrome. *Hum. Mol. Genet.* **6**, 157-164.
- Lohka, M.J., and Maller, J.L. (1988). Induction of metaphase chromosome condensation in human sperm by *Xenopus* egg extracts. *Exp. Cell Res.* **179**, 303-309.
- Long, C.R., Pinto-Correia, C., Duby, R.T., Ponce de Leon, F.A., Boland, M.P., Roche, J.F., and Robl, J.M. (1993). Chromatin and microtubule morphology during the first cell cycle in bovine zygotes. *Mol. Reprod. Dev.* **36**, 23-32.
- Long, C.R., Suncan, R.P., and Robl, J.M. (1997). Isolation and characterization of MPM-2 reactive sperm proteins: homology to components of the outer dense fibers and segmented columns. *Biol. Reprod.* **57**, 246-254.
- Lowe, M., Gonatas, N.K., and Warren, G. (2000). The mitotic phosphorylation cycle of the cis-Golgi matrix protein GM130. *J. Cell Biol.* **149**, 341-356.
- Lowe, M., and Kreis, T.E. (1998). Regulation of membrane traffic in animal cells by COPI. *Biochim. Biophys. Acta* **1404**, 53-66.
- Lowe, M., Rabouille, C., Nakamura, N., Watson, R., Jackman, M., Jamsa, E., Rahman, D., Pappin, D.J., and Warren, G. (1998). Cdc2 kinase directly phosphorylates the cis-Golgi matrix protein GM130 and is required for Golgi fragmentation in mitosis. *Cell* **94**, 783-793.

- Lu, Q., Dunn, R.L., Angeles, R., and Smith, G.D. (2002). Regulation of spindle formation by active mitogen-activated protein kinase and protein phosphatase 2A during mouse oocyte meiosis. *Biol. Reprod.* **66**, 29-37.
- Maller, J. Poceia, D., Nishioka, D., Gerhart, J., and Hartman, H. (1976). Spindle formation and cleavage in *Xenopus* eggs injected with centriole-containing fractions from sperm. *Exp. Cell Res.* **99**, 285–294.
- Manandhar, G., Simerly, C., Salisbury, J.L., and Schatten, G. (1999). Centriole and centrin degeneration during mouse spermiogenesis. *Cell Motil. Cytoskeleton* **43**, 137-144.
- Manandhar, G., Sutovsky, P., Joshi, H.C., Stearns, T., and Schatten, G. (1998). Centrosome reduction during mouse spermiogenesis. *Dev. Biol.* **203**, 424–434.
- Mazia, D. (1961). Mitosis and the physiology of cell division. In: *The Cell, Vol. III*, ed. J. Bracket and A.E. Mirsky. New York: Academic Press, 78–412.
- Mazia, D., and Zimmerman, A.M. (1958). SH compounds in mitosis. II. The effect of mercaptoethanol on the structure of the mitotic apparatus in sea urchin eggs. *Exp. Cell Res.* **15**, 138–153.
- McGaughey, R.W., Racowsky, C., Rider, V., Baldwin, K., DeMarais, A.A., and Webster, S.D. (1990). Ultrastructural correlates of meiotic maturation in mammalian oocytes. *J. Electron Microsc. Tech.* **16**, 257-280.
- McIntosh, J.R., and Koonce M.P. (1989). Mitosis. *Science* **246**, 622–628.
- Mehlmann, L.M., Terasaki, M., Jaffe, L.A., and Kline, D. (1995). Reorganization of the endoplasmic reticulum during meiotic maturation of the mouse oocyte. *Dev. Biol.* **170**, 607-615.

- Mellon, M.G., and Rebhun, L.I. (1976). Sulfhydryls and the in vitro polymerization of tubulin. *J. Cell Biol.* **70**, 226–238.
- Memili, E., and First, N.L. (1999). Control of gene expression at the onset of bovine embryonic development. *Biol. Reprod.* **61**, 1198-1207.
- Meng, L., Ely, J.J., Stouffer, R.L., and Wolf, D.P. (1997). Rhesus monkeys produced by nuclear transfer. *Biol. Reprod.* **57**, 454-459.
- Middendorp, S., Paoletti, A., Schiebel, E., and Bornens, M. (1997). Identification of a new mammalian centrin gene, more closely related to *Saccharomyces cerevisiae* CDC31 gene. *Proc. Natl. Acad. Sci. USA* **94**, 9141–9146.
- Miles, S., McManus, H., Forsten, K.E., and Storrie, B. (2001). Evidence that the entire Golgi apparatus cycles in interphase HeLa cells: sensitivity of Golgi matrix proteins to an ER exit block. *J. Cell Biol.* **155**, 543-555.
- Mitalipov, S.M., Yeoman, R.R., Nusser, K.D., and Wolf, D.P. (2002). Rhesus monkey embryos produced by nuclear transfer from embryonic blastomeres or somatic cells. *Biol. Reprod.* **66**, 1367-1373.
- Moreno, R.D., Ramalho-Santos, J., Chan, E.K.L., Wessel, G.M., and Schatten, G. (2000). The Golgi apparatus segregates from the lysosomal/acrosomal vesicle during rhesus spermiogenesis: structural alterations. *Dev. Biol.* **219**, 334-349.
- Moreno, R.D., Schatten, G., and Ramalho-Santos, J. (2002). Golgi apparatus dynamics during mouse oocyte in vitro maturation: effect of the membrane trafficking inhibitor brefeldin A. *Biol. Reprod.* **66**, 1259-1266.

- Moritz, M., Braunfeld, M.B., Sedat, J.W., Alberts, B., and Agard, D.A. (1995). Microtubule nucleation by γ -tubulin-containing rings in the centrosome. *Nature* **378**, 638–640.
- Morris, M.C., Depollier, J., Mery, J., Heitz, F., and Divita, G. (2001). A peptide carrier for the delivery of biologically active proteins into mammalian cells. *Nat. Biotechnol.* **19**, 1173–1176.
- Mountain, V., Simerly, C., Howard, L., Ando, A., Schatten, G., and Compton, D.A. (1999). The kinesin-related protein, HSET, opposes the activity of Eg5 and cross-links microtubules in the mammalian mitotic spindle. *J. Cell Biol.* **147**, 351–366.
- Murray, A.W. (1991). Cell cycle extracts. *Methods Cell Biol.* **36**, 581–595.
- Murray, A.W., and Hunt, T. (1993). *The Cell Cycle: An Introduction*. New York: W.H. Freeman.
- Nakamura, N., Rabouille, C., Watson, R., Nilsson, T., Hui, N., Slusarewicz, P., Kreis, T.E., and Warren, G. (1995). Characterization of a cis-Golgi matrix protein, GM130. *J. Cell Biol.* **131**, 1715–1726.
- Navara, C.S., First, N.L., and Schatten, G. (1994). Microtubule organization in the cow during fertilization, polyspermy, parthenogenesis, and nuclear transfer: the role of the sperm aster. *Dev. Biol.* **162**, 29–40.
- Nomura, A., Maruyama, Y.K., and Yoneda, M. (1991). Initiation of DNA replication cycle in fertilized eggs of the starfish, *Asterina pectinifera*. *Dev. Biol.* **143**, 289–296.
- Nudell, D.M., and Lipshultz, L.I. (2001). Is intracytoplasmic sperm injection safe? Current status and future concerns. *Curr. Urol. Rep.* **2**, 423–431.

- Oakley, B.R. (1992). γ -Tubulin: the microtubule organizer. *Trends Cell Biol.* **2**, 1–5.
- Oakley, C.E., and Oakley, B.R. (1989). Identification of γ -tubulin, a new member of the tubulin superfamily encoded by mipA gene of *Aspergillus nidulans*. *Nature* **338**, 662–664.
- Ohsumi, K., Katagiri, C., and Yanagimachi, R. (1986). Development of pronuclei from human spermatozoa injected microsurgically into frog (*Xenopus*) eggs. *J. Exp. Zool.* **237**, 319–325.
- Ohsumi, K., Katagiri, C., and Yanagimachi, R. (1988). Human sperm nuclei can transform into condensed chromosomes in *Xenopus* egg extracts. *Gamete Res.* **20**, 1–9.
- Oliver, J.M., Albertini, D.F., and Berlin, R.D. (1976). Effects of glutathione oxidizing agents on microtubule assembly and microtubule-dependent surface properties of human neutrophils. *J. Cell Biol.* **71**, 921–932.
- Paccaud, J.P., Reith, W., Carpentier, J.L., Ravazzola, M., Amherdt, M., Schekman, R., and Orci, L. (1996). Cloning and functional characterization of mammalian homologues of the COPII component Sec23. *Mol. Biol. Cell* **7**, 1535–1546.
- Palacios, M.J., Joshi, H.C., Simerly, C., and Schatten, G. (1993). Dynamic reorganization of γ -tubulin during murine fertilization. *J. Cell Sci.* **104**, 383–389.
- Palermo, G., Joris, H., Devroey, P., and Van Steirteghem, A.C. (1992). Pregnancies after intracytoplasmic injection of single spermatozoon into an oocyte. *Lancet* **340**, 17–18.
- Panté, N., and Kann, M. (2002). Nuclear pore complex is able to transport macromolecules with diameters of ~39 nm. *Mol. Biol. Cell* **13**, 425–434.

- Paoletti, A., Moudjou, M., Paintrand, M., Salisbury, J.L., and Bornens, M. (1996). Most of centrin in animal cells is not centrosome-associated and centrosomal centrin is confined to the distal lumen of centrioles. *J. Cell Sci.* **109**, 3089–3102.
- Parrington, J., Brind, S., De Smedt, H., Gangeswaran, R., Lai, F.A., Wojcikiewicz, R., and Carroll, J. (1998). Expression of inositol 1,4,5-triphosphate receptors in mouse oocytes and early embryos: the type 1 isoform is upregulated in oocytes and downregulated after fertilization. *Dev. Biol.* **203**, 451-461.
- Payne, C., Rawe, V., Ramalho-Santos, J., Simerly, C., and Schatten, G. (2003). Preferentially localized dynein and perinuclear dynactin associate with nuclear pore complex proteins to mediate genomic union during mammalian fertilization. *J Cell Sci.* **in press**.
- Payne, C., and Schatten, G. (2003). Golgi dynamics during meiosis are distinct from mitosis and are coupled to endoplasmic reticulum dynamics until fertilization. *Dev. Biol.* **in press**.
- Perreault, S.D. (1992). Chromatin remodeling in mammalian zygotes. *Mutat. Res.* **296**, 43-55.
- Perreault, S.D., Naish, S.J., and Zirken, B.R. (1987). The timing of hamster sperm nuclear decondensation and male pronucleus formation is related to sperm nuclear disulfide bond content. *Biol. Reprod.* **36**, 239–244.
- Perreault, S.D., Wolf, R.A., and Zirken, B.R. (1984). The role of disulfide bond reduction during mammalian sperm nuclear decondensation in vivo. *Dev. Biol.* **101**, 160–167.

- Pinto-Correia, C., Poccia, D.L., Chang, T., and Robl, J.M. (1994). Dephosphorylation of sperm midpiece antigens initiates aster formation in rabbit oocytes. *Proc. Natl. Acad. Sci. USA* **91**, 7894–7898.
- Pires-daSilva, A., Nayernia, K., Engel, W., Torres, M., Stoykova, A., Chowdhury, K., and Gruss, P. (2001). Mice deficient for spermatid perinuclear RNA-binding protein show neurologic, spermatogenic, and sperm morphological abnormalities. *Dev. Biol.* **233**, 319-328.
- Plante, L., and King, W.A. (1994). Light and electron microscopic analysis of bovine embryos derived by in vitro and in vivo fertilization. *J. Assist. Reprod. Genet.* **11**, 515-529.
- Polejaeva, I.A., Chen, S.H., Vaught, T.D., Page, R.L., Mullins, J., Ball, S., Dai, Y., Boone, J., Walker, S., Ayares, D.L., Colman, A., and Campbell, K.H.S. (2000). Cloned pigs produced by nuclear transfer from adult somatic cells. *Nature* **407**, 86-90.
- Presley, J.F., Cole, N.B., Schroer, T.A., Hirschberg, K., Zaal, K.J., and Lippincott-Schwartz, J. (1997). ER-to-Golgi transport visualized in living cells. *Nature* **389**, 81-85.
- Quintyne, N.J., and Schroer, T.A. (2002). Distinct cell cycle-dependent roles for dynactin and dynein at centrosomes. *J. Cell Biol.* **159**, 245-254.
- Ramalho-Santos, J., Sutovsky, P., Simerly, C., Oko, R., Wessel, G.M., Hewitson, L., and Schatten, G. (2000). ICSI choreography: fate of sperm structures after monospermic rhesus ICSI and first cell cycle implications. *Hum. Reprod.* **15**, 2610-2620.

- Reinsch, S., and Gönczy, P. (1998). Mechanisms of nuclear positioning. *J. Cell Sci.* **111**, 2283-2295.
- Reinsch, S., and Karsenti, E. (1997). Movement of nuclei along microtubules in *Xenopus* egg extracts. *Curr. Biol.* **7**, 211-214.
- Richter, J.D. (2001). Think globally, translate locally: what mitotic spindles and neuronal synapses have in common. *Proc. Natl. Acad. Sci. USA* **98**, 7069-7071.
- Rideout, W.M., Eggan, K., and Jaenisch, R. (2001). Nuclear cloning and epigenetic reprogramming of the genome. *Science* **293**, 1093-1098.
- Rodman, T.C., Pruslin, F.H., Hoffmann, H.P., and Allfrey, V.G. (1981). Turnover of basic chromosomal proteins in fertilized eggs: a cyto-immunochemical study of events in vivo. *J. Cell Biol.* **90**, 351-361.
- Rose, M.D., Biggins, S., and Satterwhite, L.L. (1993). Unravelling the tangled web at the microtubule-organizing center. *Curr. Opin. Cell Biol.* **5**, 105-115.
- Rouvière, C., Houliston, E., Carré, D., Chang, P., and Sardet, C. (1994). Characteristics of pronuclear migration in *Beroe ovata*. *Cell Motil. Cytoskeleton* **29**, 301-311.
- Ryan, K.J., and Wente, S.R. (2000). The nuclear pore complex: a protein machine bridging the nucleus and cytoplasm. *Curr. Opin. Cell Biol.* **12**, 361-371.
- Salina, D., Bodoor, K., Eckley, D.M., Schroer, T.A., Rattner, J.B., and Burke, B. (2002). Cytoplasmic dynein as a facilitator of nuclear envelope breakdown. *Cell* **108**, 97-107.
- Salisbury, J.L. (1995). Centrin, centrosomes, and mitotic spindle poles. *Curr. Opin. Cell Biol.* **7**, 39-45.

- Sanders, M.A., and Salisbury, J.L. (1989). Centrin-mediated microtubule severing during flagellar excision in *Chlamydomonas reinhardtii*. *J. Cell Biol.* **108**, 1751–1760.
- Sanders, M.A., and Salisbury, J.L. (1994). Centrin plays an essential role in microtubule severing during flagellar excision in *Chlamydomonas reinhardtii*. *J. Cell Biol.* **124**, 795–805.
- Sapir, T., Elbaum, M., and Reiner, O. (1997). Reduction of microtubule catastrophe events by LIS1, platelet-activating factor acetylhydrolase subunit. *EMBO J.* **16**, 6977-6984.
- Sathananthan, A.H., Kola, I., Osborne, J., Trounson, A., Ng, S.C., Bongso, A., and Ratnam, S.S. (1991). Centrioles in the beginning of human development. *Proc. Natl. Acad. Sci. USA* **88**, 4806-4810.
- Schafer, D.A., Gill, S.R., Cooper, J.A., Heuser, J.E., and Schroer, T.A. (1994). Ultrastructural analysis of the dynactin complex: an actin-related protein is a component of a filament that resembles F-actin. *J. Cell Biol.* **126**, 403-412.
- Schatten, G. (1982). Motility during fertilization. *Int. Rev. Cytol.* **79**, 59-163.
- Schatten, G. (1994). Centrosome inheritance: the reduction of the centrosome during gametogenesis and its restoration during fertilization. *Dev. Biol.* **165**, 299–335.
- Schatten, G., Simerly, C., and Schatten, H. (1991). Maternal inheritance of centrosomes in mammals? Studies on parthenogenesis and polyspermy in mice. *Proc. Natl. Acad. Sci. USA* **88**, 6785–6789.
- Schatten, H., Schatten, G., Mazia, D., Balczon, R., and Simerly, C. (1986). Behavior of centrosomes during fertilization and cell division in mouse oocytes and in sea urchin eggs. *Proc. Natl. Acad. Sci. USA* **83**, 105–109.

- Schliwa, M., Pryzwansky, K.B., and Euteneuer, U. (1982). Centrosome splitting in neutrophils: an unusual phenomenon related to cell activation and motility. *Cell* **31**, 705–717.
- Seemann, J., Pypaert, M., Taguchi, T., Malsam, J., and Warren, G. (2002). Partitioning of the matrix fraction of the Golgi apparatus during mitosis in animal cells. *Science* **295**, 848–851.
- Shalgi, R., Seligman, J., and Kosower, N.S. (1989). Dynamics of the thiol status of rat spermatozoa during maturation: analysis with the fluorescent labeling agent monobromobimane. *Biol. Reprod.* **40**, 1037–1045.
- Sheeman, B., Carvalho, P., Sagot, I., Geiser, J., Kho, D., Hoyt, M.A., and Pellman, D. (2003). Determinants of *S. cerevisiae* dynein localization and activation: implications for the mechanism of spindle positioning. *Curr. Biol.* **13**, 364–372.
- Shin, T., Kraemer, D., Pryor, J., Liu, L., Rugila, J., Howe, L., Buck, S., Murphy, K., Lyons, L., and Westhusin, M. (2002). A cat cloned by nuclear transplantation. *Nature* **415**, 859.
- Shiraishi, K., Okada, A., Shirakawa, H., Nakanishi, S., Mikoshiba, K., and Miyazaki, S. (1995). Developmental changes in the distribution of the endoplasmic reticulum and inositol 1,4,5-triphosphate receptors and the spatial pattern of Ca^{2+} release during maturation of hamster oocytes. *Dev. Biol.* **170**, 594–606.
- Shorter, J., and Warren, G. (2002). Golgi architecture and inheritance. *Annu. Rev. Cell Dev. Biol.* **18**, 379–420.
- Simerly, C., and Schatten, G. (1993). Techniques for localization of specific molecules in oocytes and embryos. *Methods Enzymol.* **225**, 516–552.

- Simerly, C., Wu, G.J., Zoran, S., Ord, T., Rawlins, R., Jones, J., Navara, C., Gerrity, M., Rinehart, J., Binor, Z., Asch, R., and Schatten, G. (1995). The paternal inheritance of the centrosome, the cell's microtubule-organizing center, in humans, and the implications for infertility. *Nat. Med.* **1**, 47–52.
- Sirard, M.A., Parrish, J.J., Ware, C.B., Leibfried-Rutledge, M.L., and First, N.L. (1988). The culture of bovine oocytes to obtain developmentally competent embryos. *Biol. Reprod.* **39**, 546-552.
- Skop, A.R., Bergmann, D., Mohler, W.A., and White, J.G. (2001). Completion of cytokinesis in *C. elegans* requires a brefeldin A-sensitive membrane accumulation at the cleavage furrow apex. *Curr. Biol.* **11**, 735-746.
- Slusarewicz, P., Nilsson, T., Hui, N., Watson, R., and Warren, G. (1994). Isolation of a matrix that binds medial Golgi enzymes. *J. Cell Biol.* **124**, 405-413.
- Smith, D.S., Niethammer, M., Ayala, R., Zhou, Y., Gambello, M.J., Wynshaw-Boris, A., and Tsai, L.H. (2000). Regulation of cytoplasmic dynein behaviour and microtubule organization by mammalian Lis1. *Nat. Cell Biol.* **2**, 767-775.
- Smith, G.D., Sadhu, A., Mathies, S., and Wolf, D.P. (1998). Characterization of protein phosphatases in mouse oocytes. *Dev. Biol.* **204**, 537-549.
- Stearns, T. (1995). The form and the substance. *Nat. Med.* **1**, 19–20.
- Stearns, T., Evans, L., and Kirschner, M. (1991). γ -Tubulin is a highly conserved component of the centrosome. *Cell* **65**, 825–836.
- Stearns, T., and Kirschner, M. (1994). In vitro reconstitution of centrosome assembly and function: the central role of γ -tubulin. *Cell* **76**, 623–637.
- Stearns, T., and Winey, M. (1997). The cell center at 100. *Cell* **91**, 303–309.

- Steffen-Zoran, S., Simerly, C.R., and Schatten, G. (1993). Microtubule organization in mouse oocytes after microinjection of sea urchin sperm heads, midpieces and centrosomal complexes. *Biol. Res.* **26**, 453–464.
- Straight, A.F., and Field, C.M. (2000). Microtubules, membranes and cytokinesis. *Curr. Biol.* **10**, R760-R770.
- Sun, F.Z., and Moor, R.M. (1995). Nuclear transplantation in mammalian eggs and embryos. *Curr. Top. Dev. Biol.* **30**, 147-176.
- Susko-Parrish, J.L., Leibfried-Rutledge, M.L., Northey, D.L., Schutzkus, V., and First, N.L. (1994). Inhibition of protein kinases after an induced Ca^{2+} transient causes transition of bovine oocytes to embryonic cycles without meiotic completion. *Dev. Biol.* **166**, 729-739.
- Sutovsky, P., Fléchon, J.E., Fléchon, B., Motlík, J., Peynot, N., Chesné, P., and Heyman, Y. (1993). Dynamic changes of gap junctions and cytoskeleton during in vitro culture of cattle oocyte cumulus complexes. *Biol. Reprod.* **49**, 1277–1287.
- Sutovsky, P., Hewitson, L., Simerly, C.R., Tengowski, M.W., Navara, C.S., Haavisto, A., and Schatten, G. (1996). Intracytoplasmic sperm injection for Rhesus monkey fertilization results in unusual chromatin, cytoskeletal, and membrane events, but eventually leads to pronuclear development and sperm aster assembly. *Hum. Reprod.* **11**, 1703-1712.
- Sutovsky, P., and Schatten, G. (2000). Paternal contributions to the mammalian zygote: fertilization after sperm-egg fusion. *Int. Rev. Cytol.* **195**, 1-65.

- Sutovsky, P., Simerly, C., Hewitson, L., and Schatten, G. (1998). Assembly of nuclear pore complexes and annulate lamellae promotes normal pronuclear development in fertilized mammalian oocytes. *J. Cell Sci.* **111**, 2841-2854.
- Swan, A., Nguyen, T., and Suter, B. (1999). Drosophila Lissencephaly-1 functions with Bic-D and dynein in oocyte determination and nuclear positioning. *Nat. Cell Biol.* **1**, 444-449.
- Swann, K. (1990). A cytosolic sperm factor stimulates repetitive calcium increases and mimics fertilization in hamster eggs. *Development* **110**, 1295-1302.
- Tai, C.Y., Dujardin, D.L., Faulkner, N.E., and Vallee, R.B. (2002). Role of dynein, dynactin, and CLIP-170 interactions in LIS1 kinetochore function. *J. Cell Biol.* **156**, 959-968.
- Takizawa, C.G., and Morgan, D.O. (2000). Control of mitosis by changes in the subcellular location of cyclin-B1-cdk1 and cdc25c. *Curr. Opin. Cell Biol.* **12**, 658-665.
- Terasaki, M., and Jaffe, L.A. (1991). Organization of the sea urchin egg endoplasmic reticulum and its reorganization at fertilization. *J. Cell Biol.* **114**, 929-940.
- Thomson, J.A., Itskovitz-Eldor, J., Shapiro, S.S., Waknitz, M.A., Swiergiel, J.J., Marshall, V.S., and Jones, J.M. (1998). Embryonic stem cell lines derived from human blastocysts. *Science* **282**, 1145-1147.
- Thornton, K.L. (2000). Advances in assisted reproductive technologies. *Obstet. Gynecol. Clin. North Am.* **27**, 517-527.
- Thyberg, J., and Moskalewski, S. (1999). Role of microtubules in the organization of the Golgi complex. *Exp. Cell Res.* **246**, 263-279.

- Vaisberg, E.A., Koonce, M.P., and McIntosh, J.R. (1993). Cytoplasmic dynein plays a role in mammalian mitotic spindle formation. *J. Cell Biol.* **123**, 849-858.
- Van Steirteghem, A., Devroey, P., and Liebaers, I. (2002). Intracytoplasmic sperm injection. *Mol. Cell. Endocrinol.* **186**, 199-203.
- Van Steirteghem, A.C., Nagy, Z., Joris, H., Liu, J., Staessen, C., Smitz, J., Wisanto, A., and Devroey, P. (1993). High fertilization and implantation rates after intracytoplasmic sperm injection. *Hum. Reprod.* **8**, 1061-1066.
- Vandré, D.D., Davis, F.M., Rao, P.N., and Borisy, G.G. (1986). Distribution of cytoskeletal proteins sharing a conserved phosphorylated epitope. *Eur. J. Cell Biol.* **41**, 72-81.
- Vaughan, K.T., and Vallee, R.B. (1995). Cytoplasmic dynein binds dynactin through a direct interaction between the intermediate chains and p150^{Glued}. *J. Cell Biol.* **131**, 1507-1516.
- Verde, F., Labbé, J.C., Dorée, M., and Karsenti, E. (1990). Regulation of microtubule dynamics by cdc2 protein kinase in cell-free extracts of *Xenopus* eggs. *Nature* **343**, 233-238.
- Verlhac, M.-H., Kubiak, J.Z., Clarke, H.J., and Maro, B. (1994). Microtubule and chromatin behavior follow MAP kinase activity but not MPF activity during meiosis in mouse oocytes. *Development* **120**, 1017-1025.
- Wakayama, T., Perry, A.C., Zuccotti, M., Johnson, K.R., and Yanagimachi, R. (1998). Full-term development of mice from enucleated oocytes injected with cumulus cell nuclei. *Nature* **394**, 369-374.

- Wang, W., Hosoe, M., Li, R., and Shioya, Y. (1997). Development of the competence of bovine oocytes to release cortical granules and block polyspermy after meiotic maturation. *Dev. Growth Differ.* **39**, 607-615.
- Ward, T.H., Polishchuk, R.S., Caplan, S., Hirschberg, K., and Lippincott-Schwartz, J. (2001). Maintenance of Golgi structure and function depends on the integrity of ER export. *J. Cell Biol.* **155**, 557-570.
- Ward, W.S., and Coffey, D.S. (1991). DNA packaging and organization in mammalian spermatozoa: comparison with somatic cells. *Biol. Reprod.* **44**, 569-574.
- Wassarman, P.M., and Josefowicz, W.J. (1978). Oocyte development in the mouse: an ultrastructural comparison of oocytes isolated at various stages of growth and competence. *J. Morphol.* **156**, 209-235.
- Waterman-Storer, C., Karki, S., and Holzbaaur, E.L.F. (1995). The p150^{Glued} component of the dynactin complex binds to both microtubules and the actin-related protein centractin (Arp-1). *Proc. Natl. Acad. Sci. USA* **92**, 1634-1638.
- Wessel, G.M., Brooks, J.M., Green, E., Haley, S., Voronina, E., Wong, J., Zaydfudim, V., and Conner, S. (2001). The biology of cortical granules. *Int. Rev. Cytol.* **209**, 117-206.
- Whitaker, M., and Swann, K. (1993). Lighting the fuse at fertilization. *Development* **117**, 1-12.
- Wilmut, I. (2002). Are there any normal cloned mammals? *Nat. Med.* **8**, 215-216.
- Wilmut, I., Schnieke, A.E., McWhir, J., Kind, A.J., and Campbell, K.H.S. (1997). Viable offspring derived from fetal and adult mammalian cells. *Nature* **385**, 810-813.

- Wilson, E.B. (1895). *An atlas of the fertilization and karyokinesis of the ovum*. New York: Macmillan and Co.
- Wolf, D.P., Meng, L., Ouhibi, N., and Zelinski-Wooten, M. (1999). Nuclear transfer in the rhesus monkey: practical and basic implications. *Biol. Reprod.* **60**, 199-204.
- Wolf, D.P., Vandevoort, C.A., Meyer-Haas, G.R., Zelinski-Wooten, M.B., Hess, D.L., Baughman, W.L., and Stouffer, R.L. (1989). In vitro fertilization and embryo transfer in the rhesus monkey. *Biol. Reprod.* **41**, 335-346.
- Xiang, X., and Morris, N.R. (1999). Hyphal tip growth and nuclear migration. *Curr. Opin. Microbiol.* **2**, 636-640.
- Xiang, X., Osmani, A.H., Osmani, S.A., Xin, M., and Morris, N.R. (1995). NudF, a nuclear migration gene in *Aspergillus nidulans*, is similar to the human LIS-1 gene required for neuronal migration. *Mol. Biol. Cell* **6**, 297-310.
- Xu, Y.-S., Overton, W.R., Marmar, J.L., Leonard, J.C., McCoy, J.P., Jr., Butler, G.H., and Li, H. (1998). Complete replication of human sperm genome in egg extracts from *Xenopus laevis*. *Biol. Reprod.* **58**, 641-647.
- Young, L.E., Sinclair, K.D., and Wilmut, I. (1998). Large offspring syndrome in cattle and sheep. *Rev Reprod.* **3**, 155-163.
- Zaal, K.J., Smith, C.L., Polishchuk, R.S., Altan, N., Cole, N.B., Ellenberg, J., Hirschberg, K., Presley, J.F., Roberts, T.H., Siggia, E., Phair, R.D., and Lippincott-Schwartz, J. (1999). Golgi membranes are absorbed into and reemerge from the ER during mitosis. *Cell* **99**, 589-601.
- Zalensky, A.O. (1998). Genome architecture. In: *Genes and Genomes, Vol. V*, ed. R.S. Verma. Greenwich, Connecticut: JAI Press, 179-210.

- Zamboni, L., and Stefanini, M. (1971). The fine structure of the neck of mammalian spermatozoa. *Anat. Rec.* **169**, 155–172.
- Zelinski-Wooten, M.B., Hutchison, J.S., Hess, D.L., Wolf, D.P., and Stouffer, R.L. (1995). Follicle stimulating hormone alone supports follicle growth and oocyte development in gonadotrophin-releasing hormone antagonist-treated monkeys. *Hum. Reprod.* **10**, 1658-1666
- Zheng, Y., Jung, M.K., and Oakley, B.R. (1991). γ -Tubulin is present in *Drosophila melanogaster* and *Homo sapiens* and is associated with the centrosome. *Cell* **65**, 817–823.
- Zheng, Y., Wong, M.L., Alberts, B., and Mitchison, T. (1995). Nucleation of microtubule assembly by a γ -tubulin-containing ring complex. *Nature* **378**, 578–583.
- Zimmerman, W., Sparks, C.A., and Doxsey, S.J. (1999). Amorphous no longer: the centrosome comes into focus. *Curr. Opin. Cell Biol.* **11**, 122–128.